2007

Equilibria and microorganism studies with analytical separation technique

Andrew W. Lantz
Iowa State University

Equilibria and microorganism studies with analytical separation techniques

by

Andrew W. Lantz

A dissertation submitted to the graduate faculty

in partial fulfillment of the requirements for the degree of

DOCTOR OF PHILOSOPHY

Major: Analytical Chemistry

Program of Study Committee:
Daniel W. Armstrong, Co-major Professor
Victor S.Y. Lin, Co-major Professor
Patricia A. Thiel
Robert J. Angelici
Byron F. Brehm-Stecher

Iowa State University

Ames, Iowa

2007

TABLE OF CONTENTS

ABSTRACT

The applications of analytical techniques to evaluate solute-ligand interactions and to analyze microbiological samples are discussed in this work. The dissertation is organized into two sections based on the natural division of studies done in the past several years. Part I includes studies involving the estimation of binding constants and partition coefficients and the modeling of pseudophase gas-liquid chromatography. The binding of solutes to pseudophases, such as micelles and cyclodextrins, is an important phenomenon in numerous areas of chemistry. Here, the ability of various native and derivatized cyclodextrins to sequester oral malodorous compounds and other volatile solutes was examined by measuring their association constants. Numerous techniques were utilized to determine the solute-cyclodextrin affinities. The results of this study indicate that cyclodextrins are capable of binding with a wide variety of oral malodorous compounds to varying degrees. The equations used in this study were then developed further and applied to the separation of several enantiomers using a methylated-cyclodextrin/polysiloxane stationary phase. These calculations allow the contributions from all three solute equilibria to retention and selectivity to be measured. This work was then extended to micellar/ionic liquid gas-liquid chromatography stationary phases, and the Abraham solvation parameter model was used in order to deconvolute the types of interactions responsible for analyte partitioning to these two phases. Part II of this dissertation focuses on the work done on the development of a rapid capillary electrophoretic sterility test. This technique coalesces all cells in a sample into a single peak and removes them from potential interferences in the sample matrix. Cationic surfactants were used in the run buffer to impart charge onto the microorganisms and sweep them out of the sample zone, while a plug of blocking agent induced cellular

aggregation and negated the cells' electrophoretic mobility. A wide variety of bacteria are compatible with this method, and analysis times are typically less than 10 minutes. Single cell detection was accomplished via laser-induced fluorescence detection and fluorescent cell staining. By coupling this capillary electrophoresis method with fluorescence in situ hybridization, a method that utilizes fluorescently tagged nucleic acid probes to selectively stain specific microorganism species or classes, identification of microbial contaminants was achieved.

PART I: BINDING AND PARTITION EQUILIBRIA STUDIES

CHAPTER 1. GENERAL INTRODUCTION

Introduction

Equilibrium processes involving noncovalent interactions take place in almost every chemical system. Numerous types of noncovalent interactions may occur between the substrate and ligand depending on their molecular structure and the characteristics of the surrounding environment. These include metal ion-ligand coordination, hydrogen bonding, ion pair interactions, dipole-dipole interactions, and dispersion forces. Association constants are often measured in order to assess the strength of substrate-ligand binding and elucidate the contribution of various intermolecular forces to complex formation. Other mathematical models and expressions may be applied to binding data in order to determine quantitative information regarding the types and magnitudes of interactions that a ligand may be capable of. This topic will be covered more in depth in the literature review section.

In order to discuss the nature of substrate-ligand complexation, an understanding of the types of noncovalent interactions involved in binding is necessary. Electrostatic interactions consist of the forces between the moments of polar molecules, such as charge-charge interactions and dipole moment interactions.[1] Ion-pairing interactions between an anion and cation tend to be relatively strong, yet are greatly affected by the presence of other ionic species in the surroundings that may compete for electrostatic interaction. The attractive interaction of two polar molecules (dipole-dipole) is highly dependent on the mutual direction of the molecules' moments. As a result, these interactions are only significant in certain binding orientations of the ligand and substrate.[1] Compounds containing substituted aromatic rings may also exhibit binding *via* π-π interactions. These

forces occur when an electron-withdrawing group is substituted on the ring of one molecule and an electron-donating group is on the ring of another molecule. This π -acid/ π -base interaction results in a staggered stacking of the two aromatic rings.[2] Induction phenomenon in which a polar molecule induces a charge separation in an adjacent molecule may also occur, however these forces are relatively weak.[1]

Nonpolar (and polar) molecules may also experience attractive interactions through a quantum mechanical phenomenon known as dispersion (London) forces.[1] In a molecule, an instantaneous dipole may be generated from an asymmetric distribution of the surrounding electrons. This temporary dipole may then induce a similar dipole on an adjacent molecule. The magnitude of these interactions is dependent on the molecule's polarizability, which is greatly affected by the size and shape of the molecule.

Hydrogen bonding is one of the strongest noncovalent interactions and is essential in numerous chemical and biological systems.[3] This interaction may exist between a molecule containing a hydrogen atom covalently bound to a highly electronegative atom (e.g. oxygen, nitrogen, fluorine) and a molecule containing an electronegative atom with a non-bonding electron pair. The covalent bond between the hydrogen and the neighboring atom is highly polar, resulting in strong dipole-dipole interactions with molecules containing non-bonding electrons. The nature of hydrogen bonding has been studied extensively and results have shown that a significant electrostatic contribution to binding exists with these interactions.[4]

As alluded to previously, the solvent plays a significant role on the magnitude and types of binding interactions that may occur between a ligand and a substrate in solution. Since the solvent is a molecular matrix, it too can interact with the substrate and ligand through similar intermolecular forces. In order for the substrate and ligand to bind, the free

energy of solute-solute binding must overcome the free energies of the individual solute-solvent interactions.[5] Solvents capable of only weak solvation interactions, such as nonpolar solvents with only dispersion forces, generally do not compete greatly with solute-solute interactions. However, in polar solvents or solvents consisting of other dissolved ionic or polar species, the solvent may interfere significantly with binding between a substrate and a ligand. Therefore, association constants are unique for the environment in which they are measured, and it is imperative to properly define this environment when reporting such values.

Another contribution of the bulk solvent towards solute-solute binding is the effect from solvent-solvent interactions. If the magnitude of solute-solvent interaction is low compared to the extent of solvent-solvent interaction, then the solvent may promote the formation of the substrate-ligand complex by forcing the solutes together.[5,6] This tendency is the driving force behind the solvophobic effect (*i.e.* hydrophobic effect in aqueous solutions). Nonpolar solutes dissolved in aqueous solution are surrounded by highly structured solvation shells. The high surface tension of water drives the reduction of solvent surface area in contact with the solute, resulting in aggregation of the nonpolar solutes. Generally speaking, solute-solute interaction is driven by enthalpic forces involved in the system and hindered by the solutes' decrease in entropy resulting from binding. However, the minimization of the solvent's surface area (and structured solvation shell) greatly increases the entropy of the surrounding solution and further promotes solute interaction.[7]

An important step in understanding and deconvoluting the noncovalent interactions that take place in a system is the measurement of their equilibrium constants. The interaction equilibrium of a substrate (*S*) with a ligand (*L*) is often described by a binding constant (also

known as an association or stability constant), which is defined as the ratio of the rate constants of the forward (association) and reverse (dissociation) reactions.

$$aS + bL \overset{K}{\longleftrightarrow} S_a \cdot L_b \tag{1}$$

$$K = \frac{k_f}{k_r} \tag{2}$$

The coefficients *a* and *b* indicate the complex stoichiometry. At equilibrium, the forward and reverse rates are equal, and the ratio of the rate constants is directly related to the concentrations of the complex and the free substrate and ligand.

$$K = \frac{[S_a \cdot L_b]}{[S]^a [L]^b} \tag{3}$$

These binding constants are dependent on the thermodynamic parameters enthalpy, entropy, and Gibbs free energy by the following equations:

$$\Delta G = -RT \ln K \tag{4}$$

$$\Delta G = \Delta H - T\Delta S \tag{5}$$

Under conditions in which these thermodynamic relationships are maintained, the van't Hoff equation (Eqn. 6) may be used to correlate the contributions of enthalpy and entropy to the magnitude of solute-ligand binding by measuring the association constants at a series of temperatures.

$$\ln K = -\frac{\Delta H}{R} \cdot \frac{1}{T} + \frac{\Delta S}{R} \tag{6}$$

If the ligand consists of a cavity or region with a defined volume that is capable of including the substrate, a partition coefficient may also be used to express the equilibrium. Partition coefficients simply state the ratio of the equilibrium concentrations of the substrate

in the two phases. In the case of ligand binding, the concentrations of the substrate (C_S) in the bulk solution (B) volume and ligand (L) cavity volume are used.

$$K = \frac{C_S^L}{C_S^B} \tag{7}$$

Such regions/ligands are often referred to as pseudophases in the sense that these species are dissolved in the surrounding medium, yet provide a micro-environment capable of different solvation interactions.[8]

Some of the most commonly used pseudophases include surfactant micelles and cyclodextrins. Surfactants are amphiphilic compounds consisting of a nonpolar and polar region. When these molecules are dissolved in aqueous or polar solutions, surfactant monomers align at the gas-liquid interface with their nonpolar portions extending out of solution. Once the surface is saturated with these monomers (at the critical micelle concentration, CMC), any additional dissolved surfactant molecules form aggregates called micelles in solution.[9] In micellar form, the hydrophobic portions of the surfactant molecules are shielded from the polar environment by their hydrophilic groups. This phenomenon results in the formation of distinct hydrophobic micro-environments inside the micelles that are capable of solvating highly lipophilic compounds. In nonpolar solutions, the opposite effect occurs and the interior cavity contains the hydrophilic portions (reverse micelles). The ability of aqueous micelles to solubilize organic solutes has been well documented and exploited in numerous areas of chemistry from reaction catalysis to chromatographic separations and solute extractions.[10-14]

Cyclodextrins however differ from micelles in that they are not dynamically formed pseudophases, but rather are large molecular compounds that are capable of including

smaller molecules. The cyclodextrin family is a unique class of compounds and one of the more important and useful pseudophase forming entities. Cyclodextrins are cyclic oligosaccharides composed of 6-8 glucopyranose units (α-, β-, and γ- cyclodextrin) connected by α-(1,4) linkages, and are the product of the natural breakdown of starch by a family of bacteria known as Bacillus macerans.[15] Cyclodextrins conform to a toroidal shape whose outer surface is hydrophilic and inner cavity is more hydrophobic. This characteristic allows a wide variety of hydrophobic molecules to form inclusion complexes within the cyclodextrin cavity in aqueous environments. Additional solute-cyclodextrin interactions may occur through hydrogen bonding, electrostatic, and dipole-dipole effects. Cyclodextrins may also be chemically modified by adding substituents to the hydroxyl groups on the cavity rim in order to change their aqueous solubility, charge, and analyte binding properties.[15] As a result of these properties, cyclodextrins have been studied extensively in a variety of fields including reaction catalysis, chromatographic separations, solubilization and bio-delivery of pharmaceuticals, preservation of food products, and cosmetics and deodorizing products. In addition to being relatively inexpensive, native cyclodextrins have negligible toxicity and their bioadaptability has been well documented.[16]

Organization

The studies presented in this portion of the dissertation focus on applications of cyclodextrins and micelles as 1) aqueous sequestering agents for oral malodorous compounds and volatile analytes and, 2) as pseudophases for use in gas-liquid chromatography stationary phases. The association constants for a wide range of volatile odoriferous molecules to a variety of native and derivatized cyclodextrins were measured. Several techniques were implemented to accomplish this task. In Chapter 2, nuclear

magnetic resonance spectroscopy and capillary electrophoresis were used to measure the ability of cyclodextrins to complex with the less volatile, more water soluble analytes. However, highly volatile and gaseous compounds cannot be analyzed using these methods, as sufficient solute concentrations could not be reached in solution to be properly detected. Therefore, a novel headspace gas chromatography method was developed that describes the partitioning of a gaseous analyte to an aqueous phase and dissolved pseudophase as a "three-phase" system. This technique was used to measure the association constants of highly volatile analytes to an assortment of cyclodextrin derivatives, and the results are published in Chapter 3. The analyte equilibria occurring in this study are also analogous to the partitioning of analytes in gas-liquid chromatography (GLC) using dissolved pseudophases. Therefore, the "three-phase" model derived for volatile-cyclodextrin binding studies may also be applied to help describe the mechanism behind pseudophase GLC. In Chapter 4, we further develop the equations behind this model and apply them to the enantiomeric separations of several compounds using a methylated-cyclodextrin/polysiloxane stationary phase. This study allows, for the first time, the contribution from all three solute equilibria to retention and selectivity to be measured. Recently, significant interest in ionic liquids as chromatographic stationary phases has arisen. In addition, it has been shown that surfactants may form micelles in ionic liquids in a similar manner as in other polar solvents. As a result, micelles may be used to alter the solvation properties of ionic liquid stationary phases to enhance selectivity. In Chapter 5, we present several micellar ionic liquid stationary phases for GLC and apply the three-phase model to determine the effect of each stationary phase component on analyte retention and selectivity. The Abraham solvation parameter model was also used in order to deconvolute the types of interactions responsible for analyte

partitioning to these two phases. Finally, Chapter 6 summarizes the conclusions of this study and points the direction of possible future studies.

Literature Review

Complex formation between a host and a guest molecule is an essential process in supramolecular chemistry. The measurement of the association constant provides important quantitative information regarding the nature of the interaction, particularly when these data are applied to further mathematical treatments. In this literature section, methods and techniques that have been developed over the past several decades to measure binding constants and partition coefficients are reviewed. However, before appropriate methods are chosen for measuring association parameters, the stoichiometry of the equilibrium should be determined. In many systems a 1:1 complex is common, however other ratios may exist either exclusively or simultaneously with the 1:1 complex. It is important to note that while the ratio of substrate and ligand in a complex is primarily based on the molecules' individual properties, the conditions used to measure the association may also play a role in determining the stoichiometric relationship. Systems in which the ligand concentration is significantly higher than the concentration of substrate generally will promote the formation of complexes with multiple ligands associated with a single substrate molecule (if possible). Conversely, higher substrate concentrations may facilitate the formation of ligand complexes with more than one substrate bound.

Numerous techniques are available for determining the stoichiometric coefficients, many of which are beyond the scope of this review. However, the most popular (and useful) means include continuous variation methods, mole ratio methods, and stoichiometric model fitting.[17-25] The method of continuous variations, or Job's method, often times allows the

determination of the stoichiometric ratio of a complex by varying the relative concentrations of substrate and ligand while maintaining the total concentration of the two species constant.[17] A property or signal that is directly related to formation of the complex is measured at each concentration and plotted against the fraction of substrate ($x=[S]/\{[S]+[L]\}$). The maxima of these plots indicate the ratio of substrate and ligand in the complex ($a/b=x_{max}/\{1-x_{max}\}$). The mole ratio method is similar to a Job's plot, however in this scenario the concentration of the substrate is held constant while the ligand concentration is varied. The complex dependent property is plotted against the ratio of ligand to substrate, and sudden changes in the slope correspond to the stoichiometric ratio. If the association is very strong, the concentration of complex will increase (and the dependent signal will change) with increasing ligand concentration until the ratio of a/b is reached, at which point little additional complex will be formed.[18]

Many applications of these methods utilize absorption spectroscopy as a technique of measuring a complex dependent signal, however other techniques may be used.[19] It has been noted, however, that most continuous variation and mole ratio treatments assume that only a single complex is formed, which may not necessarily be the case. In cases in which multiple substrate-ligand associations occur, the x-axis stoichiometry point may be highly dependent on the wavelength used for detection as these multiple complexes may produce dissimilar spectra.[20] Since most complexes conform to ratios of 1:1, 2:1, and 1:2, any significant deviation from these values is likely indicative of the formation of a second complex.

Perhaps the most useful method of determining complex stoichiometry is by fitting data to assumed binding isotherm models. Binding isotherms are commonly used functional rearrangements of the equilibrium model equations. Often times, mass balance expressions

are used as a basis for these isotherms. For the model of a simple 1:1 substrate-ligand interaction, the binding constant equation may be rearranged to produce the following binding isotherm:

$$f_{11} = \frac{K_{11}[L]}{1 + K_{11}[L]} \tag{8}$$

where f_{11} is the fraction of substrate bound to ligand at any given time and K_{11} is the association constant for the 1:1 interaction. Similarly, the binding of a single substrate to two ligands simultaneously is expressed as

$$f_{12} = \frac{K_{11}K_{12}[L]^2}{1 + K_{11}[L] + K_{11}K_{12}[L]^2} \tag{9}$$

and f_{12} and K_{12} are the fraction of bound substrate and binding constant for the 1:2 association, respectively.[21] The fraction of substrate bound to a ligand may be determined by measuring a system signal or property that is related to binding, as done with the Job's and mole ratio plots.

In order to test experimentally collected data against these isotherms in determining complex stoichiometry, these expressions are commonly rearranged so that the dependent variable (y, fraction of substrate bound) may be plotted in relation to the dependent variable (x, often ligand concentration). Assuming 1:1 binding, the general binding isotherm $y=dx/(f+ex)$ produces a parabolic plot, with y initially increasing rapidly and gradually plateauing. This equation may be derived into several forms. Log-log plots, or Hill plots, are often used in studies of enzyme inhibition and cooperative binding.[22]

$$\log\frac{y}{1-y} = \log x - \log\frac{d}{f} \tag{10}$$

For this simple system, a linear plot with a slope of 1 should be obtained. Any significant deviation from this behavior demonstrates a more complicated binding system. Three other nonlogrithmic expressions of the binding isotherm exist, and these rearrangements are more commonly used than logarithmic methods. The double-reciprocal plot produces a straight line when *1/y* is plotted against *1/x*.

$$\frac{1}{y} = \frac{f}{d} \cdot \frac{1}{x} + \frac{e}{d} \tag{11}$$

Other names for this rearrangement include the Lineweaver-Burk plot (enzyme studies) and the Benesi-Hildebrand plot (spectroscopic studies).[23,24] The y-reciprocal plot is shown below:

$$\frac{x}{y} = \frac{e}{d} \cdot x + \frac{f}{d} \tag{12}$$

The x-reciprocal plot, sometimes called a Scatchard plot or an Eadie plot in enzyme kinetics, is likely the most popular form of the binding isotherm.[21]

$$\frac{y}{x} = -\frac{e}{f} \cdot y + \frac{d}{f} \tag{13}$$

Note that this last form actually contains the dependent variable on both axes. It has been discussed that in order to accurately determine that substrate-ligand interaction exists, data must be collected in the highly curved region of the parabolic binding isotherm (low ligand concentration). This method ensures that the concentration of complex is a function of ligand concentration.[25]

The complex stoichiometry may be determined by applying the experimentally collected data to the derived isotherms for the various binding ratios and performing graphical analysis and curve fitting.[21] What makes this particular method of measuring

stoichiometric coefficients so useful is that once the proper binding isotherm has been isolated, this same equation may be used to determine the association constant itself. For example, in a 1:1 binding scenario *K* may be determined from the log-log plot as the negative inverse-log of the *y-intercept*. Similarly, for the double-reciprocal, y-reciprocal, and x-reciprocal plots *K* equals *y-int./slope*, *slope/y-int.*, and *–slope* respectively. For more complex systems involving multiple equilibria, unique equations must be derived that take into account all binding and partitioning present. Such examples are described in later chapters of this dissertation.

Methods of Analysis. As discussed previously, a system signal or property that is directly related to the formation of the substrate-ligand complex is often used in determining association constants. A wide range of techniques is available for measuring this dependent variable, and these methods may be categorized in a number of fashions. Homogeneous systems are those in which the equilibrium exists within a single phase (such as with spectroscopy or potentiometry), while heterogeneous systems involve two phases (e.g. solubility and liquid-liquid extraction methods). Methods may also be described as equilibrium or non-equilibrium processes, where measuring the equilibrium either may or may not perturb the system. Finally, direct techniques measure a signal that is the direct result of substrate-ligand binding while competitive methods measure the change in response of an indicator substrate that competes for ligand binding with the analyte of interest. Methods may have their own advantages or disadvantages depending on the binding system being investigated.[21]

Absorbance spectroscopy is one the most widely used techniques for determining binding constants. For measuring association constants with this technique, a change in the

absorption spectrum that occurs upon complexation is measured. Typically, the wavelength of detection is within the ultraviolet, visible, or infrared regions and is chosen so that the molar absorptivities of the free substrate and complex are significantly different. Recently, this technique was used to measure the affinity of several porphyrins and derivatives to jacalin, a naturally produced lectin that binds specifically to tumor-associated disaccharides.[26] Porphyrins are currently being investigated as photosensitizers in photodynamic therapy to treat malignant tumors. Also, the binding constants for several aminoglycosides to RNA of the HIV-1 virus was studied using UV absorption spectroscopy.[27] Numerous other methods are capable of measuring the formation of the substrate-ligand complex including fluorometry, refractometry, measuring reaction kinetics, electrical methods (e.g. conductometry and polarography), and solubility measurements. However, these techniques have similar data treatments as mentioned above, and are not used in the studies presented in this dissertation.

Nuclear magnetic resonance (NMR) spectroscopy has been widely used for the measurement of substrate-ligand association constants in recent years. Here, the chemical shift of a nucleus (usually a proton or carbon) on either the substrate or ligand is used as the binding dependent variable. Upon complexation, the magnetic environment around the nucleus is altered by the electronic structure of the associated molecule, resulting in a change in the chemical shift of the target nucleus. This shift may then be related to the fraction of substrate bound to the ligand.[28] Recent studies include association measurements of crown ethers with tropylium cations,[29] calixarenes with various ligands,[30] nitrophenol with ternary complex amide oligomers,[31] and cyclodextrin complexes.[32] In addition to providing information regarding the strength of substrate-ligand association, NMR may also reveal

valuable structural information about the orientation of these molecules in the complex. Numerous studies have been performed that examine the binding of various ligands to proteins and viruses receptor sites. These include the association of carbohydrates to wheat germ agglutinin (WGA) protein[33] and neuraminic acid to influenza viruses.[34] A more comprehensive review of modern NMR studies on the screening of ligands bound to protein receptors may be found in the literature.[35]

Chromatography may also be used as a method to study substrate ligand interactions in either the mobile or stationary phases. Much of the progress made towards the study of binding by chromatography has been motivated by optimizing chromatographic separations that utilize specific intermolecular interactions (i.e. affinity and complexation chromatography).[36] Two general methods are commonly used for the measurement of binding constants by chromatography: zonal and frontal analysis. In zonal analysis, a small injection of substrate is applied to a column that contains an equilibrated mixture of mobile phase, ligand, and stationary phase. The ligand may be dissolved in either phase or immobilized on the stationary phase. The retention time of the solute is tracked as the concentration of ligand present in either phase changes with each run, and these data are related back to the appropriate binding isotherms.[37] In frontal analysis, the ligand of interest is immobilized on the stationary phase and the substrate solution is continuously applied to the column. As the stationary phase binding sites become saturated, the concentration of eluted substrate increases until it matches the composition of the injected solution. Often times a competing ligand is added to the stationary phase to further control the affinity process or determine two association interactions simultaneously.[38]

Methods that utilize gas-liquid chromatography (GLC) focus on the association of solutes with nonvolatile ligands dissolved in the liquid stationary phase. This often requires separate column preparations of different ligand concentrations, and as a result the method is quite time consuming and not commonly performed. An early example by Gil-Av and Herling of such a study involves silver ion-olefin complexes.[39] Many modern studies use GLC as a technique for monitoring the complexation of volatile aroma compounds to various protecting or sequestering ligands.[40] Headspace analysis or solid phase microextraction may also be coupled with gas chromatography to study the partitioning of volatile solutes to either a ligand dissolved in solution or immobilized on a solid support.[41,42] Liquid chromatographic methods allow the determination of association constants between a substrate and a ligand either dissolved in the mobile phase or immobilized to the stationary phase. The ability to study substrate-ligand associations in common aqueous or polar solvents is an attractive feature of LC binding studies. Recently, LC has been used significantly to characterize biospecific interactions between proteins, enzymes, and other biomolecules,[43] as well as to optimize chiral interactions for the separation of enantiomers.[44]

With the recent development of commercial capillary electrophoresis (CE) instrumentation, considerable interest has arisen in using CE as a technique for measuring association constants.[45] Its inherently low sample requirements and solvent consumption are advantageous over traditional LC methods, particularly for studies involving biomolecules that are available only in small quantities. As with chromatographic techniques, several methods are available for the determination of binding constants with CE. The most popular of these techniques is affinity capillary electrophoresis (ACE) and fontal analysis by CE. Estimation of substrate-ligand affinity by ACE is performed by dissolving the ligand in the

bulk running buffer and injecting a small plug of substrate onto the capillary. If these two molecules have unique electrophoretic mobilities, the substrate-ligand complex will have a migration velocity that is different than the free substrate. The change in the experimentally measured mobility of the substrate with increasing dissolved ligand concentration may then be related to the fraction of bound substrate.[45] This method has been widely used for measuring association constants between various solutes and cyclodextrins.[46,47] Frontal analysis is often performed when there is insufficient amounts of ligand available to dissolve in the entire run buffer at the appropriate concentrations. Here, the substrate and ligand are mixed, allowed to equilibrate prior to analysis, and then injected together as a large plug into the capillary. In a properly designed experiment, the unbound substrate will migrate away from the sample plug containing the ligand and substrate-ligand complex, resulting in a plateau to the side of the initial sample peak. The height of this plateau is directly proportional to the concentration of free substrate, and a Scatchard plot may be used to estimate the association constant.[48] This method is often used to probe biomolecular interactions and drug-protein systems.[49,50] Several other methods exist for calculating binding constants by CE, including the partial-filling technique, vacancy peak method, and the Hummel-Dreyer method, however these variations are not as widely used.[51]

Calculating Interaction Parameters. In addition to calculating association constants, many of the previously mentioned techniques provide valuable information that may be used for elucidating the types of noncovalent interactions that are responsible for substrate-ligand binding. In all cases, the experimentally obtained data (whether it is an absorbance, retention factor, chemical shift, or electrophoretic mobility) are related to the formation of the complex and therefore to the interaction properties of the substrate and the

ligand. If the affinities to a ligand are measured for a series of solutes whose interaction capabilities are known, then it is possible to determine the contribution of each of these interactions to ligand binding. Most of the methods applied for this purpose utilize a linear solvation energy relationship (LSER) that correlates the dependent variable with the solvation and interaction parameters of the substrate and the ligand. One of the first LSER models was developed by Kamlet and Taft in the late 1970s to measure the solvation effects in physiochemical processes.[52]

$$\log k' = c + mV_1 + s\pi^* + b\beta + a\alpha \qquad (14)$$

Here, *k'* is the retention factor obtained chromatographically, *c* is a constant, V_1 is the intrinsic volume of the solute, π^* denotes solute polarizability, and α and β are the hydrogen bond acidity and basicity of the solute respectively. Multiple linear regression may then be used to solve for the corresponding interaction parameters of the solvent or ligand (*m*, dispersion; *s*, polarizability; *b*, hydrogen acidity; *a*, hydrogen basicity).

This model was later revised by Abraham in the early 1990s to include the effect of n- and π-electron interactions on solvation by adding an rR_2 term to the equation. The mV_1 term was also replaced by the gas-hexadecane partition coefficient, $l\log L_{16}$, however the same interaction parameter is measured. A large quantity of more thermodynamically valid solute descriptors were also published in this work.[53]

$$\log k = c + rR_2 + s\pi_2^H + a\alpha_2^H + b\beta_2^H + l\log L^{16} \qquad (15)$$

Since this time, such LSERs have been used to determine the interaction parameters for a wide variety of systems including micellar solutions and chromatographic systems.[54,55]

Concluding Remarks. Through the methods described here, the magnitude of substrate-ligand interaction may be calculated for a variety of chemical systems. In addition,

the contributions from different noncovalent interactions to complexation may also be derived. These data provide insights into the thermodynamic nature of the chemical system under investigation. However, it is important to note that the binding constants estimated with these methods are dependent on the conditions in which they were measured (e.g. solvent, temperature, matrix species, etc.). Small changes in solvent polarity, ionic strength, and competing substrate concentration can significantly influence the magnitude of substrate-ligand interaction(s). Therefore, it is important to choose a method that is compatible with the target analytes (i.e. solubility and detection method) and design the experiment to mimic the environment of the target system.

References

(1) Hirschfelder, J.O.; Curtiss, C.F.; Bird, R.B. In *Molecular Theory of Gases and Liquids*, Wiley: New York, 1954, Ch. 1.

(2) Hirschfelder, J.O.; Curtiss, C.F.; Bird, R.B. In *Molecular Theory of Gases and Liquids*, Wiley: New York, 1954, pp. 968-983.

(3) Pimentel, G.C.; McClellan, A.L.; In *The Hydrogen Bond*, Freeman: San Francisco, 1960, p 195.

(4) Morokuma, K. *Acc. Chem. Res.*, **1977**, *10*, 294.

(5) Jencks, W.P. In *Catalysis in Chemistry and Enzymology*, McGraw-Hill: New York, 1969, Ch. 5-9.

(6) Tanford, C. In *The Hydrophobic Effect*, 2nd ed., Wiley-Interscience: New York, 1980.

(7) Abraham, M.H. *J. Am. Chem. Soc.* **1982**, *104,* 2085.

(8) Armstrong, D.W. *J. Liq. Chromatogr.* **1980**, *3*, 895-900.

(9) McIntire, G.L. *CRC Anal. Chem.* **1990**, *21*, 257-278.

(10) Fendler, J.H. *Chem. Rev.* **1987**, *87*, 877-899.

(11) Tascioglu, S. *Tetrahedron* **1996**, *52 (34),* 11113-11152.

(12) Breslow, R.; Dong, S.D. *Chem.Rev.* **1998**, *98*, 1997-2011.

(13) Tabushi, I.; Kuroda,Y. In *Cyclodextrins and Cyclophanes as Enzyme Models*; Eley, D.D., Pines, H., Weisz, P.B., Eds.; Advances in Catalysis 32; Academic Press: NewYork, 1983.

(14) Armstrong, D.W.; Nome, F. *Anal.Chem.* **1981**, *53*, 1662-1666.

(15) Armspach, D.; Gattuso, G.; Koniger, R.; Stoddart, J.F. *Cyclodextrins*, In *Bioorganic Chemistry: Carbohydrates*, Oxford University Press: New York, 1999.

(16) Uekama, K.; Irie, T. *Pharmaceutical Use of Cyclodextrins in Various Drug Formulations,* In *Comprehensive Supramolecular Chemistry, Vol 3*, Elsevier: New York, 1996.

(17) Job, A. *Annales de Chimie* **1928**, *9*, 113.

(18) Meyer, A.S.; Ayres, G.H. *J. Am. Chem. Soc.* **1957**, *79*, 49.

(19) Chriswell, C.D.; Schilt, A.A. *Anal. Chem.* **1975**, *47*, 1623.

(20) Vosburgh, W.C.; Cooper, G.R. *J. Am. Chem. Soc.* **1941**, *63*, 437.

(21) Conners, K.A. *Binding Constants*, Wiley: New York, 1987.

(22) Saroff, H.A.; Minton, A.P. *Science* **1972**, *175,* 1253.

(23) Lineweaver, H; Burk, D. *J. Am. Chem. Soc.* **1934**, *56*, 658.

(24) Benesi, H.; Hildebrand, J.H. *J. Am. Chem. Soc.* **1949**, *71*, 2703.

(25) Person, W.B. *J. Am. Chem. Soc.* **1965**, *87*, 167.

(26) Komath, S.S.; Bhanu, K.; Maiya, B.G.; Swamy, M.J. *Biosci. Rep.* **2000**, *20*, 255-276.

(27) Sullivan, J.M.; Goodisman, J.; Dabrowiak, J,C. *Bioorg. Med. Chem. Lett*. **2002**, *12*, 615-618.

(28) Becker, E.D. *High Resolution NMR,* Academic: New York, 1969, Ch. 10.

(29) Lamsa, M.; Pursiainen, J.; Rissanen, K.; Huuskonen, J. *Acta Chem. Scand*. **1998**, *52*, 563-570.

(30) Yanagihara, R.; Tominaga, M.; Aoyama, Y. *J. Org. Chem* **1994**, *59*, 6865-6867.

(31) Bisson, A.P.; Hunter, C.A.; Morales, J.C.; Young, K. *Chem. Eur. J*. **1998**, *4*, 845-851.

(32) Dodziuk, H.; Ejchart, A.; Lukin, O.; Vysotsky, M.O. *J. Org. Chem*. **1999**, *64*, 1503-1507.

(33) Klein, J.; Meinecke, R.; Mayer, M.; Meyer, B. *J. Am. Chem. Soc.* **1999**, *121*, 5336-5337.

(34) Hanson, J.E.; Sauter, N.K.; Skehel, J.J.; Wiley, D.C. *Virology* **1992**, *189*, 525-533.

(35) Meyer, B.; Peters, T. *Angew. Chem. Int. Ed.* **2003**, *42*, 864-890.

(36) Andrews, P.; Kitchen, B.J.; Winzor, D.J. *Biochem. J.* **1973**, *135*, 897.

(37) Dunn, B.M.; Chaiken, J.M. *Proc. Natl. Acad. Sci. USA* **1974**, *71*, 2382.

(38) Winzor, D.J. *J. Biochem. Biophys. Methods* **2001**, *49*, 99.

(39) Gil-Av, E.; Herling, J. *J. Phys. Chem.* **1962**, *66*, 1208.

(40) Guichard, E. *Food Rev. Int.* **2002**, *18*, 49-70.

(41) Guichard, E.; Langourieux, S. *Food Chem*. **2000**, *71*, 301–308.

(42) Yuan, H.; Pawliszyn, J. *Anal. Chem.* **2001**, *73*, 4410-4416.

(43) Hage, D.S. *J. Chromatogr. B* **2002**, *768*, 300.

(44) Ringo, M.C.; Evans, C.E. *Anal. Chem.* **1998**, *70*, 315A-321A.

(45) Rundlett, K.L.; Armstrong, D.W. *J. Chromatogr. A* **1996**, *721*, 173-186.

(46) Li, J.; Waldron, K.C. *Electrophoresis* **1999**, *20*, 171-179.

(47) Larsen, K.K.; Endo, T.; Ueda, H.; Zimmerman, W. *Carbohydr. Res.* **1998**, *309*, 153-159.

(48) Shibukawa, A.; Kuroda, Y.; Nakagawa, T. *Pharm. Biomed. Anal.* **1999**, *18*, 1047-1055.

(49) Fung, Y.S.; Sun, D.X.; Yeung, C.Y. *Electrophoresis*, **2000**, *21*, 403-410.

(50) Koruda, Y.; Shibukawa, A.; Nakagawa, T. *Anal. Biochem.* **1999**, *268*, 9-14.

(51) Rundlett, K.L.; Armstrong, D.W. *Electrophoresis* **2001**, *22*, 1419-1427.

(52) Kamlet, M.J.; Taft, R.W. *J. Am. Chem. Soc*. **1976**, *98*, 377.

(53) Abraham, M.H. *Chem. Soc. Rev.* **1993**, *22*, 73-83.

(54) Quina, F.H.; Alonso, E.O.; Farah, J.P.S. *J. Phys. Chem.* **1995**, *99*, 11708-11714.

(55) Trone, M.; Khaledi, M. *J. Chromatogr. A* **2000**, *886*, 245-257.

CHAPTER 2. ESTIMATION OF ASSOCIATION CONSTANTS BETWEEN ORAL MALODOR COMPONENTS AND VARIOUS NATIVE AND DERIVATIZED CYCLODEXTRINS

Published in *Analytica Chimica Acta*

Andrew W. Lantz, Michael A. Rodriguez, Sean M. Wetterer, Daniel W. Armstrong*

Department of Chemistry, Iowa State University, Ames, IA USA 50011

GlaxoSmithKline, Parsippany, NJ USA 07054

Abstract

The association constants of 33 oral malodorous compounds and odor precursors (9 organic acids, 7 amine-containing bases, 11 organic neutral and aromatic compounds, and 6 amino acids) with native and derivatized cyclodextrins were measured using one or more of a variety of techniques including affinity capillary electrophoresis, nuclear magnetic resonance titrations, and head-space gas chromatography. With the exception of formic acid and urea, which had binding constants that were too small to measure, all analytes showed significant binding to at least one of the cyclodextrins studied. In most cases, the native cyclodextrins exhibited the most stable complexes with these analytes. However, with cationic analytes under acidic conditions, the negatively charged sulfated and carboxymethyl cyclodextrins had higher association constants. The six amino acid precursor molecules only bound significantly with the sulfated cyclodextrins. In addition, several analyte-cyclodextrin combinations were observed to form insoluble complexes, indicating that these cyclodextrins are particularly effective at extracting these compounds from aqueous solution.

Introduction

Halitosis is a common condition that afflicts many individuals, and is generally described as an unpleasant or offensive odor emanating from the oral cavity. While halitosis may be emitted from the gastrointestinal tract or the upper respiratory system, the mouth is the source of 90% of breath odors [1]. Halitosis may be classified as either physiological halitosis, where odors arise from the natural putrefaction of food particulates by saliva or bacteria present in the mouth, or pathologic halitosis that results from a disease or condition such as periodontal disease. Numerous chemicals are responsible for oral malodor and include the volatile sulfur compounds (VSC), as well as a wide variety of short chain fatty acids, polyamines, alcohols, and aromatic compounds [1,2].

The treatment and control of malodorous compounds in the mouth is an important focus of the oral hygiene industry. In 2004, breath freshening products had an estimated retail value of $2.4 billion, a significant portion of the $7.2 billion oral care industry [3]. Clearly, there is a significant demand for consumer products that effectively extract and eliminate the compounds and precursor compounds responsible for halitosis. Several methods are available for controlling oral malodorous compounds. Antimicrobial agents may be used to limit the growth of bacteria that produce malodorous compounds in the oral cavity [2]. However, while this technique effectively limits the production of new malodorous compounds, it should be coupled with another method to extract or suppress pre-existing odor molecules. The introduction of a pleasant smelling fragrance may mask the perception of odor molecules, although the odor causing chemicals will still be present. Another option is to chemically change (oxidize, reduce, decompose, etc.) the malodorous compounds [4,5], however in this case the toxicity and chemical strength of both the reactive

agents and the product may be an issue. Finally, the use of a complexation agent that effectively binds to the malodorous compounds is an attractive approach. By complexing the odor chemicals with a ligand, it is possible to limit their ability to reach the vapor phase and therefore reduce their odor. This method could also allow the extraction of odor compounds from the aqueous environment of the mouth altogether.

A promising complexation agent for this purpose is cyclodextrin (CD). Cyclodextrins are cyclic oligosaccharides consisting of glucopyranose units connected by α-(1,4) linkages (Figure 1) [6].

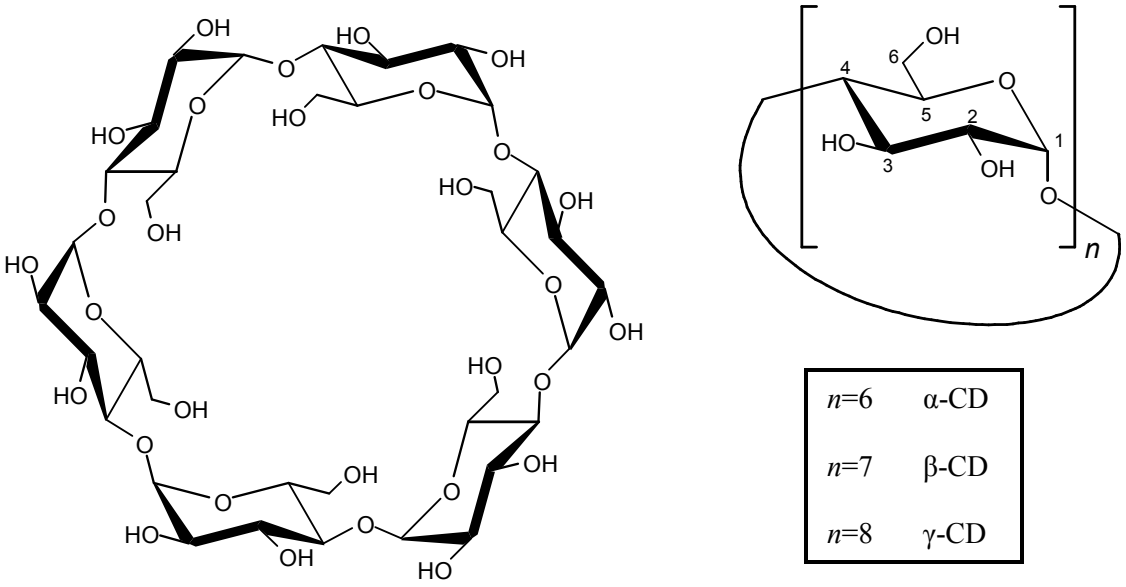

Figure 1. The structure of native cyclodextrin.

Three forms of cyclodextrin commonly exist: α-, β-, and γ-cyclodextrin, composing 6, 7, and 8 units respectively. These macromolecules are produced by the natural breakdown of starch by the cyclodextrin glucosyl transferase (CGTase) enzyme found in *Bacillus macerans* bacteria. Their basic shape is toroidal, with a hydrophilic exterior and more lipophilic interior. This characteristic allows a wide variety of hydrophobic compounds to form

inclusion complexes within the cyclodextrin cavity in aqueous environments. Additional solute-cyclodextrin interactions may occur through hydrogen bonding, electrostatic, and dipole-dipole effects. Cyclodextrins may also be derivatized by adding substituents to the hydroxyl groups on the cavity rim in order to change their aqueous solubility, binding properties, and charge [7]. In addition to being relatively inexpensive, native cyclodextrins have negligible toxicity and their bioadaptability has been well documented [8], which make them ideal additives in oral care products. Cyclodextrins have already been used extensively for the protection and solubilization of drugs [8,9] and the extraction of unwanted tastes and odors in foodstuffs [10].

In this study, we measure the binding constants of 33 malodorous compounds and odor precursors commonly present in the mouth with a variety of cyclodextrins and cyclodextrin derivatives. These compounds include 9 organic acids, 7 amine-containing bases, 11 organic neutral and aromatic compounds, and 6 amino acid precursor molecules. Binding constants, also called association constants, between an analyte and a ligand may be obtained by measuring an instrumental system response with varying ligand concentration and constant analyte concentration. This response can then be related back to the concentrations of the free and bound analyte, and therefore to the extent of binding [11-13]. Here, binding constants were determined using a combination of affinity capillary electrophoresis (ACE), nuclear magnetic resonance (NMR) titrations, and a recently developed head-space GC method [13]. To our knowledge, no previous study has examined the binding of such a wide variety of oral malodorous compounds to cyclodextrins.

Materials and Methods

Materials. Native α-, β-, and γ-cyclodextrin were obtained from Advanced Separation Technologies (Whippany, NJ, USA). Sulfated-α-cyclodextrin (S-α-CD), sulfated-β-cyclodextrin (S-β-CD), and hydroxypropyl-β-cyclodextrin (HP-β-CD) were all purchased from Aldrich Chemical Company (Milwaukee, WI, USA), with degrees of substitution (DS) of approximately 1.8, 1.5, and 0.8 respectively. Carboxymethyl-β-cyclodextrin (CM-β-CD, DS~0.8) was obtained from Cerestar USA Inc. (Hammond, IN, USA). Arginine, lysine, ornithine, tryptophan, citrulline, and cysteine were all received from Sigma (St. Louis, MO, USA). Pyridine was bought from Fisher Scientific (St. Louis, MO, USA), and all other analyte studied were purchased from Aldrich. Sodium phosphate, sodium hydroxide, and 85% phosphoric acid were all purchased from Fisher Scientific. D_2O (99.9%) used in the NMR titrations were also obtained from Aldrich.

Methods. Due to the wide variety of analytes examined in this study, multiple techniques were needed to determine all the analyte-cyclodextrin association constants (see Table 1). Analytes that had significant water solubility and contained a UV-absorbing chromophore were analyzed by ACE. These compounds include pyridine, 3-methyl pyridine, phenyl acetate, m-cresol, phenol, indole, and skatole. Indirect detection was not used for non-UV absorbing analytes, as the addition of a UV absorbing buffer additive may compete with the analytes for cyclodextrin binding. Because ACE requires that the ligand and analyte have differing electrophoretic mobilities, the binding constants of neutral analytes with neutral cyclodextrins could not be performed. These analyte-cyclodextrin combinations were examined by H^1-NMR titrations. In addition, the cyclodextrin binding of the six amino acid precursors were also determined with ACE. ACE was performed at

various acidic and basic conditions (pH 4.5, 8.5, and 9.4) in most cases. NMR titrations were used to measure the binding of the remaining analytes, such as the organic acids and non-aromatic amines, with cyclodextrin.

ACE was performed on a Beckman PACE 2100 (Fullerton, CA, USA) with a 50 μm I.D. x 358 μm O.D. capillary, 37 cm in length (30 cm to the detector). The amino acid analytes, however, were analyzed using a Beckman PACE MDQ (capillary 30 cm, 20 cm to detector) because of its higher detection sensitivity. Capillaries were purchased from Polymicro Technologies (Phoenix, AZ, USA). Detection was accomplished by UV absorbance at 214 nm. Data analysis was done with Beckman System Gold software. Buffer solutions of 10 mM sodium phosphate buffer and cyclodextrin were made from deionized filtered water, and brought to the desired pH with 85% phosphoric acid and 1 M sodium hydroxide. Cyclodextrin concentrations of 0, 20, 40, 60, and 80 mg/mL were used for each series of runs. Samples were prepared by diluting the analyte samples directly into the phosphate buffer to a concentration of 2 mM. Mesityl oxide was used as an electroosmotic flow marker. All buffers and sample solutions were sonicated for 5 min prior to their first run. The capillary was conditioned before its first use by rinsing with 1 M sodium hydroxide for 3 min, water for 3 min, sodium hydroxide for 1 min, and finally water for 1 min. Between each run, 1 min sodium hydroxide, water, and run buffer rinses were performed. Samples were injected for 2 s via hydrodynamic pressure of 0.5 psi. All separations were performed in the normal polarity mode with an applied voltage of 15 kV. The capillary was maintained at a temperature of 25°C.

The association constant determinations for formate, acetate, propionate, butyrate, isobutyrate, valerate, isovalerate, lactate, succinate, ammonia, methylamine, cadaverine,

putrescine, diphenylamine, urea, dodecanol, and tetradecanol were performed by H^1-NMR titrations using a 7.05T Varian VXR-300 Spectrometer. All analytes were diluted to 2 mM or lower using 99.9% D_2O as a solvent. Cyclodextrin was added to the series of NMR samples resulting in concentrations of 0, 20, 40, 60, and 80 mg/mL. However, due to its limited solubility native β-cyclodextrin concentrations of 0, 5, 10, 15 and 20 mg/mL were used with an analyte concentration of 1 mM. All H^1 spectra were analyzed using MestReC software (MestreLab Research, A Coruńa, Spain), and the D_2O (δ 4.80) signal was used as an internal reference.

The complexation of the volatile sulfur compounds (VSCs) with cyclodextrin was measured *via* a previously described method using head-space gas chromatography mass spectrometry (HS-GCMS) [13]. Briefly, the analyte vapor pressure above an aqueous phase is monitored by HS-GCMS with the addition of cyclodextrin to the solution. Upon analyte-cyclodextrin binding, the analyte vapor pressure decreases. By applying the known Henry's constants for these analytes, one is able to quantitate the number of moles of analyte in the gas phase, aqueous phase, and bound to cyclodextrin. From these data, the association constant between the aqueous analyte and cyclodextrin may be obtained. The full method description can be found in the literature [13].

Theory

As stated earlier, binding constants of an analyte with a ligand are commonly measured by tracking an instrumental response while varying the ligand concentration with constant analyte concentration. For example, in ACE the electrophoretic mobility of an analyte plug through a buffer filled capillary is measured as the cyclodextrin concentration in the buffer is increased (Figure 2, left). Similarly, in an NMR titration it is the chemical shift

of the analyte that is measured with increasing concentration of cyclodextrin in solution (Figure 2, right) [11,14].

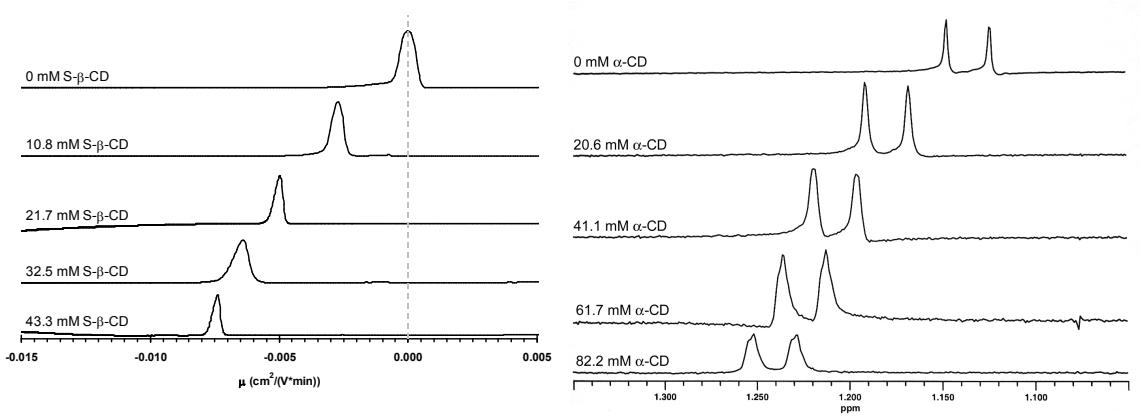

Figure 2. *Left*: Change in the electrophoretic mobility of indole with increasing S-β-CD concentration using ACE at pH 4.5. *Right*: Change in the chemical shift of the β-hydrogens of isobutyric acid with increasing α-CD concentration.

The change in these values upon analyte complexation with the ligand can be related to the relative amounts of free and bound analyte. All binding isotherms exhibited appropriate hyperbolic curvature, indicating the formation of a 1:1 complex. Generally, the 1:1 binding of an analyte with a ligand can be described by the following equilibria:

$$S + L \overset{K}{\longleftrightarrow} S \cdot L \qquad K = \frac{[S \cdot L]}{[S][L]} \tag{1}$$

where S is the analyte, L is the ligand, $S{\cdot}L$ is the complex, and K is the association constant. The change in instrumental response can be applied to Eqn. 1 to obtain

$$K[L] = \left(\frac{r_f - r_i}{r_i - r_c} \right) \tag{2}$$

where r_f and r_c are the instrumental responses of the free and fully complexed analyte and r_i is the analyte response at a certain concentration of ligand. Isolating the experimentally measured response, $(r_i\text{-}r_f)$, the following equation is produced:

$$(r_i - r_f) = \frac{(r_c - r_f)K[L]}{1 + K[L]} \quad (3)$$

Because of the inherent difficulty of measuring r_c, it is advantageous to rearrange Eqn. 3 to a form in which the r_c value is not needed to calculate K. One such form is a Scatchard-type (also known as the x-reciprocal) equation

$$\frac{(r_i - r_f)}{[L]} = -K(r_i - r_f) + K(r_c - r_f) \quad (4)$$

Plotting $(r_i-r_f)/[L]$ vs. (r_i-r_f) results in a line with a negative slope of K (Figure 3A and 3B) [11,14]. An approximation was made that the equilibrium concentration of the ligand is equal to the initial ligand concentration. This assumption is reasonable when the concentration of the ligand is significantly greater than the concentration of the analyte. These equations were used to determine the association constants reported in this research using ACE and NMR titrations. Data was plotted in Excel, and fit to a line using the least squares method. The error in the reported binding constants were based on the uncertainties of the slopes measured by the software. Briefly, these uncertainties were calculated using propagation of error analysis methods. The formula $\delta m^2 = \Sigma(\delta m/\delta y_i)^2 \delta y_i^2$ was used to calculate the uncertainties, where δm is the uncertainty in the slope and δy are the uncertainties in the actual y values. The operation $(\delta m/\delta y_i)^2$ is performed on the equation used to determine the slope based on the experimental values. The error values reported here represent 67% confidence limit. HS-CGMS calculations and methods are described in detail in a previous publication [13]. An example plot of the change in the apparent gas-liquid partition coefficient for methanethiol with HP-b-CD concentration is shown in Figure 3C.

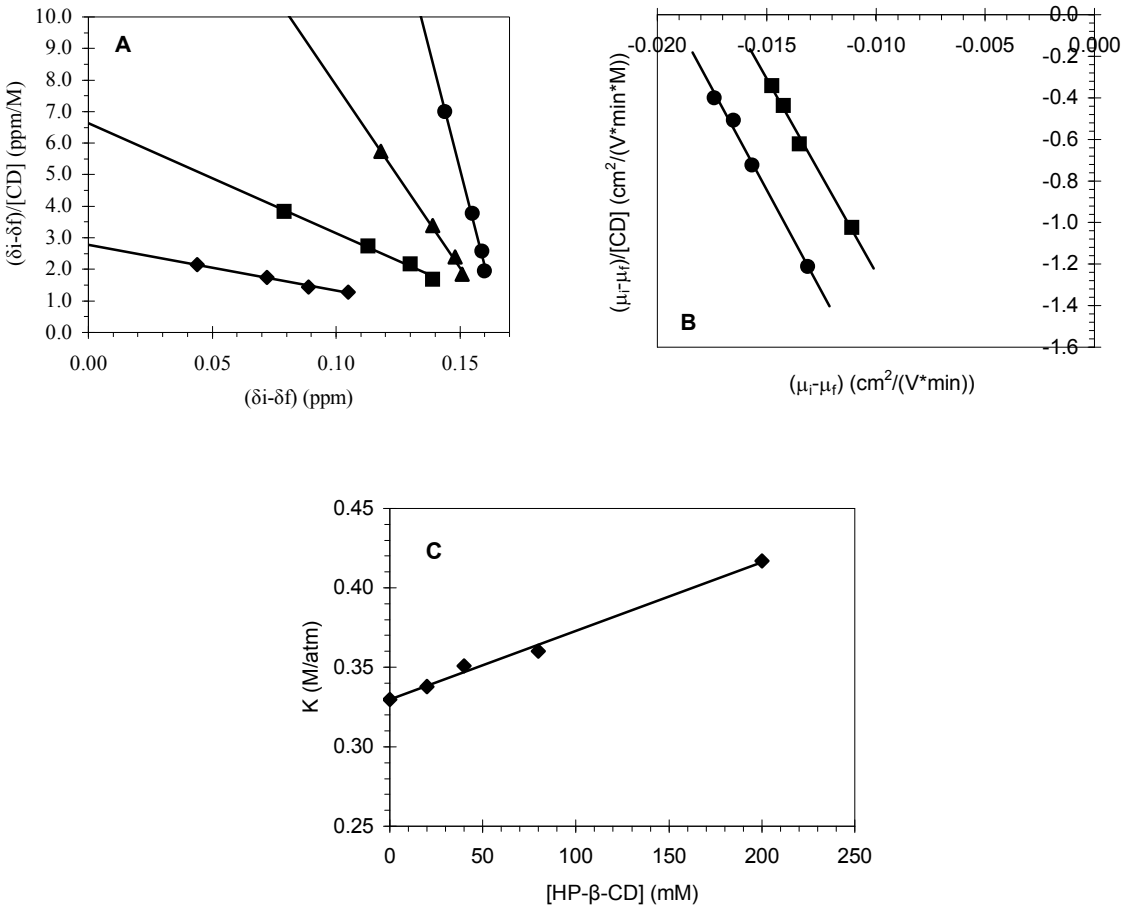

Figure 3. A: x-Reciprocal plots (Eqn. 4) for α-CD at 22ºC with: (■) propionic acid, (▲) butyric acid, (♦) isobutyric acid, and (●) valeric acid. **B:** x-Reciprocal plots (Eqn. 4) for S-β-CD at 22ºC and pH 4.5 with: (■) pyridine, and (●) 3-methyl pyridine. **C:** Plot of the apparent partition coefficient vs. HP-β-CD concentration for methanethiol (see reference 13).

Results and Discussion

Table 1 lists the association constants of all the malodorous compounds with various cyclodextrins examined in this study. Dashes in the table indicate that the extent of binding was too low to be measured by the performed method, while empty spaces designate analyte-cyclodextrin combinations or methods that were not performed. Several analytes were observed to form insoluble complexes with certain cyclodextrins when sufficient concentrations of each were present in solution. These combinations are starred in Table 1,

and include complexes involving propionate, butyrate, isobutyrate, isovalerate, diphenylamine, hydrogen sulfide, methanethiol, dimethyl sulfide, m-cresol, indole, dodecanol, and tetradecanol. Coincidentally, a majority of these compounds are also the most offensive and strongest odor producing components of halitosis. The formation of these insoluble complexes demonstrates that some cyclodextrins are particularly effective at extracting these compounds from the aqueous phase, and therefore may be promising agents for the suppression of the analytes' volatility/odor. Precipitation of the analyte-cyclodextrin complex invalidates our association constant equation (Eqn. 4) by introducing new equilibria and reducing the actual aqueous concentration of analyte and cyclodextrin in solution. Therefore, for ACE and NMR studies analyte and cyclodextrin concentrations low enough to prevent the formation of the precipitates were used for all association constant determinations. However, some HS-GCMS experiments could not be performed without producing the insoluble complex, and as a result the association constants for the VSCs that precipitated are misleadingly high [13].

The acidic analytes examined generally bound most strongly to native α- and β-CD. Small compounds, such as acetic and propionic acid, only formed stable complexes with α-CD, while formic acid did not bind appreciably to any of the cyclodextrins in this study. Native β-CD, by and large, exhibited higher association constants than the β-CD derivatives with these analytes. This effect is likely due to electrostatic repulsion by the negatively charged analytes and cyclodextrin derivatives. Steric hindrance produced by the substituents attached to the cyclodextrin's rim may also play a role in inhibiting analyte binding [15,16].

Table 1. Aqueous binding constants[a] for various malodorous compounds with cyclodextrins at 22ºC.[b,c,d]

Acids	α-CD	β-CD	γ-CD	HP-β-CD	S-α-CD	S-β-CD	CM-β-CD	Method
Formic Acid	--	--	--	--		--	--	NMR Titration
Acetic Acid	31.4 ± 2.9	--	--	--		--	--	NMR Titration
Propionic Acid	34.4 ± 4.0*	--	--	--		--	--	NMR Titration
Butyric Acid	117.1 ± 5.9*	120.5 ± 57.2	3.3 ± 1.1	45.5 ± 4.1		2.1 ± 1.5	1.5 ± 0.8	NMR Titration
Isobutyric Acid	14.5 ± 0.8	201.5 ± 2.4*	--	33.2 ± 3.9		2.5 ± 1.4	3.1 ± 1.0	NMR Titration
Valeric Acid	313.5 ± 21.0	190.6 ± 12.6	13.6 ± 1.0	100.1 ± 5.9		13.2 ± 2.7	29.7 ± 2.7	NMR Titration
Isovaleric Acid	35.4 ± 1.2	203.8 ± 54.2*	21.6 ± 3.4	144.8 ± 16.0		5.2 ± 1.2	19.0 ± 1.7	NMR Titration
Lactic Acid	23.2 ± 5.3	--	--	--		3.6 ± 1.1	327.3 ± 31.3	NMR Titration
Succinic Acid	64.3 ± 1.1	21.6 ± 16.3	6.6 ± 3.2	4.3 ± 1.3		44.4 ± 7.6	270.4 ± 25.1	NMR Titration

Bases	α-CD	β-CD	γ-CD	HP-β-CD	S-α-CD	S-β-CD	CM-β-CD	Method
Ammonia	--	--	--	--		19.6 ± 4.8	2.3 ± 0.8	NMR Titration
Methylamine	--	--	--	--		13.7 ± 3.8	4.8 ± 1.0	NMR Titration
Cadaverine	28.9 ± 2.8	42.1 ± 2.1	11.2 ± 2.3	16.1 ± 0.2		96.0 ± 9.8	13.9 ± 1.1	NMR Titration
Putrescine	32.2 ± 5.1	39.3 ± 11.6	15.2 ± 1.7	6.4 ± 0.9		82.0 ± 6.7	8.8 ± 1.2	NMR Titration
Pyridine	12.7 ± 1.6	54.3 ± 1.8	19.1 ± 1.8	25.9 ± 3.1		3.5 ± 0.1	9.5 ± 0.4	NMR Titration
					75.6 ± 15.8	189.7 ± 10.6	38.8 ± 3.6	ACE pH 4.5
3-Methyl Pyridine	18.6 ± 1.3	32.0 ± 2.6	29.1 ± 3.2	28.0 ± 3.2		3.9 ± 0.3	10.2 ± 0.7	NMR Titration
					66.1 ± 9.1	264.1 ± 11.7	27.5 ± 1.4	ACE pH 4.5
Diphenylamine	24.1 ± 2.4	216.7 ± 12.2*	57.4 ± 7.7*	248.6 ± 16.1		33.2 ± 2.9	82.7 ± 5.8	NMR Titration

Neutrals	α-CD	β-CD	γ-CD	HP-β-CD	S-α-CD	S-β-CD	CM-β-CD	Method
Hydrogen Sulfide	20.73 ± 0.76*	7.38 ± 2.20	4.98 ± 0.83	6.29 ± 0.48	1.12 ± 0.14	0.88 ± 0.07	1.65 ± 0.38	HS-GCMS[e]
Methanethiol	23.05 ± 0.30*	1.70 ± 0.47	2.53 ± 0.10	1.90 ± 0.12	0.75 ± 0.13	0.18 ± 0.06	0.35 ± 0.07	HS-GCMS[e]
Dimethyl Sulfide	24.84 ± 2.19*	17.27 ± 3.19*	8.31 ± 0.45*	4.34 ± 0.12	0.37 ± 0.06	0.43 ± 0.03	1.57 ± 0.15	HS-GCMS[e]
Urea	--	--	--	--		--	--	NMR Titration
Phenyl Acetate	6.9 ± 1.2	106.5 ± 5.3	14.0 ± 1.6	111.8 ± 7.2				NMR Titration
					6.4 ± 0.6	2.6 ± 0.2	65.6 ± 5.4	ACE pH 8.5
					4.6 ± 1.8	6.0 ± 3.6	24.3 ± 8.3	ACE pH 4.5
m-Cresol	48.4 ± 2.3	124.7 ± 27.5	97.4 ± 8.2*	130.5 ± 13.9				NMR Titration
					3.2 ± 2.4	5.9 ± 0.8	35.1 ± 2.8	ACE pH 8.5
					4.3 ± 3.7	17.9 ± 8.8	6.5 ± 2.4	ACE pH 4.5
Phenol	18.6 ± 1.3	59.6 ± 5.8	2.6 ± 1.4	52.4 ± 5.6				NMR Titration
					4.4 ± 2.5	7.5 ± 0.7	29.4 ± 0.9	ACE pH 8.5
					10.7 ± 4.0	16.8 ± 9.1	23.1 ± 2.1	ACE pH 4.5
Indole	5.5 ± 0.8	166.4 ± 0.4	20.8 ± 2.0*	136.8 ± 8.5				NMR Titration
					15.1 ± 1.4	15.6 ± 2.9	71.1 ± 1.2	ACE pH 8.5
					24.0 ± 19.8	45.4 ± 21.1	70.7 ± 17.9	ACE pH 4.5
Skatole	4.1 ± 0.6	162.3 ± 1.3	29.7 ± 2.9	171.8 ± 6.9				NMR Titration
					15.5 ± 6.1	18.9 ± 1.0	72.1 ± 4.3	ACE pH 8.5
					13.9 ± 5.2	22.6 ± 4.0	86.8 ± 24.6	ACE pH 4.5
Dodecanol	142.0 ± 20.3*	100.7 ± 33.6*	80.5 ± 14.6*	157.6 ± 14.3		8.1 ± 2.2	25.3 ± 3.0	NMR Titration
Tetradecanol	425.5 ± 71.1*	200.3 ± 25.0*	85.6 ± 7.8*	104.4 ± 6.9		14.5 ± 3.3	35.6 ± 2.5	NMR Titration

Amino Acids	α-CD	β-CD	γ-CD	HP-β-CD	S-α-CD	S-β-CD	CM-β-CD	Method
Arginine	--	--	--	--	121.6 ± 18.9	324.9 ± 93.8	--	ACE pH 9.4
	--	--	--	--	87.3 ± 18.3	151.8 ± 10.6	--	ACE pH 4.5
Lysine	--	--	--	--	167.2 ± 12.4	142.0 ± 13.7	--	ACE pH 9.4
	--	--	--	--	103.3 ± 11.9	173.6 ± 3.1	--	ACE pH 4.5
Ornithine	--	--	--	--	139.1 ± 4.8	192.2 ± 22.0	--	ACE pH 9.4
	--	--	--	--	181.8 ± 14.8	368.8 ± 24.6	--	ACE pH 4.5
Tryptophan	--	--	--	--	--	--	--	ACE pH 9.4
	--	--	--	--	--	49.5 ± 4.9	--	ACE pH 4.5
Citrulline	--	--	--	--	231.8 ± 24.7	1068.6 ± 57.8	--	ACE pH 9.4
	--	--	--	--	222.1 ± 97.8	231.8 ± 24.7	--	ACE pH 4.5
Cysteine	--	--	--	--	40.3 ± 17.8	719.5 ± 37.8	--	ACE pH 9.4
	--	--	--	--	--	250.5 ± 49.1	--	ACE pH 4.5

α-CD: α-cyclodextrin, **β-CD:** β-cyclodextrin, **γ-CD:** γ-cyclodextrin, **HP-β-CD:** Hydroxypropyl-β-cyclodextrin, **S-α-CD:** Sulfated-α-cyclodextrin, **S-β-CD:** Sulfated-β-cyclodextrin, **CM-β-CD:** Carboxymethyl-β-cyclodextrin

[a] All binding constants in units of M^{-1}.
[b] For method details, see Experimental section.
[c] Spaces indicate binding constant determination not performed.
[d] Dashes indicate extent of binding too low to be measured
[e] Data from reference [13]
* Precipitation of CD-Analyte complex

However lactic and succinic acid, both dicarboxylic acids, exhibited significantly higher binding to CM-β-CD and slightly higher binding to S-β-CD than to the native β-CD. The two carboxylate groups on these analytes may interact strongly with the numerous hydrogen-bond donor and acceptor sites provided by the carboxylate and sulfate groups attached to these cyclodextrins. Association constants of the acidic analytes to native γ-CD were lower than with α- and β-CD, likely due to the larger size of the γ-CD cavity. As a result, analyte inclusion into the CD will be a poorer fit, and therefore weaker [15,16]. Generally, less polar analytes formed more stable associations with the cyclodextrins, supporting the formation of a hydrophobic inclusion complex within the cyclodextrin cavity.

In most cases, similar trends seen for the acidic analytes were observed for the basic compounds examined, where the largest association constants were achieved with native α- and β-CD. Under acidic conditions in which the analyte was positively charged, however, higher association constants were exhibited with the negatively charged cyclodextrins (S-β-CD and CM-β-CD) apparently due to strong electrostatic interactions. Pyridine and 3-methyl pyridine formed notably more stable complexes in acidic conditions (pH 4.5 ACE) with these anionic cyclodextrins than under near neutral conditions (D_2O NMR). The highly hydrophobic diphenylamine bound most strongly to native β- and γ-CD.

The VSCs, a major source of odor in halitosis, formed the most stable complexes with the native cyclodextrins and HP-β-CD, while sulfated- and carboxymethyl-CDs had significantly less binding behavior with these analytes. The neutral aromatic compounds exhibited the highest association constants with native β-CD, and generally exhibited weaker binding to α- and γ-CD. This data may be due to the tightness-of-fit of the analyte within the cyclodextrin cavity, where matching of the size and shape of the host cavity and guest

molecule increases the stability of the complex [15,16]. Of the long chain alcohols, tetradecanol complexed with α-CD more strongly than β-CD, again possibly due to a tightness-of-fit within the cyclodextrin cavity. HP-β-CD associated with these analytes to a similar extent as native β-CD, whereas the CM- and S-CDs generally had lower binding constants.

Apparently, only the sulfated derivatives of α- and β-CD showed significant binding behavior to the six amino acids examined in this study with ACE. While amino acids themselves have no odor, these molecules are known to be precursors to a number of malodorous compounds [1,2]. All other cyclodextrins had association constants too low to be measured by ACE. Arginine, lysine, and ornithine, which all contain basic side chains, bound strongly to both the anionic S-α-CD and S-β-CD. The zwitterionic amino acids citrulline and cysteine also complexed to these two cyclodextrins, however tryptophan only weakly interacted S-β-CD. In addition, pH appeared to have an effect on the magnitude of analyte-cyclodextrin complexation. Arginine, citrulline, and cysteine produced more stable cyclodextrin complexes in slightly basic conditions as compared to acidic solutions, while lysine interacted more strongly at low pH (see Table 1).

It should be noted, however, that the environment in the mouth may be significantly more complex than the aqueous systems in which these binding constant experiments were performed. Saliva contains a wide array of salts, proteins, and bacteria which may compete with the analyte for cyclodextrin binding. Furthermore, the matrix of the cyclodextrin oral hygiene product may also alter the magnitude of analyte binding. Development of a specific product application of cyclodextrins would eventually require binding determinations be performed under more accurate conditions.

Cyclodextrins and their derivatives bind to a wide variety of malodorous compounds and precursor molecules commonly found in the mouth. In this study, less polar analytes generally exhibited higher association constants with these cyclodextrins, likely due to the formation of a hydrophobic inclusion complex. Size and shape matching between the analyte and the cyclodextrin cavity also increased the stability of the analyte-cyclodextrin complex. Electrostatics may play a large role in binding through either attractive or repulsive interactions. The formation of several analyte-cyclodextrin precipitates further indicates that some cyclodextrins can effectively remove these analytes from solution. Ideally, a mixture of α-, β-, and sulfated-CDs would suppress the volatility of the greatest number of analytes from this study. While the toxicities of many derivatized cyclodextrins are not yet fully evaluated [8], the known negligible toxicity and low cost of native cyclodextrins currently make them attractive complexation agents for malodorous compounds in oral hygiene products.

References

[1] M. Sanz, S. Roldán, D. Herrera, J. Contemp. Dent. Pract., 2 (2001) 1.

[2] W.J. Loesche, C. Kazor, Periodontology 2000, 28 (2002) 256.

[3] Packaged Facts, The U.S. Market for Oral Care Products, New York, 2004.

[4] N.F. Schmidt, W.J. Tarbet, Oral. Surg. Oral. Med. Oral. Pathol. Oral. Radiol. Endod., 45 (1978) 560.

[5] R.B. Greenstein, S. Goldberg, S. Marku-Cohen, N. Sterer, M. Rosenberg, J. Periodontol., 68 (1997) 1176.

[6] Hinze, Sep. Purif. Methods, 10 (1981) 159.

[7] D. Armspach, G. Gattuso, R. Königer, J.F. Stoddart, Cyclodextrins (Bioorganic Chemistry: Carbohydrates), Oxford Univ. Press, New York, 1999.

[8] K. Uekama, T. Irie, Pharmaceutical Use of Cyclodextrins in Various Drug Formulations (Comprehensive Supramolecular Chemistry, vol. 3: Cyclodextrins), Elsevier, New York, 1996.

[9] T. Nagai, H. Ueda, Aspects of Drug Formulation with Cyclodextrins (Comprehensive Supramolecular Chemistry, vol. 3: Cyclodextrins), Elsevier, New York, 1996.

[10] H. Hashimoto, Cyclodextrins in Foods, Cosmetics, and Toiletries (Comprehensive Supramolecular Chemistry, vol. 3: Cyclodextrins), Elsevier, New York, 1996.

[11] K.L. Rundlett, D.W. Armstrong, J. Chromatogr. A, 721 (1996) 173.

[12] K.L. Rundlett, D.W. Armstrong, Electrophoresis, 18 (1997) 2194.

[13] A.W. Lantz, S.M. Wetterer, D.W. Armstrong, Anal. Bioanal. Chem., (2005) In press.

[14] L. Fielding, Tetrahedron, 56 (2000) 6151.

[15] W. Saenger, T. Steiner, Acta. Cryst., A54 (1998) 798.

[16] Y. Liu, C. You, J. Phys. Org. Chem., 14 (2001) 11.

CHAPTER 3. USE OF THE THREE-PHASE MODEL AND HEAD-SPACE ANALYSIS FOR THE FACILE DETERMINATION OF ALL PARTITION/ASSOCIATION CONSTANTS FOR HIGHLY VOLATILE SOLUTE-CYCLODEXTRIN-WATER SYSTEMS

Published in *Analytical and Bioanalytical Chemistry*

Andrew W. Lantz, Sean M. Wetterer, Daniel W. Armstrong*

Department of Chemistry, Iowa State University, Ames, IA USA 50011

GlaxoSmithKline, Parsippany, NJ USA 07054

Abstract

A versatile method for measuring the partition coefficients of volatile analytes with an aqueous pseudophase using headspace gas chromatography is reported. A "three-phase" model accounts for all equilibria present in the system, including the partitioning of the analyte in the gas and aqueous phases to the pseudophase. This method is applicable to a wide variety of volatile analytes and aqueous pseudophases, providing that sufficient pseudophase may be used to reduce the analyte partial pressure. Generally, the method offers good reproducibility and high sensitivity. The associations of five volatile analytes (hydrogen sulfide, methanethiol, dimethyl sulfide, dichloromethane, and ethyl ether) with various cyclodextrins were examined. All analytes were found to partition preferentially to the cyclodextrin pseudophase compared to the aqueous phase. In addition, several analyte-cyclodextrin combinations formed insoluble complexes in solution that enhanced the

extraction of the analyte from the gas and aqueous phases. Derivatization of the cyclodextrins generally decreased the extent of analyte-cyclodextrin interaction.

Introduction

Studies involving the association of dissolved analytes with aqueous pseudophases (e.g., micelles, cyclodextrins, polymers, proteins, etc.) are an important area of research. It has been well established that the presence of a pseudophase in water can significantly increase the solubility of lipophilic compounds [1]. Various industrial processes, such as tertiary oil recovery and chlorinated solvent removal [2-4], implement surfactant micelles to increase the efficiency of aqueous solutions to extract highly hydrophobic compounds. In addition, pseudophases have been utilized to increase the solubility of organic reaction reagents, and facilitate and control reaction rates and products in aqueous environments [5]. The binding of volatile aroma compounds by aqueous pseudophases is of particular interest in the food and hygiene industry to either protect and control the release of desirable odor molecules or suppress unwanted aromas [6-9]. Drug formulations can use pseudophases as excipients to enhance the solubility of lipophilic molecules [10, 11]. Such cases in which the pseudophase may be ingested require that the additive have very low toxicity and is easily metabolized by the body. The cyclodextrin family of molecules contributes one of the more important and useful pseudophase forming entities. Cyclodextrins (CD) are cyclic oligosaccharides composed of 6-8 glucopyranose units connected by α-(1,4) linkages, and are the product of the natural breakdown of starch by a family of bacteria known as *Bacillus macerans* [12]. Cyclodextrins conform to a toroidal shape whose outer surface is hydrophilic and inner cavity is more hydrophobic. This characteristic allows a wide variety of hydrophobic molecules to form inclusion complexes within the cyclodextrin cavity in

aqueous environments. The bio-adaptability of native cyclodextrins has been well documented [10]. In fact, cyclodextrins have been studied extensively for the solubilization, protection, and bio-delivery of drug molecules in the pharmaceutical industry [10, 11]. Cyclodextrins may also be chemically modified by adding substituents to the hydroxyl groups on the cavity rim in order to change their aqueous solubility, charge, and analyte binding properties [12].

The partition coefficient of a volatile analyte between the gas and aqueous phase is traditionally defined by Henry's Law and the Henry's constant (K_H):

$$K_H = C_S / P_S \tag{1}$$

where C_S is the analyte concentration in the aqueous phase and P_S is the partial pressure of the analyte in the gas phase. It should be noted that in most environmental studies the Henry's constant is commonly defined inversely ($K_H = P_S / C_S$). However, throughout this paper, K_H will be defined according to Eqn. 1. These constants are related to the physical and thermodynamic properties of the analyte and the solvent, and have been well established in the literature for a wide variety of compounds. Additional solute equilibria present in either phase will result in changes to the analyte concentrations in both phases, as the Henry's constant ratio is maintained. For example, the introduction of a solubilizing pseudophase to the aqueous environment will result in a decrease in the analyte's aqueous concentration and partial pressure. Numerous studies have been performed that examine the ability of various pseudophases to solubilize volatile lipophilic compounds[3-6, 9, 13, 14]. However, these papers often attribute the increased aqueous solubility of the volatile analyte simply to a change in its gas-aqueous phase partition coefficient [6], or they determine only the binding constant of the analyte between the aqueous phase and the hydrophobic

pseudophase [3-5, 14]. These studies neglect to report the contribution of the analyte partitioning directly between the gas phase and the aqueous pseudophase. Since the solubilization of the hydrophobic analyte is highly dependent on the presence of this hydrophobic pseudophase, it is likely that this equilibrium plays a role. A "three-phase" model, which takes into account all three of the equilibria present in the system, has been used previously to describe micellar and cyclodextrin liquid chromatography [15, 16], as well as for the determination of octanol-water-pseudophase partition coefficients [17, 18]. Versions of this method have been adapted for and widely used in capillary electrophoresis [19-21]. This model can easily be applied to any number of similar systems in which an analyte is partitioning between two phases and a pseudophase (Figure 1). Although this work focuses on the use of cyclodextrins, the pseudophase can consist of any molecule or colloid entity (e.g., micelle, polymer, protein, cyclodextrin, nanoparticle, etc.)

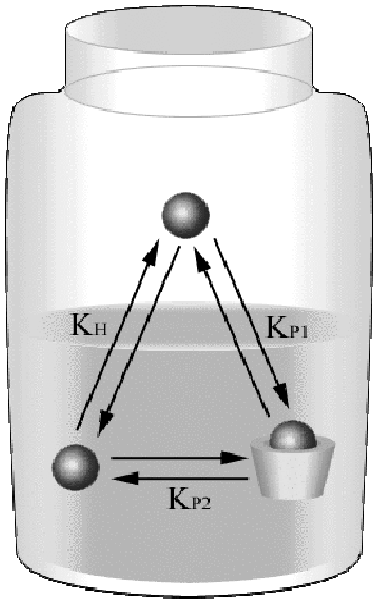

Figure 1. A representation of the "three-phase" model in which the analyte (sphere) is in dynamic equilibrium between the gas phase, the aqueous phase, and bound to aqueous cyclodextrin (torus). K_H is the Henry's constant, and K_{P1} and K_{P2} are the respective partition coefficients.

Here we report a simple headspace gas chromatography (HSGC) method utilizing the "three-phase" model for the estimation of all partition coefficients of volatile analytes between the aqueous phase, gas phase, and dissolved cyclodextrin. Gas chromatography has already been recognized as a valuable and reliable method for investigating solute-solvent interactions [22, 23]. In this study we obtain the analyte partition coefficients by monitoring the depression of the analyte partial pressure upon addition of cyclodextrin to the aqueous phase. Several sulfur-containing volatiles (hydrogen sulfide, methanethiol, and dimethyl sulfide) were investigated to determine their degree of partitioning to cyclodextrin pseudophases. These compounds are well known to be the primary components of halitosis [24, 25], and also are the products of numerous bio-industries/technologies including waste-treatment and compost plants [26]. To demonstrate the versatility of the method dichloromethane and ethyl ether, two commonly used organic solvents, also were studied. The Henry's constant data for these compounds are shown in Table 1 as reported in previous literature [27-31].

Table 1. List of Henry's Constants at 22 °C for Compounds of Interest as Reported in the Literature

Volatile Compound	Henry's Constant (K_H, M/atm)	Reference
Hydrogen Sulfide	0.10	24
Methanethiol	0.33	25
Dimethyl Sulfide	0.56	26
Dichloromethane	0.40	27
Ethyl Ether	1.2	28

Materials and Methods

Reagents and Materials. Hydrogen sulfide, methanethiol, and dimethyl sulfide were all purchased from Aldrich Chemical Company (Milwaukee, WI). Dichloromethane and ethyl ether were bought from Fisher Scientific (St. Louis, MO). Of the cyclodextrins

studied, the native α-, β-, and γ-cyclodextrin were obtained from Advanced Separation Technologies (Whippany, NJ). Sulfated-α-cyclodextrin (S-α-CD), sulfated-β-cyclodextrin (S-β-CD), hydroxypropyl-β-cyclodextrin (HP-β-CD), and hydroxypropyl-γ-cyclodextrin (HP-γ-CD) were all acquired from Aldrich, with degrees of substitution (DS) of approximately 1.8, 1.5, 0.8, and 0.6 respectively. Dimethyl-β-cyclodextrin (DM-β-CD, DS~1.9) was purchased from Sigma (St. Louis, MO), while carboxymethyl-β-cyclodextrin (CM-β-CD, DS~0.8) was received from Cerestar USA Inc. (Hammond, IN).

The 6-mL and 2-mL headspace vials and their crimp-caps with gas tight Teflon® septa, lecture bottle regulator (part Z148512-1EA) and fittings, and gas tight syringes with Teflon® tipped plungers (250 μL) were all obtained from Supelco (Bellefonte, PA). Fused-silica capillary tubing (250 μm i.d.) was purchased from Polymicro Technologies (Phoenix, AZ), and the calibrated 1-mL transfer syringes were from Becton Dickinson & Co. (Franklin Lakes, NJ).

Apparatus. Analysis was carried out on a Varian CP-3800 GC equipped with a Saturn 2000 MS/MS detector (Walnut Creek, CA). Helium carrier gas was utilized with a flow rate of 1.0 mL/min through a 30m x 0.25mm i.d. Varian CP-Sil 8CB capillary column. The GC conditions were as follows: split ratio, 100:1; injector temperature, 250 ˚C; oven temperature, 75 ˚C. MS was operated in electron impact ionization scan mode between m/z 20 and 100. All headspace sample vials were equilibrated and analyzed at 22 °C.

Standard Curves. The standards of the gaseous analytes (hydrogen sulfide and methanethiol) were prepared by flushing a Teflon® sealed 6-mL vial with pure analyte gas through a fused-silica capillary for several hours. The gas lecture bottles were connected to the capillary through a pressure regulator and custom fittings. A second capillary was used

as a gas outlet for the vial. The gaseous standards were prepared by injecting increasing volumes (45, 90, 180, 360, and 720 µL) of pure analyte gas from the 6-mL vial into a series of sealed argon flushed 2-mL vials using gas tight syringes. These volumes were then converted to partial pressures *via* the ideal gas law. The analytes obtained in the liquid phase (dimethyl sulfide, dichloromethane, and ethyl ether) were initially diluted to known concentrations (0.179, 0.143, 0.301 M respectively) in a sealed vial with deionized, filtered water. Again, increasing volumes (0.1, 0.2, 0.4, 0.8, and 1.0 mL) of the diluted analyte solution were injected respectively into a series of sealed argon flushed 2-mL vials. Enough deionized, filtered water was then injected into the vials until all had a total volume of 1.0 mL. To reduce pressurization, a capillary was pierced through the Teflon® septa of each vial during the injections, and quickly removed after the injection to limit the escape of analyte vapor. These vials were shaken every 10 min. and allowed to equilibrate for at least 2 hrs. Using the known Henry's constants for each of these analytes, the analyte concentration in each vial could be converted to a partial pressure above the solution. All of the standards were analyzed by headspace-GC/MS using a gas tight syringe with a large injection volume (100 µL) to limit the error from injection. The analytes were detected by EI-MS using the following m/z values: hydrogen sulfide, 34; methanethiol, 47; dimethyl sulfide, 62; dichloromethane, 49; ethyl ether, 74. The peak areas of these m/z were used to produce linear standard curves relating analyte partial pressure to detector response for each of the analytes of interest.

Sample Preparation. Initially, stock solutions of each analyte were prepared in sealed vials. Gaseous analytes were bubbled through deionized, filtered water in sealed vials for at least 1 hr in order to infuse the solution. Liquid analytes were diluted in the same

manner as described in the "Standard Curves" section. A series of ten 2-mL vials were prepared for each analyte: one empty vial, and nine vials each containing one of the nine cyclodextrins studied. Each cyclodextrin vial contained the correct amount of cyclodextrin needed to produce a 200 mM solution when dissolved in 1 mL of water. The native α-, β-, and γ-cyclodextrins however were prepared to be 125, 15, and 150 mM respectively due to their limited solubilities. Once sealed, these vials were all injected with exactly 1 mL of the same analyte stock solution using a calibrated 1 mL syringe. This method dictates that each vial must contain the same amount of analyte, and also limits the analyte's ability to transfer from the aqueous phase to the vapor phase before it is transferred to the 2-mL vial. The vials were then vortexed and sonicated to dissolve the cyclodextrin, and then allowed to equilibrate for at least 2 hrs with intermittent shaking. Headspace-GC/MS was then performed as described in the "Standard Curves" section. The analyte partial pressure in each vial was calculated using the previously prepared standard curves. This entire procedure was repeated three times with each analyte-cyclodextrin combination in order to determine method reproducibility and error measurements.

Results and Discussion

Calculations. A system involving an analyte that partitions between the gas phase, aqueous phase, and cyclodextrin pseudophase (Figure 1) includes the following three equilibria:

$$S_{(g)} \xleftrightarrow{K_H} S_{(aq)} \qquad K_H = \frac{C_S^W}{P_S} \tag{2}$$

$$S_{(g)} \xleftrightarrow{K_{P1}} S_{(CD)} \qquad K_{P1} = \frac{C_S^{CD}}{P_S} \tag{3}$$

$$S_{(aq)} \xleftrightarrow{K_{P2}} S_{(CD)} \qquad K_{P2} = \frac{C_S^{CD}}{C_S^W} \tag{4}$$

where S is the volatile analyte in the gas and aqueous phases and bound to the cyclodextrin pseudophase, $C_S{}^W$ and $C_S{}^{CD}$ are the concentrations of the analyte in the water and cyclodextrin pseudophase, P_S is the partial pressure of the analyte, K_H is the Henry's constant, and K_{P1} and K_{P2} are the respective partition coefficients. Based on these equilibria, a relationship between K_H, K_{P1}, and K_{P2} is found:

$$K_H = \frac{K_{P1}}{K_{P2}} \tag{5}$$

As a result of analyte-CD binding the partial pressure of the analyte, P_S, will decrease. This may occur directly *via* equation 3, or indirectly by means of equations 2 and 4. Simple mass balance equations can be developed to summarize the total number of moles of analyte present in each prepared sample vial:

$$n_S^{total} = n_S^G + n_S^W \qquad \text{Vials without aqueous cyclodextrin} \tag{6}$$

$$n_S^{total} = n_S^G + n_S^W + n_S^{CD} \qquad \text{Vials with aqueous cyclodextrin} \tag{7}$$

where $n_S{}^G$, $n_S{}^W$, and $n_S{}^{CD}$ are the number of moles of analyte in the gas and aqueous phases and the cyclodextrin pseudophase. In order to determine the number of moles of analyte in the gas and aqueous phases, headspace GC/MS measurements were performed, and the Henry's constant equation (Eqn. 2) was applied to translate the measured analyte partial pressure to the corresponding aqueous solution concentration. The ideal gas law and the solution volumes were then used to convert these data into the number of moles of analyte in each phase. This procedure was performed for vials with and without aqueous cyclodextrin present. Since our methodology dictates that each vial is injected with the same number of

moles of analyte (see Experimental section), the vials without cyclodextrin (Eqn. 6) were used to determine the total number of moles of analyte present in the vials containing cyclodextrin (Eqn. 7). Therefore, the following equation can be used to calculate the amount of analyte in the cyclodextrin pseudophase:

$$n_S^{CD} = n_S^{total} - n_S^G - n_S^W \tag{8}$$

The partition coefficients of the analyte between the gas phase and the pseudophase (Eqn. 3, K_{P1}) and the aqueous phase and pseudophase (Eqn. 4, K_{P2}) are defined as

$$K_{P1} = \left(n_S^{CD}/V_{CD}\right)/P_S \tag{9}$$

$$K_{P2} = \left(n_S^{CD}/V_{CD}\right)/\left(n_S^W/V_W\right) \tag{10}$$

where V_{CD} and V_W are the volumes of the cyclodextrin and water. The volume of the cyclodextrin pseudophase may be easily calculated multiplying the partial specific volume of cyclodextrin (α-CD, 0.6114 L/mol; β-CD, 0.7038 L/mol; γ-CD, 0.8012 L/mol) [32] by the number of moles of cyclodextrin present, n_{CD}. For this study, the partial specific volumes of the native cyclodextrins were used for all corresponding derivatized cyclodextrins. The experimentally obtained n_S and P_S values, along with the appropriate phase volumes, were applied to Eqns. 9 and 10 to obtain the partition coefficients shown in Table 2.

Alternatively, the association of a solute with a cyclodextrin can be given in terms of a binding constant. The 1:1 complexation of the aqueous analyte with cyclodextrin may be described by the equilibrium

$$S_{(aq)} + CD_{(aq)} \overset{K_2}{\longleftrightarrow} S \cdot CD_{(aq)} \qquad K_2 = \frac{[S \cdot CD]}{[S][CD]} \tag{11}$$

where K_2 is the equilibrium binding constant. Using Eqns. 11 and 4, the relationship between K_{P2} and K_2 is found to be

$$K_2 = K_{P2}\left(\frac{V_{CD}}{n_{CD}^{W}}\right) \tag{12}$$

where $n_{CD}{}^{W}$ is the number of moles of free cyclodextrin in the water

$$n_{CD}^{W} = n_{CD}^{total} - n_{S}^{CD} \tag{13}$$

The K_2 values calculated by this method are shown in Table 3 below.

Analyte Partitioning. The partition coefficient data in Table 2 provide useful information concerning the ability of cyclodextrin to solubilize and/or sequester these volatile analytes in aqueous solution. First, by comparing K_{P1} and K_H (both in units of M/atm) for each analyte, it is clear that the analyte partition coefficient between the gas phase and the cyclodextrin is much higher than the Henry's law constant in most cases. This trend indicates that these volatile compounds preferentially partition to the cyclodextrin pseudophase over the aqueous phase. It should be noted that this partitioning can only occur between cyclodextrins at the gas-liquid interface.

Table 2. Partition Coefficients of Volatile Analytes with Native and Derivatized Aqueous Cyclodextrins at 22ºC.

	Hydrogen Sulfide		Methanethiol		Dimethyl Sulfide		Dichloromethane		Ethyl Ether	
	K_{P1}	K_{P2}	K_{P1}	K_{P2}	K_{P1}	K_{P2}	K_{P1}	K_{P2}	K_{P1}	K_{P2}
α-CD	**2.27 ± 0.07***	**22.77 ± 0.69***	**11.95 ± 3.12***	**36.20 ± 9.46***	**10.00 ± 1.18***	**17.85 ± 2.12***	**10.14 ± 1.56***	**25.34 ± 3.89***	**7.45 ± 0.25***	**6.21 ± 0.21***
S-α-CD	0.17 ± 0.02	1.74 ± 2.11	0.37 ± 0.06	1.12 ± 0.18	0.32 ± 0.05	0.58 ± 0.10	2.18 ± 0.05	5.44 ± 0.13	2.17 ± 0.18	1.81 ± 0.15
β-CD	0.77 ± 0.17	7.65 ± 1.70	0.62 ± 0.13	1.88 ± 0.40	**4.81 ± 0.34***	**8.60 ± 0.61***	**4.38 ± 0.59***	**10.96 ± 1.47***	3.51 ± 0.81	2.92 ± 0.67
HP-β-CD	0.75 ± 0.05	7.48 ± 0.51	0.74 ± 0.04	2.23 ± 0.12	2.61 ± 0.06	4.67 ± 0.11	4.29 ± 0.80	10.73 ± 2.00	7.21 ± 1.23	6.01 ± 1.03
DM-β-CD	0.34 ± 0.01	3.38 ± 0.09	0.95 ± 0.10	2.87 ± 0.30	**10.40 ± 2.12***	**18.58 ± 3.91***	3.03 ± 0.29	7.59 ± 0.74	1.69 ± 0.22	1.41 ± 0.18
S-β-CD	0.12 ± 0.01	1.19 ± 0.10	0.08 ± 0.03	0.25 ± 0.08	0.33 ± 0.02	0.58 ± 0.04	0.40 ± 0.15	1.00 ± 0.37	1.71 ± 0.33	1.43 ± 0.27
CM-β-CD	0.22 ± 0.05	2.19 ± 0.47	0.15 ± 0.03	0.47 ± 0.09	1.09 ± 0.09	1.94 ± 0.16	1.09 ± 0.24	2.71 ± 0.60	1.93 ± 0.16	1.61 ± 0.13
γ-CD	0.53 ± 0.08	5.27 ± 0.77	0.78 ± 0.03	2.37 ± 0.08	**3.74 ± 0.15***	**6.68 ± 0.26***	**5.02 ± 0.41***	**12.56 ± 1.03***	**4.99 ± 0.37***	**4.16 ± 0.31***
HP-γ-CD	0.48 ± 0.03	4.82 ± 0.26	1.16 ± 0.08	3.53 ± 0.26	0.82 ± 0.05	1.46 ± 0.10	1.42 ± 0.43	3.56 ± 1.08	2.25 ± 0.82	1.88 ± 0.69

α-CD: α-cyclodextrin, **S-α-CD:** Sulfated-α-cyclodextrin, **β-CD:** β-cyclodextrin, **HP-β-CD:** Hydroxypropyl-β-cyclodextrin, **DM-β-CD:** Dimethyl-β-cyclodextrin, **S-β-CD:** Sulfated-β-cyclodextrin, **CM-β-CD:** Carboxymethyl-β-cyclodextrin, **γ-CD:** γ-cyclodextrin, **HP-γ-CD:** Hydroxypropyl-γ-cyclodextrin

K_{P1} is the partition coefficient of the analyte between the gas phase and bound to the cyclodextrin (units of M/atm)
K_{P2} is the partition coefficient of the analyte between the aqueous phase and bound to the cyclodextrin (unitless)
Standard deviations calculated with n=3
* Precipitation of CD-Analyte complex (Values for K_{P1} and K_{P2} are not accurate, see text)

Clearly, since all experiments were performed in an aqueous environment the ratio of K_{P1} and K_{P2} in Table 2 equals the K_H of the analyte (Eqn. 5), indicating that the results conform to the "three-phase" model. Interestingly, several analyte-cyclodextrin combinations produced an insoluble complex that resulted in a turbid solution. All five analytes precipitated with α-CD, while only dimethyl sulfide and dichloromethane precipitated with β-CD. Complexes between γ-CD and dimethyl sulfide, dichloromethane, and ethyl ether also fell out of solution. In addition, binding between dimethyl sulfide and DM-β-CD resulted in an insoluble complex. Numerous compounds are known to form insoluble inclusion complexes with cyclodextrin [33], however to our knowledge this is the first report of hydrogen sulfide, methanethiol, and dimethyl sulfide precipitating upon cyclodextrin complexation. Obviously precipitation produces a fourth phase that is not accounted for in our model, and therefore these results are not accurate. This fourth phase complicates the equilibria, and causes the values shown for K_{P1}, K_{P2}, and K_2 to be misleadingly high. Since our model assumes that the insoluble complex is still in the aqueous phase, in reality these partition coefficients and binding constants are lower than those reported in Tables 2 and 3. However, this phenomenon demonstrates that these cyclodextrins are particularly effective at extracting these compounds from both the gas and aqueous phases, and therefore may be promising agents for the suppression of the analytes' volatility/odor. In the few cases where precipitation occurred the data (in Tables 2 and 3) are given in bold and starred.

Derivatization of the cyclodextrin rim groups affected the magnitude of analyte cyclodextrin partitioning. The native cyclodextrins generally had a higher affinity than their derivatized forms for the analytes studied.

Table 3. Equilibrium Binding Constants (K_2) for Aqueous Analyte-Cyclodextrin Binding at 22ºC.

	Hydrogen Sulfide	Methanethiol	Dimethyl Sulfide	Dichloromethane	Ethyl Ether
α-CD	**20.73 ± 0.76***	**23.05 ± 0.30***	**24.84 ± 2.19***	**37.85 ± 9.61***	**23.03 ± 2.42***
S-α-CD	1.12 ± 0.14	0.75 ± 0.13	0.37 ± 0.06	4.72 ± 0.15	1.22 ± 0.11
β-CD	7.38 ± 2.20	1.70 ± 0.47	**17.27 ± 3.19***	**30.18 ± 13.40***	6.71 ± 3.88
HP-β-CD	6.29 ± 0.48	1.90 ± 0.12	4.34 ± 0.12	13.94 ± 3.38	5.57 ± 1.11
DM-β-CD	2.63 ± 0.08	2.74 ± 0.40	**23.55 ± 2.29***	7.44 ± 0.96	1.35 ± 0.22
S-β-CD	0.88 ± 0.07	0.18 ± 0.06	0.43 ± 0.03	0.78 ± 0.30	1.10 ± 0.23
CM-β-CD	1.65 ± 0.38	0.35 ± 0.07	1.57 ± 0.15	2.25 ± 0.57	1.62 ± 0.18
γ-CD	4.98 ± 0.83	2.53 ± 0.10	**8.31 ± 0.45***	**18.01 ± 1.99***	**12.16 ± 2.49***
HP-γ-CD	4.46 ± 0.27	3.86 ± 0.35	1.32 ± 0.10	3.95 ± 1.49	1.72 ± 0.69

α-CD: α-cyclodextrin, **S-α-CD:** Sulfated-α-cyclodextrin, **β-CD:** β-cyclodextrin, **HP-β-CD:** Hydroxypropyl-β-cyclodextrin, **DM-β-CD:** Dimethyl-β-cyclodextrin, **S-β-CD:** Sulfated-β-cyclodextrin, **CM-β-CD:** Carboxymethyl-β-cyclodextrin, **γ-CD:** γ-cyclodextrin, **HP-γ-CD:** Hydroxypropyl-γ-cyclodextrin

All equilibrium constants in units of M^{-1}.
Standard deviations calculated with n=3
* Precipitation of CD-Analyte complex (Values for K_2 are not accurate, see text)

Carboxymethyl- and sulfated-cyclodextrin varieties showed the greatest decrease in partition coefficients, whereas the hydroxypropyl-cyclodextrins produced data more similar to the native forms. However, with some analytes DM-CDs and HP-CDs achieved greater partitioning than their native forms. It is known that derivatizing cyclodextrins can distort their cavity shape or change the hydrophobicity of the rim, altering the cyclodextrin's ability to include guest molecules [34, 35]. Hydrophobic interactions are likely the primary driving force behind the partitioning of these lipophilic volatiles with cyclodextrin. The addition of a hydrophilic group to the cyclodextrin, such as a sulfate or carboxyl substituent, may limit analyte partitioning with the cyclodextrin by reducing the overall hydrophobicity of the cyclodextrin cavity [34]. Conversely, hydroxypropyl groups are more hydrophobic than the secondary hydroxy groups of native cyclodextrin, and therefore may promote the formation of hydrophobic inclusion complexes [34]. The substituents attached to the cyclodextrin rim likely do not produce significant steric hindrance with these small analytes.

Method Versatility and Reproducibility. This headspace-GC/MS method is quite versatile in that a wide variety of volatile analyte and pseudophase combinations may be utilized. The primary requirement is that a sufficient concentration of pseudophase be present in solution to lower the analyte partial pressure. This may require that a lower analyte concentration be used if the pseudophase has limited solubility or if the analyte has a high K_H value. Since an analyte with a higher K_H value will produce a lower partial pressure, the detection limit of the GC/MS for a compound is a controlling factor when using this approach for evaluating partition/binding behavior. In cases involving a micellar pseudophase, it is important to note that the pseudophase concentrations in the above calculations will need to be adjusted to reflect the critical micelle concentration (CMC) [15].

As seen in Tables 2 and 3, method reproducibility is reasonable with standard deviations mostly within 10-15% (n=3). Partition coefficients and association constants with native β-CD, however, had larger standard deviations due to the limited solubility of the cyclodextrin (~17 mM). As a result, the measured change in analyte partial pressure was significantly smaller than with the other cyclodextrins examined. The accuracy of the calculated partition coefficients and association constants is dependent on several factors. First, allowing sufficient time to achieve analyte equilibrium between the gas and aqueous phases and the pseudophase prior to HSGC analysis is imperative for accurate and reliable measurements. If this is not accomplished, the Henry's constant values used throughout the calculations are not valid and run-to-run reproducibility will be low. Equilibration for 2 hrs is ample time for the partitioning of these volatiles, and shaking or stirring the well-sealed vials will accelerate the process [27-31]. The low standard deviations in our data and the lack of change in the values of the coefficient with greater equilibration time also indicate

that equilibrium was reached. Secondly, the linearity of the standard curves is important since the experimentally measured analyte partial pressures are used in the calculations. For this study, the R^2 values of the analyte standard curves are as follows: hydrogen sulfide, 0.9896; methanethiol, 0.9815; dimethyl sulfide, 0.9882; dichloromethane, 0.9802; ethyl ether, 0.9831. In addition, the accuracy of the binding constants is based on the Henry's constant value used in the calculations. Therefore, it is necessary to choose a Henry's constant value that is well established in the literature or measured independently. Also, changes in room temperature will also have an effect on the validity of the results, as K_H values vary with temperature. Generally, at low temperatures Henry's constants for these analytes decrease with increasing temperature [27, 29, 30]. Finally, this study assumes that all analyte-cyclodextrin complexes are 1:1, which is not necessarily always valid. Studies have reported that other stoichiometries exist for cyclodextrin complexes [32]. Often more than one cyclodextrin may bind to a single analyte molecule, or in the case of small analytes multiple guest molecules may simultaneously include in a single cyclodextrin cavity [32, 36]. If 1:1 complexation occurs, a linear relationship between the apparent partition coefficient between the aqueous and gas phases (K_{app}) and cyclodextrin concentration should exist [18, 37]. Figure 2 shows the linearity of K_{app} of methanethiol with increasing concentration of HP-β-CD in solution (R^2=0.9925), and indicates that 1:1 complexes form within the range of analyte and cyclodextrin concentrations used in this study. However, it is well known that with an excessively high concentration of analyte, multiple analyte molecules may complex with a single cyclodextrin [32, 36].

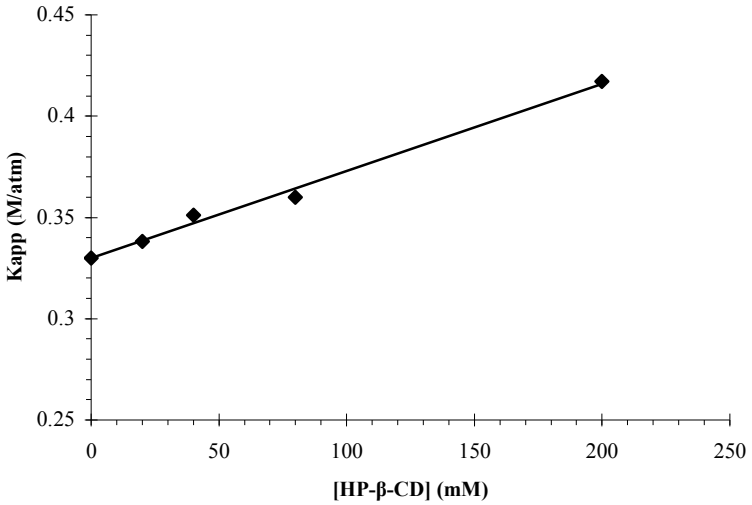

Figure 2. Linearity of methanethiol K_{app} with increasing concentration of HP-β-CD (R^2=0.9925).

Conclusions

Here we have demonstrated a simple versatile method for determining the partition coefficients of volatile analytes with an aqueous pseudophase. The "three-phase" model takes into account all equilibria present in the system, including partitioning of the analyte from the gas and aqueous phases to the pseudophase. The method offers good reproducibility, provided that sufficient pseudophase is used to depress the analyte partial pressure. The partition coefficients of five volatile analytes with various cyclodextrins were measured with this technique. Overall, analyte-cyclodextrin partitioning was low, however several analyte-cyclodextrin combinations produced insoluble complexes. These precipitates enhanced the extraction of the analyte from the solution and the headspace. In addition, the data suggests that native cyclodextrins achieve the highest partition coefficients with these compounds, as adding substituents to the rim of the cyclodextrin cavity generally decreased

partitioning. These results are particularly useful for understanding the ability of cyclodextrins to solubilize and extract volatile compounds for the vapor and aqueous phases.

References

1. Christian SD, Scamehorn JF (eds) (1995) Solubilization in Surfactant Aggregates. In *Surfactant Science Series Vol 55.* Marcel Dekker, New York.
2. Miller CA, Qutubuddin S (1986) Enhanced Oil Recovery Using Microemulsions. In *Interfacial Phenomenon in Nonaqueous Media*. Elicke HF, Prafitt G. (eds) Marcel Dekker, New York.
3. Vane LM, Giroux EL (2000) J. Chem. Eng. Data 45:38-47.
4. Kashiyama N, Boving TB (2004) Environ. Sci. Technol. 38(16):4439-4444.
5. Winters LJ, Grunwald EJ (1965) Am. Chem. Soc. 87(20):4608-4611.
6. Kant A, Linforth RST, Hort J, Taylor AJ (2004) J. Agric. Food Chem. 52:2028-2035.
7. Goubet I, Dahout C, Sémon E, Guichard E, Le Quéré JL, Voilley A (2001) J. Agric. Food Chem. 49:5916-5922.
8. Reineccius TA, Reineccius GA, Peppard TL (2005) J. Agric. Food Chem. 53(2):388-392.
9. Qu Q, Tucker E, Christian SD (2003) J. Incl. Phenom. Macrocycl. Chem. 45(1-2):83-89.
10. Uekama K, Irie T (1996) Pharmaceutical Use of Cyclodextrins in Various Drug Formulations. In *Comprehensive Supramolecular Chemistry, vol. 3: Cyclodextrins.* Elsevier, New York.

11. Ueda H, Nagai T (1996) Aspects of Drug Formulation with Cyclodextrins. In *Comprehensive Supramolecular Chemistry, vol. 3: Cyclodextrins.* Elsevier, New York.

12. Armspach D, Gattuso G, Königer R, Stoddart JF (1999) Cyclodextrins. In *Bioorganic Chemistry: Carbohydrates.* Oxford Univ. Press, New York.

13. Hai M, Han B (2003) J. Colloid. Interface Sci. 267:173-177.

14. Hussam A, Basu SC, Hixon M, Olumee Z (1995) Anal. Chem. 67:1459-1464.

15. Armstrong DW, Nome F (1981) Anal. Chem. 53:1662-1666.

16. Armstrong DW, Stine GY (1983) J. Am. Chem. Soc. 105:2962-2964.

17. Janini GM.; Attari SA (1983) Anal. Chem. 55:659-661.

18. Menges RA, Armstrong DW (1991) Anal. Chim. Acta 255:157-162.

19. Rundlett KL, Armstrong DW (1995) Anal. Chem. 34:2088-2095.

20. Armstrong DW (1985) Sep. Purif. Methods 14:213-304.

21. Nishi H, Fukuyama T, Terabe S (1991) J. Chromatogr. 553:503-516.

22. Conder JR, Young CL (1979) Physicochemical Measurements by Gas Chromatography. Wiley, New York.

23. Laub RJ, Pecsok RL (1978) Physicochemical Applications of Gas Chromatography. Wiley: New York.

24. Loesche WJ, Kazor C (2002) Periodontology 2000 28:256-279.

25. Sanz M, Roldán S, Herrera D (2001) J. Contemp. Dent. Pract. 2:1-13.

26. Smet E, Van Langenhove H (1998) Biodegredation 9:273-284.

27. Carroll JJ, Mather AE (1989) Geochim. Cosmochim. Acta. 53:1163-1170.

28. Hine J, Weimar RD Jr (1965) J. Am. Chem. Soc. 87:3387-3396.

29. Dacey JWH, Wakeham SG, Howes BL (1984) Geophys. Res. Lett. 11:991-994.

30. Wright DA, Sandler SI, DeVoll D (1992) Environ. Sci. Technol. 26:1828-1831.

31. Nielson F, Olson E, Fredenslund A (1994) Environ. Sci. Technol. 28:2133-2138.

32. Szejtli J (1996) Chemistry, Physical and Biological Properties of Cyclodextrins. In *Comprehensive Supramolecular Chemistry, vol. 3: Cyclodextrins*. Elsevier, New York.

33. Sanemasa I, Wu J, Toda K (1997) Bull. Chem. Soc. Jpn. 70:365-369.

34. Liu Y, You C (2001) J. Phys. Org. Chem. 14:11-16.

35. Saenger W, Steiner T (1998) Acta Cryst. A54:798-805.

36. Szejtli J (1982) *Cyclodextrins and Their Inclusion Complexes*. Akademai Kiado, Budapest.

37. Armstrong DW, Nome F, Spino LA, Golden TD (1986) J. Am. Chem. Soc. 108:1418-1421.

CHAPTER 4. THEORY AND USE OF THE PSEUDOPHASE MODEL IN GAS-LIQUID CHROMATOGRAPHIC ENANTIOMERIC SEPARATIONS

Published in *Analytical Chemistry*

Verónica Pino[‡], Andrew W. Lantz, Jared L. Anderson, Alain Berthod, and Daniel W. Armstrong*

Iowa State University, Chemistry Department, 1605 Gilman Hall, Ames, Iowa 50011, USA.

Abstract

The theory and use of the "three-phase" model in enantioselective gas-liquid chromatography utilizing a methylated cyclodextrin/polysiloxane stationary phase is presented for the first time. Equations are derived which account for all three partition equilibria in the system, including partitioning between the gas mobile phase and both stationary phase components, and the analyte equilibrium between the polysiloxane and cyclodextrin pseudophase. The separation of the retention contributions from the achiral and chiral parts of the stationary phase can be easily accomplished. Also it allows the direct examination of the two contributions to enantioselctivity, i.e., that which occurs completely in the liquid stationary phase versus the direct transfer of the chiral analyte in the gas phase to the dissolved chiral selector. Six compounds were studied to verify the model: 1-phenyl-ethanol, α-ionone, 3-methyl-1-indanone, *ortho*-chloromethylphenylsulfoxide, *ortho*-bromomethylphenylsulfoxide, and ethyl-*para*-tolyl-sulfonate. Generally, the cyclodextrin component of the stationary phase contributes to retention more than the bulk liquid

[‡] Current Address: University of La Laguna, Analytical Chemistry, Nutrition and Food Science Department, Campus de Anchieta, E-38205, La laguna, Spain.

polysiloxane. This may be an important requirement for effective GC chiral stationary phases. In addition, the roles of enthalpy and entropy toward enantiorecognition by this stationary phase were examined. While enantiomeric differences in both enthalpy and entropy provide chiral discrimination, the contribution of entropy appears to be more significant in this regard. The "three-phase" model may be applied to any gas-liquid chromatography stationary phase involving a pseudophase.

Introduction

Separations involving micelles or cyclodextrins (aka pseudophase separations [1]) are often highly specific. Indeed, the complex combination of hydrophobic, electrostatic and steric interactions of a solute with a micelle or cyclodextrin molecule cannot be duplicated by any traditional pure or mixed solvent system [2,3]. Moreover, the partitioning or binding of compounds to micelles or cyclodextrins is an important phenomena in many other areas of study, such as membrane mimetic chemistry [4], catalysis [5,6], enzyme modeling [7], chromatography [8-10], spectroscopic analysis [11], emulsion polymerization [12], and over the last twenty years, enantiomer separations [13-17]. Since the initial reports by Armstrong and coworkers on the use of micellar and cyclodextrins pseudophases in separations [1,8-10,13-17], there has been constant development of this area in both chromatography and capillary electrophoresis (CE) [18-21]. In liquid chromatography, there are three solute equilibria: between the bulk solvent and the stationary phase; solvent and the pseudophase; plus pseudophase and the stationary phase. These equilibria can be characterized either as partition coefficients or as binding constants [8-10,22]. This "three-phase" model provided a thermodynamic description of retention in these systems. The pseudophase model was extended to capillary electrophoresis using micelles, cyclodextrins, and other additives [23].

Either a two or three "phase" model is used in CE depending on whether one or two pseudophase components are added to the running buffer, respectively. Despite the tremendous impact and utility of pseudophase separations in LC and CE, the pseudophase model has not been used in gas chromatography.

One goal of this work was to apply the model to gas-liquid chromatography. This might seem illogical at first, since the pseudophase in all past separations of this type is part of a liquid mobile phase (for HPLC) or running buffer (for CE). Obviously non-volatile cyclodextrins, surfactants, etc., cannot be part of the carrier gas/mobile phase in gas-liquid chromatography (GLC). However, GLC using dissolved cyclodextrins as chiral stationary phases must have three equilibria that control the separation, i.e., the partition equilibrium of the solute chromatographed between the gas mobile phase and the cyclodextrin in the stationary phase (K_{GC}), the equilibrium of the solute between the gas mobile phase and the bulk liquid component of the stationary phase (often a polysiloxane) (K_{GS}), and the equilibrium of the solute between the cyclodextrin dissolved in the stationary phase and that in the bulk liquid stationary phase (K_{SC}). Previously, several studies have been published that describe complexation and inclusion GLC using a two-equilibria model (retention increment concept) [24,25]. However, the complete separation must be characterized by three partition coefficients (Figure 1). It is apparent that this system also can be described by a three-phase model, in a manner somewhat analogous to the original LC model [8,10]. Furthermore, this model provides a more accurate description of GLC enantiomeric separations for these specific systems, in that it can (for the first time) deconvolute the interactions that occur exclusively within the stationary phase, from those that occur directly between the gas phase and the cyclodextrins. Thermodynamic data, generally obtained using a two-phase model

[24,26] and retention increment concept [24,25], may also be obtained using this method, and may provide information regarding the process that drives the solute mobile-stationary phase exchange.

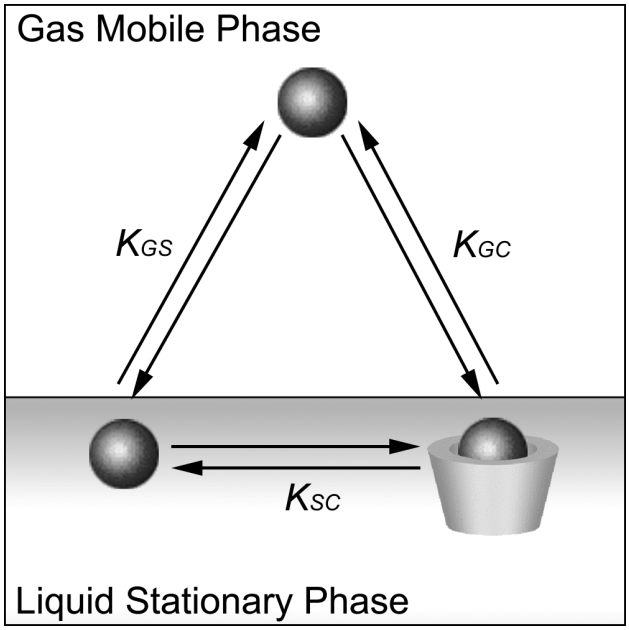

Figure 1. Three-phase model showing the equilibria implicated in gas-chromatography when using dissolved cyclodextrins in a liquid polysiloxane stationary phase.

Experimental

Materials. The chiral analytes studied were 1-phenyl-ethanol, α-ionone, 3-methyl-1-indanone, all purchased from Aldrich (Milwaukee, WI), and *ortho*-chloromethylphenylsulfoxide, *ortho*-bromomethylphenylsulfoxide, and ethyl-*para*-tolyl-sulfonate which were prepared according to Anderson *et al*. [27]. These chiral analytes were dissolved in methylene chloride (Fisher Scientific, Pittsburgh, PA) with concentrations of approximately 2-5 ppm. The cyclodextrin used was heptakis-2,3,6-trimethyl-β-cyclodextrin (PM-β-CD) from Advanced Separation Technologies (ASTEC), Whippany, NJ [28]. The coating solution consisted polysiloxane OV®-1701 (14% cyanopropyl phenyl dimethyl

polysiloxane) from Supelco (Bellefonte, PA) in dichloromethane. Dimethylphenyl deactivated polar fused silica capillary columns (0.25 mm ID) were purchased from Supelco.

Methods. All capillary columns were coated by the static coating method. 44 mg of OV-1701 polysiloxane was weighed and dissolved in 10 mL dichloromethane. Increasing weights of permethylated cyclodextrin were added to the solution to produce a concentration range of 5.8% to 38.2% (w/w). The 0.25 mm i.d. capillary was filled with the solution and sealed on both ends. The capillary was immersed in a 40 °C thermostatic bath, and one of its ends was opened and connected to a vacuum pump. Following the coating process, the coated columns were flushed with dry helium gas overnight and then conditioned from 30 to 150 ºC at 1 ºC/min. Evaporation of dichloromethane produced the deposition on the capillary internal wall of a regular polysiloxane film. The progress of the dichloromethane meniscus was watched and adjusted to be around 1 cm/s. Overall, about 3 hours were needed to prepare a 10 m column. This procedure produces a film thickness of 0.28 μm. The exact characteristics of the columns are listed in Table 1. Column efficiency was tested using naphthalene at 100 ºC. All columns had efficiencies between 2700-3400 plates/meter. The stationary phase enantioselectivity was evaluated daily using 1-phenyl-ethanol at 100 ºC.

The partial specific volume of PM-b-CD was determined using a pycnometer. A set amount of cyclodextrin was added to the pycnometer, which was then filled to the mark with a hexane. The difference in weight between the known volume of pure hexane and the same volume including cyclodextrin was used to calculate the partial specific volume of the cyclodextrin.

Table 1. Physicochemical characteristics of the 8 capillary columns[1].

Cyclodextrin (% w/w)	0	5.8	7.9	12.5	22.4	24.9	30	38.2
column length (meters)	10.85	8.23	11.22	6.95	8.00	10.48	8.18	10.35
V_s (mm3)	2.39	1.82	2.48	1.54	1.76	2.32	1.81	2.29
m_s (mg)	2.39	1.84	2.52	1.58	1.83	2.42	1.90	2.43
st. phase density (g/cm^3)	1.000	1.012	1.016	1.024	1.041	1.045	1.052	1.063
mass cyclodextrin (mg)[2]	0.00	2.55	3.48	5.50	9.86	10.96	13.20	16.81
mass OV-1701 (mg)[2]	44.00	44.00	44.00	44.00	44.00	44.00	44.00	44.00
approx. molar fraction CD	0.000	0.670	0.734	0.814	0.887	0.897	0.913	0.930
approx. molar fraction OV-1701	1.000	0.330	0.266	0.186	0.113	0.103	0.087	0.070
conc. cyclodextrin (M)	0.000	0.039	0.052	0.080	0.133	0.146	0.170	0.206
approx. conc. OV-1701 (M)	0.0200	0.0191	0.0188	0.0182	0.0170	0.0167	0.0162	0.0154

1) For all columns, the capillary internal diameter is 0.25 mm, the stationary phase film thickness is ~0.28 µm, and the geometrical phase ratio $\phi = V_s/V_m$ is 0.0045; the experimental phase ratios used in our calculations (V_s/(dead volume)) were 2 to 40% higher depending on column length, temperature and mobile phase inlet pressure since gases are compressible.
2) Masses weighted and dissolved in 10 mL dichloromethane, the solution used to coat the columns.

A Hewlett Packard 5890 Model II gas chromatograph (GC) was used for all separations. Split injection was utilized with a split ratio of 100:1 and a flow rate of 1.0 mL/min. The flow rate was determined using a soap bubble flow-meter at the outlet of the GC column. Flame ionization detection was employed with injection and detection temperatures of 250 ºC. Helium was used as the carrier gas. Methane was used to determine the dead volume of the column. All separations were performed under isothermal conditions.

Results and Discussion

Theory

Derivation of partition coefficient relationships. Separations in gas-liquid chromatography using derivatized cyclodextrins as chiral dissolved components in achiral stationary phase liquids are the result of three equilibria: i.e., the partition equilibria of the solutes chromatographed between the mobile phase and the cyclodextrin in the stationary phase; mobile phase and the bulk polysiloxane of the stationary phase; cyclodextrins in the stationary phase and the polysiloxane of the stationary phase, which are characterized by the

partition coefficients K_{GS}, K_{GC} and K_{SC}, respectively (Figure 1). The partitioning of the analyte from the mobile phase to the stationary phase is a surface adsorption process, in which the solute adsorbs to the surface of the polysiloxane or to a cyclodextrin at the gas-liquid interface. Upon adsorption, the analyte may then distribute itself throughout the volume of the stationary phase. The likelihood of a solute molecule partitioning directly from the mobile phase to either the polysiloxane or a cyclodextrin is regulated by the relative coverage of the two on the surface of the stationary phase. However, in accordance with the traditional definition of partition coefficients, the total volume of polysiloxane or cyclodextrin in the stationary phase was used in the calculations for the K_{GS} and K_{GC} partition coefficients in this study, despite the fact that an adsorption step is initially involved [8]. These equilibrium expressions may then be described by the following equations:

$$S_{(g)} \xleftrightarrow{K_{GS}} S_{(Si)} \qquad K_{GS} = \frac{C_S^{Si}}{C_S^G} \tag{1}$$

$$S_{(g)} \xleftrightarrow{K_{GC}} S_{(CD)} \qquad K_{GC} = \frac{C_S^{CD}}{C_S^G} \tag{2}$$

$$S_{(Si)} \xleftrightarrow{K_{SC}} S_{(CD)} \qquad K_{SC} = \frac{C_S^{CD}}{C_S^{Si}} \tag{3}$$

where S is the analyte in the gas and liquid polysiloxane phases, and the cyclodextrin pseudophase; $C_S{}^G$, $C_S{}^{Si}$ and $C_S{}^{CD}$ are the concentrations of the analyte in the gas and polysiloxane phases and cyclodextrin pseudophase respectively; and K_{GS}, K_{GC}, and K_{SC} are the respective partition coefficients. Based on these equilibria, a relationship between K_{GS}, K_{GC}, and K_{SC} is found:

$$K_{GC} = K_{GS} \cdot K_{SC} \tag{4}$$

The measured apparent partition coefficient (K) obtained through experimental gas chromatography can be defined as

$$K = \frac{(m_S^{Si} + m_S^{CD})/(V_{Si} + V_{CD})}{m_S^G / V_G} \tag{5}$$

where m_S is the mass of the analyte in each respective phase and V is the volume of each phase. This expression is analogous to the equations previously used to describe micelle- and cyclodextrin-water-octanol partition coefficients [29,30]. V_G is equivalent to the void volume of the column, which was calculated using the void time and the column flow-rate ($V_G = t_m \cdot F$). The total volume of the stationary phase (V_S) is simply obtained by $V_S = V_{Si}+V_{CD} = L \cdot \pi \cdot [R^2-(R-R_a)^2]$ where L is the length of the column, R is the radius of the column, and R_a is the thickness of the stationary phase. R_a is calculated using $R_a=R/(2 \cdot c)$ [31] with c being the ratio of the solvent volume (dichloromethane) to the stationary phase volume (CD and polysiloxane) in the coating solution. Using the partition coefficient between the bulk polysiloxane liquid and the cyclodextrin,

$$K_{SC} = \frac{(m_S^{CD} / V_{CD})}{(m_S^{Si} / V_{Si})} \tag{6}$$

the following equation can be produced by solving for m_S^{CD} in Eqn. 6 and substituting this into Eqn. 5:

$$K = \left\{ \left(m_S^{Si} / V_{Si}\right) \left[K_{SC} \left(\frac{V_{CD}}{V_{CD} + V_{Si}} \right) - \left(\frac{V_{CD}}{V_{CD} + V_{Si}} \right) + 1 \right] \right\} \left\{ m_S^G / V_G \right\}^{-1}. \tag{7}$$

A relationship between the concentration of cyclodextrin (C_{CD}) and the volumes of the cyclodextrin and polysiloxane phases exists involving the partial specific volume of the cyclodextrin (v_p):

$$C_{CD}v_p = V_{CD}/(V_{CD} + V_{Si}). \quad (8)$$

The partial specific volume of PM-β-CD used in all calculations in this experiment was 1.122 L/mol. This value was determined as stated in the Experimental section. Finally, by substituting Eqn. 8 into Eqn. 7 one obtains:

$$K = v_p K_{GS}(K_{SC} - 1)C_{CD} + K_{GS}. \quad (9)$$

Plotting K vs. C_{CD} allows all three partition coefficients to be determined. K_{GS} can be found directly from the y-intercept, while the $K_{SC} = slope/(y\text{-}int.\cdot v_p)+1$. K_{GC} may then simply be calculated using Eqn. 4 [29,30]. Alternately, the experimental partition ratio (k') may be used in place of K, producing a y-intercept of k'_{GS}, and a slope of $v_p k'_{GS}(K_{SC}\text{-}1)$. From this data it is possible to obtain definitive information about the interactions that each enantiomer experiences when undergoing an enantiomeric separation by GC. Additionally one can pin-point the particular interactions/equilibria that contribute to both retention and enantioselectivity.

Alternatively, the association of the analyte in the bulk liquid polysiloxane phase with a cyclodextrin dissolved in the stationary phase can be given in terms of a binding constant [26]. The 1:1 complexation of the analyte with cyclodextrin may be described by the equilibrium

$$S_{(Si)} + CD_{(Si)} \xleftrightarrow{K_{eq}} S \cdot CD_{(Si)} \qquad K_{eq} = \frac{[S \cdot CD]}{[S][CD]} \quad (10)$$

where K_{eq} is the equilibrium binding constant. Using Eqns. 10 and 8, the relationship between K_{SC} and K_{eq} is found to be

$$K_{eq} = K_{SC} \cdot v_p \quad (11)$$

at relatively low cyclodextrin concentrations (at high [CD], the activity of the CD should be used in place of the concentration). It is important to note that these equations are completely valid for any GC experiment involving a pseudophase (e.g. micelle, polymer, protein, cyclodextrin, nanoparticle, etc.). Indeed, it is the only method currently known that provides both the association constant of an analyte in the gas phase to a ligand in the condensed phase and the liquid phase association of the two molecules, from the same experiment.

Results

Analyte partitioning. Using Eqn. 9, *K* was plotted against the cyclodextrin concentration in the stationary phase. Figure 2 shows examples of the types of plots that are produced. Good correlations were obtained for these plots ($R^2 > 0.95$), particularly considering that each point in the plot corresponds to a separate column prepared with a different concentration of the cyclodextrin derivative.

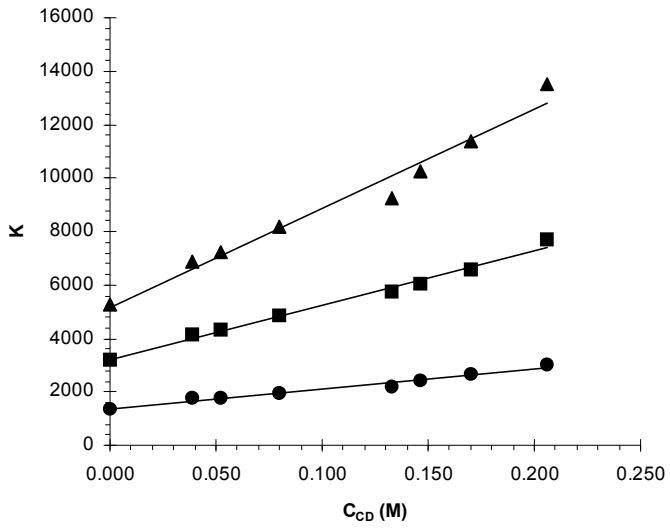

Figure 2. Plots of Eqn. 9 for the first eluted enantiomer of *ortho*-bromomethylphenylsulfoxide (■), *ortho*-chloromethylphenylsulfoxide (▲), and 3-methyl-1-indanone (●).

Table 2. Calculated partition coefficients for the studied compounds.

Compound	Enantiomer	T (°C)	K_{GS} ± SD[b]	K_{GC} ± SD[b]	K_{SC} ± SD[b]
o-chloromethylphenylsulfoxide	1[a]	130	3190 ± 150	21500 ± 300	6.8 ± 0.3
	2[a]		3170 ± 160	23900 ± 100	7.5 ± 0.4
1-phenyl-1-ethanol	1[a]	100	690 ± 40	17700 ± 900	25.6 ± 0.6
	2[a]		600 ± 70	20800 ± 500	34.5 ± 2.7
α-ionone	1[a]	120	3150 ± 110	11100 ± 300	3.5 ± 0.1
	2[a]		3110 ± 100	13200 ± 400	4.2 ± 0.1
3-methyl-1-indanone	1[a]	130	1380 ± 60	8020 ± 210	5.8 ± 0.3
	2[a]		1380 ± 40	9250 ± 180	6.7 ± 0.1
o-bromomethylphenylsulfoxide	1[a]	130	5180 ± 290	38100 ± 200	7.4 ± 0.5
	2[a]		5120 ± 330	43600 ± 300	8.5 ± 0.7
ethyl-*p*-tolylsulfonate	1[a]	115	7880 ± 430	43800 ± 300	5.6 ± 0.4
	2[a]		7860 ± 480	48300 ± 800	6.1 ± 0.5

[a] Based on the elution order of the enantiomers
[b] SD: standard deviations of the calculated partition coefficients (determined from four independent measurements)

The corresponding calculated partition coefficients are shown in Table 2. K_{eq}, the binding constant of the analyte dissolved in the bulk polysiloxane to the dissolved cyclodextrin pseudophase, was calculated using Eqn. 11, and the results are shown in Table 3. The standard deviations of these data, based on four independent measurements, are generally <5%. For all the analytes in this study, the K_{GS} values for both enantiomers are statistically equivalent within the margin of error. This trend is expected since the polysiloxane stationary phase is an achiral environment, and cannot discriminate between enantiomers. However, each analyte's enantiomers have differing K_{GC}, K_{SC}, and K_{eq} values, indicating that the cyclodextrin in the stationary phase is controlling the chiral separation. Furthermore, by definition, the second eluting enantiomer always produces a higher K_{GC}, K_{SC}, and K_{eq}.

The data in Table 2 also indicate several other interesting aspects about cyclodextrin-based GC chiral stationary phases (which may be true for other types of CSPs as well).

Table 3. Calculated binding constants for the studied compounds between the polysiloxane phase and bound to cyclodextrin.

Compound	Enantiomer	T (°C)	$K_{eq} \pm SD^b$
o-chloromethylphenylsulfoxide	1[a]	130	7.6 ± 0.3
	2[a]		8.5 ± 0.4
1-phenyl-1-ethanol	1[a]	100	28.7 ± 0.6
	2[a]		38.7 ± 3.0
α-ionone	1[a]	120	4.0 ± 0.1
	2[a]		4.8 ± 0.1
3-methyl-1-indanone	1[a]	130	6.5 ± 0.3
	2[a]		7.6 ± 0.1
o-bromomethylphenylsulfoxide	1[a]	130	8.2 ± 0.5
	2[a]		9.6 ± 0.8
ethyl-*p*-tolylsulfonate	1[a]	115	6.2 ± 0.4
	2[a]		6.9 ± 0.6

[a] Based on the elution order of the enantiomers
[b] SD: standard deviations of the calculated partition coefficients (determined from four independent measurements)

Clearly the association/partitioning of the solute to the chiral selector portion of the stationary phase (K_{GC}) is much greater than its association/partitioning to the bulk achiral portion of the stationary phase (K_{GS}). Hence the cyclodextrin has a relatively greater effect on retention than the polysiloxane component of the stationary phase. This fact permits lower concentrations of cyclodextrins to be used in the stationary phase while still maintaining their effectiveness, since the solutes preferentially partition to the cyclodextrin over the bulk polysiloxane. Indeed, it may be this preferential partitioning to the chiral selector over the achiral matrix that helps make the entire class of cyclodextrin and polysiloxane CSPs so effective in GC. Figure 3 shows the effect of methylated cyclodextrin concentration in the stationary phase on the measured enantioselectivity, resolution, and efficiency for the separation of α-ionone enantiomers.

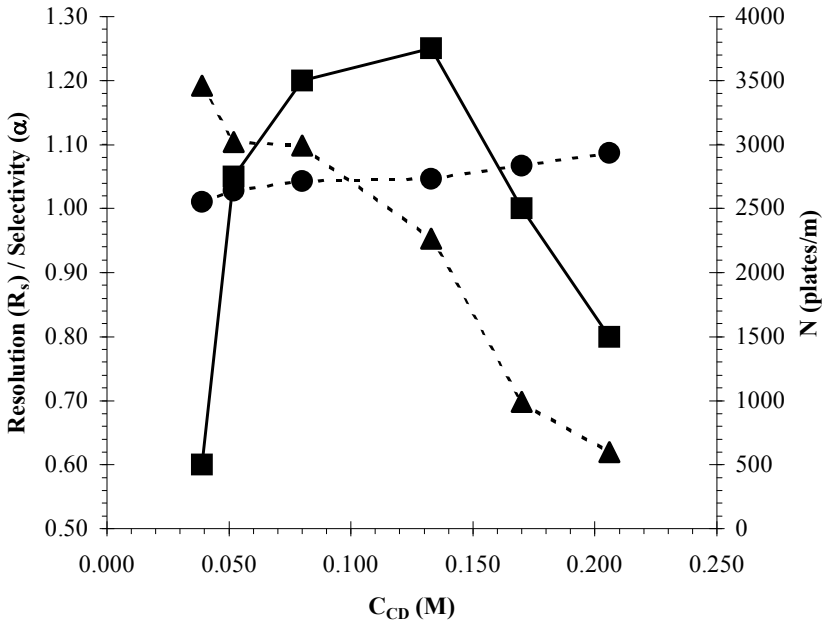

Figure 3. Effect of stationary-phase cyclodextrin concentration on selectivity (●), resolution (■), and efficiency (▲) of the enantioseparation of α-ionone.

Generally, the selectivity of the enantioseparation increases with the cyclodextrin concentration. However, as reported by Schurig *et al*. [32], it is likely that a maximum selectivity could be reached at a higher cyclodextrin concentration than was examined in this study. Generally, a maximum peak-to-peak separation may be obtained at a defined cyclodextrin concentration. Beyond this point, each solute enantiomer experiences too long of a residence time in the cyclodextrin. The cyclodextrin may therefore no longer effectively discriminate between the solute moieties, resulting in a loss of enantioselectivity [20]. 38.2 % w/w cyclodextrin was the highest concentration examined here, as columns with higher cyclodextrin concentrations are difficult to produce due to the limited solubility of methylated cyclodextrin in the bulk liquid polysiloxane. Despite the increasing enantioselectivity, the efficiency of the separations decreases steadily with increasing

cyclodextrin in the stationary phase due to poor mass transfer. Therefore by balancing these two factors, a maximum resolution may be obtained at relatively low cyclodextrin concentrations. As shown in Figure 3, the optimum resolution for α-ionone enantiomers was at approximately 0.130 M cyclodextrin.

Stationary phase surface coverage. As stated earlier, it is important to note that the partitioning of the analyte directly between the gas mobile phase and the cyclodextrin (K_{GC}) may only occur with cyclodextrins at the gas-liquid interface. Furthermore, the probability of a solute molecule in the mobile phase partitioning directly to either the polysiloxane or a cyclodextrin is controlled by their relative stationary phase surface coverage. As a result, it may be useful to approximate the polysiloxane and cyclodextrin coverage on the surface of the stationary phase that is available for analyte partitioning. To accomplish this, the total surface area of the stationary phase exposed to the gas mobile phase was calculated by

$$A = L \cdot 2 \cdot \pi \cdot \left(R - R_a\right) \tag{12}$$

The relative coverage of the polysiloxane and the methylated cyclodextrin differs for each column, correlating directly to the level of cyclodextrin dissolved in the stationary phase. Using the percent volume of cyclodextrin present in the stationary phase, an approximation of the stationary phase surface area occupied by cyclodextrin molecules may be calculated. Table 4 shows the calculated polysiloxane and cyclodextrin coverage area for each of the prepared columns. Clearly, the partitioning kinetics of the analyte is greatly affected by the relative surface coverage of the polysiloxane and cyclodextrin. Therefore, as the cyclodextrin area increases, analyte partitioning to this pseudophase (K_{GC}) must play a more significant role.

Table 4. Calculated polysiloxane and cyclodextrin coverage on the surface of the stationary phase for the 8 columns in this study.

Cyclodextrin % (w/w)	Total Surface Area (mm^2)	Polysiloxane Surface Area (mm^2)	Cyclodextrin Surface Area (mm^2)	Polysiloxane Area / Cyclodextrin Area
0	15300	15300	0.0	N/A
5.8	12400	11900	500	23.8
7.9	15700	14800	900	16.4
12.5	10900	9900	1000	9.9
22.4	12100	10300	1800	5.7
24.9	14900	12500	2400	5.2
30.0	12300	10000	2300	4.3
38.2	14800	11400	3400	3.4

Thermodynamic study. A thermodynamic examination was carried out to study the magnitude of the free energies for each equilibrium, and to determine the contribution of enthalpy and entropy toward the chiral recognition of enantiomers by the stationary phase. The free energies relating to each individual partition coefficient may be easily calculated using

$$\Delta G = -RT \ln K \tag{13}$$

These values are shown in Table 5, and provide useful information regarding the thermodynamic process that drives the solute mobile-stationary phase exchange. In addition, the relationship between all three free energies ($\Delta G_{GS} + \Delta G_{SC} = \Delta G_{GC}$) can be confirmed.

Table 5. Gibbs free energies corresponding to the individual partition coefficients.

Compound	Enantiomer	T (°C)	K_{GS}	**ΔG_{GS} (J/mol)**	K_{SC}	**ΔG_{SC} (J/mol)**	K_{GC}	**ΔG_{GC} (J/mol)**
o-chloromethyl-phenyl-sulfoxide	1[a]	130	3190	**-27000**	6.8	**-6400**	21500	**-33400**
	2[a]		3170	**-27000**	7.5	**-6770**	23900	**-33800**
1-phenyl-1-ethanol	1[a]	100	690	**-20300**	25.6	**-10100**	17700	**-30400**
	2[a]		600	**-19900**	34.5	**-11000**	20800	**-30900**
α-ionone	1[a]	120	3150	**-26300**	3.5	**-4130**	11100	**-30500**
	2[a]		3110	**-26300**	4.2	**-4720**	13200	**-31000**

[a] Based on the elution order of the enantiomers
Column 12.5% w/w CD with $\%_{CD}$=8.9% v/v and $\%_{Si}$=91.1% v/v.

The enthalpy and entropy contributions to the free energy of the global solute mobile-stationary phase exchange are typically studied by preparing van't Hoff plots using the following equation:

$$\ln \frac{k}{\phi} = \frac{\Delta S}{R} - \frac{\Delta H}{R} \cdot \frac{1}{T} \qquad (14)$$

A plot of *ln(k/ϕ)* versus *1/T* allows *ΔS*, *ΔH* and *ΔG* for each enantiomer to be obtained [33]. The working range of temperatures was selected to provide enantioresolution of both enantiomers. This equation produces straight lines with regression coefficients (R^2) higher than 0.9995 for each studied enantiomer (Figure 4).

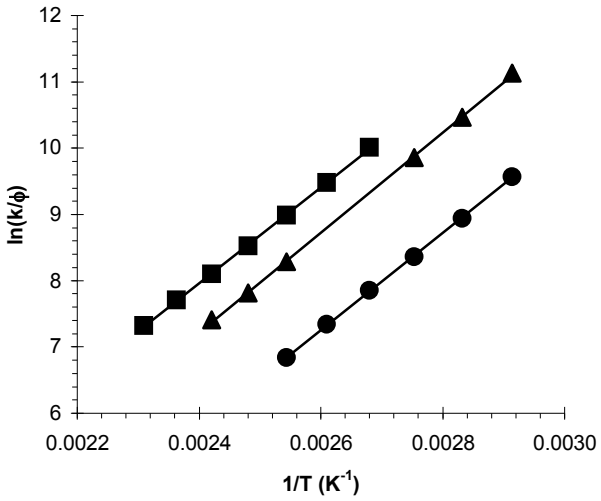

Figure 4. Van't Hoff plots for the first eluted enantiomer of *ortho*-chloromethylphenylsulfoxide (■), α-ionone (▲), and 1-phenyl-1-ethanol (●).

Furthermore, by performing separate K_{GS}, K_{GC}, and K_{SC} determinations at varying temperatures and applying these values to Eqn. 14 ($K=k/\phi$), it should be possible to determine *ΔS*, *ΔH,* and *ΔG* for each partition coefficient. While only the global thermodynamic properties of the solute mobile-stationary phase exchange were examined in

this work, using this model it is theoretically possible (for the first time) to determine the contribution of ΔS and ΔH to ΔG for each individual partition exchange.

Alternatively, an adaptation of Eqn. 13 may be used to relate the partition coefficients to the free energy of the global analyte mobile-stationary phase exchange

$$\Delta G = -RT \ln\left(\%_{CD} K_{GC} + \%_{Si} K_{GS}\right) \tag{15}$$

where the % factors are the volume fractions of the cyclodextrin and polysiloxane components in the stationary phase, respectively. Therefore, a comparison can be made between the ΔG values obtained using the van't Hoff plot (Eqn. 14) and the free energies calculated using the partition coefficients (Eqn. 15). Table 6 shows the values of ΔG calculated using both techniques, as well as the contributions of ΔS and ΔH to the free energy. Excellent correlation (within 2%) between the two free energy calculations exists, indicating the validity of equation 9.

Generally, the difference between the ΔG values of enantiomers (~0.1-0.4 kJ/mol) is relatively small when compared to the free energy of the global solute-stationary phase exchange (~20-30 kJ/mol). This two orders of magnitude difference demonstrates that these enantioselective interactions can be delicate and difficult to obtain. It is apparent from the measured enthalpy and entropy values (Table 6) that ΔH facilitates the free energy of transfer of solutes to the stationary phase while ΔS has the opposite effect. However, the magnitude of the entropic contribution ($T\Delta S$) to the free energy is roughly 50% that of the enthalpic contribution, resulting in a net negative free energy. Despite this trend, enantiorecognition benefits from both the enantiomeric differences in entropy and enthalpy, as shown by the ratio of the enantiomers' enthalpies and entropies in Table 6. Overall, the entropy term

provides more differentiation between enantiomers than the enthalpy term for all three of the analytes studied.

Table 6. Comparison of the Gibbs free energies obtained using van't Hoff plot regression and solute partition coefficients.

Compound	Enantiomer	T (°C)	ΔH (J/mol)	$\Delta H_2/\Delta H_1$	ΔS (J/mol K)	$\Delta S_2/\Delta S_1$	**ΔG (J/mol)**	K_{GS}	K_{GC}	**ΔG (J/mol)**
o-chloromethyl-phenyl-sulfoxide	1[a]	130	-60000	1.024	-77.9	1.041	**-28700**	3190	21500	**-28400**
	2[a]		-61500		-81.1		**-28800**	3170	23900	**-28600**
1-phenyl-1-ethanol	1[a]	100	-60900	1.038	-98.0	1.056	**-24300**	690	17700	**-23900**
	2[a]		-63200		-103.5		**-24600**	600	20800	**-24200**
α-ionone	1[a]	120	-62700	1.040	-90.4	1.065	**-27100**	3150	11100	**-27000**
	2[a]		-65200		-96.3		**-27300**	3110	13200	**-27100**

[a] Based on the elution order of the enantiomers
Column 12.5% w/w CD with $\%_{CD}$=8.9% v/v and $\%_{Si}$=91.1% v/v.

However, as discussed by Schurig, *et al*. [25,34] the selectivity of the system, in terms of free energy, is temperature dependent as defined by

$$-\Delta_{R,S}(\Delta G) = -\Delta_{R,S}(\Delta H) + T \cdot \Delta_{R,S}(\Delta S) \qquad (16)$$

Because a stronger analyte-cyclodextrin complex has less disorder, the contributions of $-\Delta_{R,S}(\Delta H)$ and $\Delta_{R,S}(\Delta S)$ compete for determining the selectivity, $-\Delta_{R,S}(\Delta G)$. At the isoenantioselective temperature (T_{iso}) the two contributions balance one another completely, resulting in a net $-\Delta_{R,S}(\Delta G)$ of zero. Therefore, at temperatures below T_{iso} the selectivity of the system is influenced more heavily by $-\Delta_{R,S}(\Delta H)$, while at temperatures above T_{iso} $\Delta_{R,S}(\Delta S)$ provides a greater contribution [25,34].

Conclusions

For the first time, the "three-phase" model has been applied to gas-liquid chromatography utilizing a cyclodextrin pseudophase. Important information regarding the mechanism of chiral recognition in cyclodextrin GLC may be obtained. With this model one can assess the relative importance of analyte partitioning to/between the three phases in

regard to both enantioselectivity and retention. Generally, analyte partitioning to the cyclodextrin pseudophase was greater than to the bulk liquid polysiloxane, resulting in the cyclodextrin having a more significant effect on retention. This may be one of the more important factors that control the overall effectiveness of any CSP that is composed of distinct chiral and achiral components. The analyte partitioning between the polysiloxane and cyclodextrin components of the stationary phase was several orders of magnitude smaller than the equilibria from the gas mobile phase. As expected, enantiorecognition was isolated only to equilibria involving the cyclodextrin component of the stationary phase. The thermodynamic studies indicated that the entropy was pivotal in the chiral recognition process. Further Van't Hoff plots of the three individual partition coefficients may eventually allow the thermodynamic components of each to be isolated.

References

[1] Armstrong, D.W. *J. Liq. Chromatogr.* **1980**, *3*, 895-900.

[2] Hinze, W.L. "Colloid and Interface Science", Kerket, M. Ed.: Academic Press: New York, 1976, p. 425.

[3] Fendler, J.H.; Fendler, E.J. "Catalysis in Micellar and Macromolecular Systems"; Academic Press: New York, 1973.

[4] Fendler, J.H.*Chem. Rev.* **1987**, *87*, 877-899.

[5] Taşcioğlu, S. *Tetrahedron* **1996**, *52(34)*, 11113-11152.

[6] Breslow, R.; Dong, S.D. *Chem. Rev.* **1998**, *98*, 1997-2011.

[7] Tabushi, I.; Kuroda, Y. "Cyclodextrins and Cyclophanes as Enzyme Models", In Advances in Catalysis, Vol 32. Eley, D.D.; Pines, H.; Weisz, P.B. Eds. Academic Press: New York, 1983.

[8] Armstrong, D.W.; Nome, F. *Anal. Chem.* **1981**, *53*, 1662-1666.

[9] Armstrong, D.W.; Stine, G.Y. *J. Am. Chem. Soc.* **1983**, *105*, 2962-2964.

[10] Armstrong, D.W. *Sep. Purif. Methods* **1985**, *14*, 213-304.

[11] Ueno, A. *Supramol. Sci.* **1996**, *3*, 31-36.

[12] Capek, I.; Chern, C. *Adv. Polym. Sci.* **2001**, *155*, 101-165.

[13] Armstrong, D.W.; Terrill, R.Q. *Anal. Chem.* **1979**, *51*, 2160.

[14] Singh, H.N.; Hinze, W.L. *Analyst.* **1982**, *107*, 1073.

[15] Armstrong, D.W.; Ward, T.J.; Armstrong, D.R.; Beesley, T.E. *Science* **1986**, *232*, 1132-1135.

[16] Armstrong, D.W.; DeMond, W.; Alak, A.; Hinze, W.L.; Riehl, T.E.; Bui, K.H. *Anal. Chem.* **1985**, *57*, 234-237.

[17] Armstrong, D.W.; DeMond, W. *J. Chromatogr. Sci.* **1984**, *22*, 411-415.

[18] Terabe, S.; Otsuka, K.; Ichikawa, K.; Tsuchiya, A.; Ando, T. *Anal. Chem.* **1984**, *56*, 113-116.

[19] Liu, J.; Cobb, K.A.; Novotny, M. *J. Chromatogr.* **1990**, *519*, 189-197.

[20] Wren, S.A.; Rowe, R.C. *J. Chromatogr.* **1992**, *603*, 235-241.

[21] Rundlett, K.L.; Armstrong, D.W. *Anal. Chem.* **1995**, *67*, 2088-2095.

[22] Arunyanart, M.; Cline-Love, L.J. *Anal. Chem.* **1984**, *56*, 1557.

[23] Nishi, H.; Fukuyama, T.; Terabe, S. *J. Chromatogr.* **1991**, *553*, 503-516.

[24] Schurig, V.; Schmidt, R. *J. Chromatogr. A* **2003**, *1000*, 311-324.

[25] Schurig, V. *J. Chromatogr. A* **2002**, *965*, 315-356.

[26] Schurig, V.; Chang, R.C.; Zlatkis, A.; Feibush, B. *J. Chromatogr.* **1974**, *99*, 147-171.

[27] Anderson, J.L., Ding, J.; McCulla, R.D.; Jenks, W.S.; Armstrong, D.W. *J. Chromatogr. A* **2002**, *946*, 197-208.

[28] Schurig, V.; Nowotny, H.P. *J. Chromatogr*. **1988**, *441*, 155-163.

[29] Janini, G.M.; Attari, S.A. *Anal. Chem.* **1983**, *55*, 659-661.

[30] Menges, R.A.; Armstrong, D.W. *Anal. Chim. Acta* **1991**, *255*, 157-162.

[31] Bouche, J.; Verzele, M. *J. Gas Chromatogr.* **1968**, *6*, 501.

[32] Jung, M.; Schmalzing, D.; Schurig, V. *J. Chromatogr.* **1991**, *552*, 43-57.

[33] Berthod, A.; Li, W.; Armstrong, D.W. *Anal. Chem.* **1992**, *64*, 873.

[34] Schurig, V. *Angew. Chem. Int. Ed.* **1984**, *23*, 747-765.

CHAPTER 5. DETERMINATION OF SOLUTE PARTITION BEHAVIOR WITH ROOM-TEMPERATURE IONIC LIQUID BASED MICELLAR GAS-LIQUID CHROMATOGRAPHY STATIONARY PHASES USING THE PSEUDOPHASE MODEL

Published in *Journal of Chromatography A*

Andrew W. Lantz, Verónica Pino, Jared L. Anderson, Daniel W. Armstrong*[‡]

Iowa State University, Chemistry Department, 1605 Gilman Hall, Ames, Iowa 50011.

Abstract

The use of micelles in ionic liquid-based gas-chromatography stationary phases was evaluated using equations derived for a "three-phase" model. This model allows the determination of all three partition coefficients involved in the system, and elucidates the micellar contribution to retention and selectivity. Four types of micellar-ionic liquid columns were examined in this study: 1-butyl-3-methylimidazolium chloride with sodium dodecylsulfate or dioctyl sulfosuccinate, and 1-butyl-3-methylimidazolium hexafluorophosphate with polyoxyethylene-100-stearyl ether or polyoxyethylene-23-lauryl ether. The partition coefficients were measured for a wide range of probe molecules capable of a variety of types and magnitudes of interactions. In general, most probe molecules preferentially partitioned to the micellar pseudophase over the bulk ionic liquid component of the stationary phase. Therefore, addition of surfactant to the stationary phase usually resulted in greater solute retention. It is also shown that the selectivity of the stationary phase is

[‡] Current Address: University of Texas Arlington, Department of Chemistry and Biochemistry, Arlington, TX 76091 email: sec4dwa@uta.edu

significantly altered by the presence of micelles, either by enhancing or lessening the separation. The effects of surfactant on the interaction parameters of the stationary phase are determined using the Abraham solvation parameter model. The addition of sodium dodecylsulfate and dioctyl sulfosuccinate to 1-butyl-3-methylimidazolium chloride stationary phases generally increased the phase's hydrogen bond basicity and increased the level of dispersion interaction. Polyoxyethylene-100-stearyl ether and polyoxyethylene-23-lauryl ether surfactants, however, enhanced the π-π/n-π, polarizability/dipolarity, and hydrogen bond basicity interactions of 1-butyl-3-methylimidazolium hexafluorophosphate to a greater degree than the ionic surfactants with 1-butyl-3-methylimidazolium chloride. However, these nonionic surfactants appeared to hinder the ability of the stationary phase to interact with solutes *via* dispersion forces. Therefore, it is possible to effectively predict which analytes will be most highly retained by these micellar-ionic liquid stationary phases.

Introduction

Room temperature ionic liquids (RTILs) are a class of low melting point, nonmolecular, ionic solvents that are currently of major interest in numerous branches of chemistry [1-19]. Most commonly used RTILs are composed of an imidazole, pyrrole, or pyridine based cation and an inorganic anion, such as Cl^-, PF_6^-, or NTF_2^- [1]. These solvents possess unique properties that provide advantages over traditional aqueous or organic solvents. They have high thermal stabilities and negligible vapor pressures, allowing them to be used in both high temperature and high vacuum systems. Furthermore, these solvents are attractive alternatives to environmentally unfriendly solvents that produce volatile organic carbons (VOCs) [1]. Some RTILs are immiscible with aqueous solutions, while others are immiscible with nonpolar solvents, and still others are immiscible with both thereby

providing multiphased systems [1]. Given their complex structure and numerous functional groups, ionic liquids (IL) can participate in multiple types of solvation interactions, including π-π and n-π, dipolar, hydrogen bonding, dispersive, and ionic interactions [2]. Consequently, ionic liquids are known to solvate a wide range of both polar and nonpolar molecules. In contrast, simple molecular solvents provide only a limited number of solvation interactions with solutes. As a result of their unique properties, ionic liquids have been found to be useful in a variety of fields including liquid-liquid extractions [3, 4], solvents for organic synthesis and enzyme catalyzed reactions [1, 5-8], electrochemical studies [9-10], matrix-assisted laser desorption/ionization mass spectrometry [11], additives in capillary electrophoresis [12], and as stationary phases in gas-liquid chromatography (GLC) [13-19].

The first molten salt GLC stationary phase was published by Barber *et al*. in 1959 using bivalent metal stearate salts [20]. Several other ionic liquid stationary phases based on tetra-n-pentylammonium, tetra-n-hexylammonium, and ethylammonium salts were also investigated over the past few decades [21]. While these columns exhibited good selectivity for polar and hydrogen-bonding solutes, they had poor efficiencies and a limited working temperature range of below 160 ºC. It was not until recent years that imidazole, pyrrole, and pyridine based ionic liquids were found to fulfill the requirements of effective liquid stationary phases for gas chromatography (i.e. high thermal stabilities, high efficiencies, high viscosities, and uniform coatings on fused-silica capillary columns) [13]. These RTIL stationary phases exhibit "dual nature" behavior, acting as a nonpolar stationary phase for nonpolar analytes and as a polar stationary phase for polar analytes. This phenomenon has been shown to be due the ability of these RTILs to interact with analytes through numerous types of solvation interactions, as mentioned above [2]. Recently, our group reported on

several new high-stability monocationic and dicationic ionic liquid stationary phases that have thermal ranges up to 260 ºC and 400 ºC respectively, and maintain the unique solvation characteristics of other RTILs [16-18]. The uses of ionic liquids have also been expanded to include chiral separations with the development of chiral ionic liquid stationary phases [19].

The ability of various ionic and nonionic surfactants to form micelles in ionic liquids was recently examined by Armstrong *et al*. [22]. It was found that the presence of surfactant in ILs depressed the surface tension, and likely forms normal micellar aggregates. Here, we attempt to further study the effect of micelles in RTIL stationary phases by applying the "three phase" model to these unique GLC columns (Figure 1).

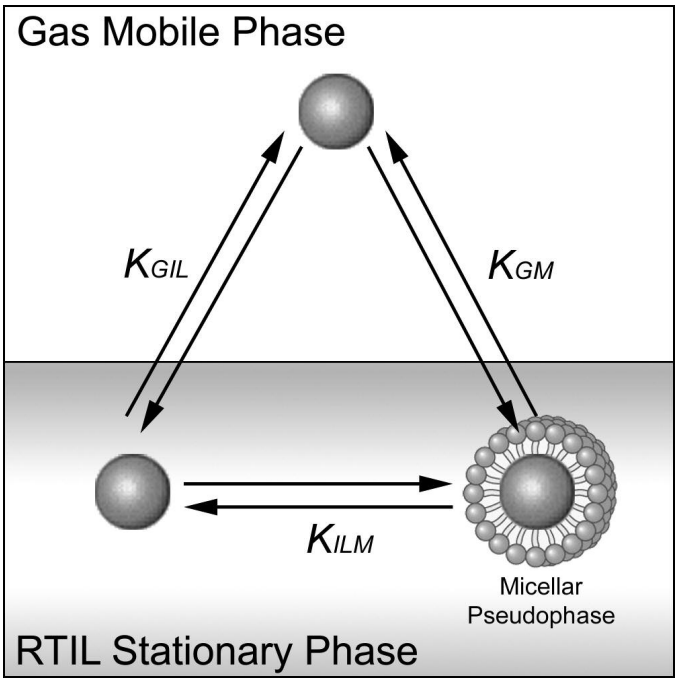

Figure 1. Diagram of the three-phase model and appropriate partition equilibria implicated in gas-chromatography when using dissolved micelles in a room temperature ionic liquid stationary phase.

The "three-phase" model has been used previously to describe micellar liquid chromatography [23] and, since then, numerous other separation systems involving pseudophases including capillary electrophoresis [24], headspace gas chromatography [25],

and gas-liquid chromatography using dissolved cyclodextrins [26]. This method allows the determination of all three partition coefficients involved in the system, and also deconvolutes the contributions of all three equilibria in regard to both selectivity and retention. Furthermore, we attempt to characterize these micellar ionic liquid based stationary phases in order to determine the solvation interactions that are involved in probe molecule partitioning.

Experimental

Materials. The selected surfactants were sodium dodecylsulfate (SDS), obtained from Fisher Scientific (St. Louis, MO, USA); polyoxyethylene-23-laurylether (Brij35), obtained from Sigma (St. Louis, MO, USA); and polyoxyethylene-100-stearylether (Brij700) and dioctyl sulfosuccinate (docSS), both obtained from Aldrich (Milwaukee, WI, USA). 1-methylimidazole, chlorobutane and hexafluorophosphoric acid were all purchased from Fluka Chemical Co. (Ronkonkoma, NY, USA) or Aldrich. HPLC grade ethyl acetate was purchased from Fisher. Probe molecules were all obtained from Aldrich (Table 1).

The ionic liquids 1-butyl-3-methylimidazolium chloride (BMIMCl) and 1-butyl-3-methylimidazolium hexafluorophosphate ($BMIMPF_6$) were selected due to their ability to dissolve high concentrations of ionic or nonionic surfactants. The syntheses of these compounds have been reported elsewhere [13]. Briefly, BMIMCl was prepared by adding equal amounts (0.5 mol) of 1-methylimidazole and chlorobutane and reacting them for 48-72 hours at 70 ºC under reflux conditions. The resulting viscous liquid was allowed to cool to room temperature and then was washed three times with 50-mL portions of ethyl acetate. After the last washing, the remaining ethyl acetate was removed by heating the liquid to 70 ºC under vacuum. $BMIMPF_6$ was prepared from BMIMCl by slowly adding hexafluorophosphoric acid (0.13 mol) to a solution of BMIMCl (0.1 mol) in 100 mL of

water. After stirring for 12 h, the lower liquid portion was washed with water until the washings were no longer acidic. The ionic liquid was heated under vacuum at 70 ºC to remove any excess water. The yield was >80%.

Table 1. List of probe molecules and their solute descriptors used to characterize each micelle-RTIL stationary phase. Data from ref. [2].

Probe Molecules	R_2	π_2^H	α_2^H	β_2^H	$log\ L^{16}$
Acetic Acid	0.265	0.65	0.61	0.44	1.750
Acetophenone	0.818	1.01	0	0.49	4.501
Aniline	0.955	0.96	0.26	0.53	3.993
Benzaldehyde	0.820	1.00	0	0.39	4.008
Benzonitrile	0.742	1.11	0	0.33	4.039
Butanol	0.224	0.42	0.37	0.48	2.601
2-Chloroaniline	1.033	0.92	0.25	0.31	4.674
1-Chlorohexane	0.201	0.40	0	0.10	3.777
p-Cresol	0.820	0.87	0.57	0.31	4.312
Cyclohexanol	0.460	0.54	0.32	0.57	3.758
Cyclohexanone	0.403	0.86	0	0.56	3.792
1,2-Dichlorobenzene	0.872	0.78	0	0.04	4.518
N,N-Dimethylformamide	0.367	1.31	0	0.74	3.173
Dioxane	0.403	0.86	0	0.56	3.792
Ethylphenylether	0.681	0.70	0	0.32	4.242
Methyl Caproate	0.080	0.60	0	0.45	3.874
Naphthalene	1.340	0.92	0	0.20	5.161
Nitrobenzene	0.871	1.11	0	0.28	4.511
1-Nitropropane	0.242	0.95	0	0.31	2.894
1-Octanol	0.199	0.42	0.37	0.48	4.619
Octyl Aldehyde	0.160	0.65	0	0.45	4.360
2-Pentanone	0.143	0.68	0	0.51	2.755
Phenol	0.805	0.89	0.60	0.31	3.766
Proprionitrile	0.162	0.90	0.02	0.36	2.082
Pyridine	0.794	0.87	0	0.62	3.003
Pyrrole	0.613	0.73	0.41	0.29	2.865
Toluene	0.601	0.52	0	0.14	3.325
m-Xylene	0.623	0.52	0	0.16	3.839
o-Xylene	0.663	0.56	0	0.16	3.939
p-Xylene	0.613	0.52	0	0.16	3.839

Methods. Solutions of surfactants in RTILs were prepared on a weight/volume basis and diluted volumetrically. Solutions were slightly heated to increase the rate of dissolution. The solutions were clarified by filtration using glass syringes and 0.45 μm PTFE filters with an external diameter of 25 mm (Alltech, Lexington, KY, USA). Due to the high viscosity of the solutions, a pump-syringe was used to accelerate this filtration step. The apparent molar volume of each surfactant was determined by adding a known amount of surfactant to a set volume of ionic liquid. The difference in weight between the set volume of pure ionic liquid and the same volume including surfactant was used to calculate the partial specific volume of the surfactant monomer. Because the volumes of ionic liquids used in these determinations were much greater than the volumes of surfactant added, the calculated apparent molar volumes of the surfactants may approximate their partial molar volumes.

Untreated fused silica capillary tubing (0.25 mm I.D.) was obtained from Supelco (Bellefonte, PA, USA). All capillaries were prepared by the static coating method using a 0.24% (w/v) solution of each RTIL-surfactant mixture in dichloromethane. The capillary was immersed in a 40 °C thermostatic bath, and one of its ends was opened and connected to a vacuum pump. The coated columns were then flushed with dry helium gas overnight and then conditioned from 30 to 150 ºC at 1 ºC/min. Column efficiencies were tested using naphthalene at 100 ºC. All columns had efficiencies between 2300-3400 plates/meter. Interestingly, column efficiencies increased steadily with increasing concentration of surfactant in the stationary phase due to a more uniform capillary coating.

Probe molecules were dissolved in dichloromethane to a concentration between 1-5 ppm. A Hewlett Packard 5890 Model II gas chromatograph (GC) was used for analysis. Split injection was utilized with a split ratio of 100:1 and a flow rate of 1.0 mL/min. The flow

rate was determined using a soap bubble flow-meter at the outlet of the GC column. Flame ionization detection was employed with injection and detection temperatures of 250 ºC. The column oven was set to a temperature of 70 ºC for all runs. Helium was used as the carrier gas, and methane was used to determine the dead volume of the column. Multiple linear regression analysis (MLR) was performed using Analyze-it software (Analyze-it Software Ltd., Leeds, England) and Excel (Microsoft, USA). All partition coefficients and binding constant plots were done using Excel, and fit to a line using the least squares method. Uncertainties in the slope and y-intercept values were used to determine the error in the reported partition coefficients and binding constants.

Results and Discussion

Theory. The equations here are similar to those used to determine the partition coefficients and binding constants of analytes in cyclodextrin GLC, and have been explained thoroughly in a previous work [26]. Briefly, the equilibrium of an analyte in an IL GC column involving micelles can be described by three partition coefficients (Figure 1):

$$S_{(g)} \xleftrightarrow{K_{GIL}} S_{(IL)} \qquad K_{GIL} = \frac{C_S^{IL}}{C_S^G} \tag{1}$$

$$S_{(g)} \xleftrightarrow{K_{GM}} S_{(M)} \qquad K_{GM} = \frac{C_S^M}{C_S^G} \tag{2}$$

$$S_{(IL)} \xleftrightarrow{K_{ILM}} S_{(M)} \qquad K_{ILM} = \frac{C_S^M}{C_S^{IL}} \tag{3}$$

where S is the analyte in the gas (G) and ionic liquid (IL) phases, and the micellar (M) pseudophase; C_S^G, C_S^{IL} and C_S^M are the concentrations of the analyte in the gas and ionic liquid phases and micellar pseudophase respectively; and K_{GIL}, K_{GM}, and K_{ILM} are the

respective partition coefficients (Figure 1). Therefore, the relationship between all three partition coefficients is as follows:

$$K_{GM} = K_{GIL} \cdot K_{ILM} \tag{4}$$

The measured apparent partition coefficient (K) obtained through experimental gas chromatography can be defined as

$$K = \frac{(m_S^{IL} + m_S^M)/(V_{IL} + V_M)}{m_S^G / V_G} \tag{5}$$

where m_S is the mass of the analyte in each respective phase and V is the volume of each phase. By substituting Eqn. 1, Eqn. 3, and the expression $C_M v_p = V_M/(V_{IL}+V_M)$ into Eqn. 5, the following expression is developed:

$$K = v_p K_{GIL}(K_{ILM} - 1)C_M + K_{GIL} \tag{6}$$

where C_M is the concentration of surfactant in the micellar phase, and v_p is the partial molar volume of the surfactant micelle. The surfactant concentration in the micellar phase may be calculated as the difference between the total surfactant concentration and the critical micelle concentration (CMC) of the surfactant in the ionic liquid. In this work, all CMC values were taken from ref. [22], and were determined using surface tension measurements. The partial molar volumes of each surfactant in their respective ionic liquid solvent are 0.269, 0.406, 3.509, and 0.931 M^{-1} for SDS, docSS, Brij700, and Brij35, as measured using the procedure described in the Methods section. Plotting K vs. C_M in Eqn. 6 allows all three partition coefficients to be determined. K_{GIL} can be found directly from the y-intercept, while the K_{ILM} = *slope/(y-int.*$\cdot v_p$*)+1*. K_{GM} may then simply be calculated using Eqn. 4.

The association of the analyte in the bulk ionic liquid phase with a micelle dissolved in the stationary phase also may be given in terms of a binding constant. The 1:1 complexation of the analyte (*S*) with the micelle (*M*) may be described by the equilibrium

$$S_{(IL)} + M_{(IL)} \xleftrightarrow{K_{eq}} S \cdot M_{(IL)} \qquad K_{eq} = \frac{C_{S \cdot M}}{C_S C_M} \tag{7}$$

where K_{eq} is the equilibrium binding constant. Using Eqn. 7 and the expression $C_M v_p = V_M/(V_{IL}+V_M)$, the relationship between K_{ILM} and K_{eq} may be derived

$$K_{eq} = K_{ILM} \cdot v_p \tag{8}$$

It is important to note that the partition coefficients and binding constants calculated here are expressed per surfactant monomer. Currently, the aggregation numbers of these micelles in ionic liquid solvents are unknown. However, as reported previously [23], the partition coefficients and binding constants per micelle may be easily calculated by multiplying their respective monomer values by the aggregation number.

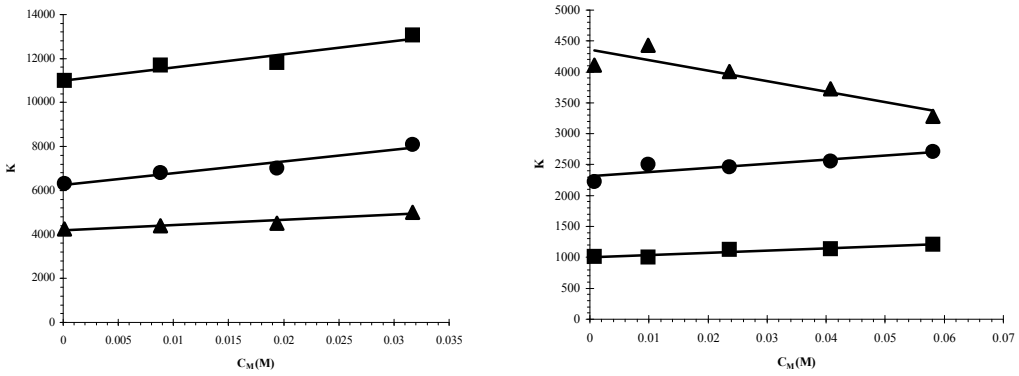

Figure 2. Plots of Eqn. 6 of cyclohexanol (■), acetophenone (●), and benzaldehyde (▲) on docSS-BMIMCl columns (left); and N,N-dimethylformamide (▲), pyrrole (●), and cyclohexanol (■) on Brij700-BMIMPF$_6$ columns (right).

Analyte Partitioning and Binding. The apparent partition coefficient (*K*) was plotted against the micellar surfactant concentration in the stationary phase (C_M) using Eqn.

6. Examples of these plots are shown in Figure 2. The resulting analyte partition coefficients with the BMIMCl columns and the $BMIMPF_6$ columns are shown in Tables 2 and 3 respectively.

Table 2. Partition coefficients of probe molecules with BMIMCl based micellar GLC columns.[a,b]

	SDS-BMIMCl			docSS-BMIMCl		
	K_{GIL}	K_{ILM}	K_{GM}	K_{GIL}	K_{ILM}	K_{GM}
Acetophenone	6350 ± 80	4.5 ± 1.2	28300 ± 7300	6250 ± 190	22.1 ± 4.2	138000 ± 26000
Benzaldehyde	3890 ± 130	8.0 ± 2.8	31200 ± 10900	4200 ± 90	14.8 ± 3.1	61900 ± 13100
Benzonitrile	5760 ± 10	3.8 ± 0.23	21900 ± 1300	6100 ± 20	13.2 ± 0.70	80500 ± 4200
Butanol	2580 ± 100	10.7 ± 3.2	27700 ± 8200	2760 ± 60	13.6 ± 2.8	37400 ± 7700
Cyclohexanol	10400 ± 300	11.3 ± 2.7	117000 ± 28000	11000 ± 300	14.5 ± 3.1	159000 ± 34000
Cyclohexanone	670 ± 40	9.7 ± 4.7	6420 ± 3140	640 ± 20	15.8 ± 7.9	10100 ± 5100
1,2-Dichlorobenzene	2000 ± 80	8.2 ± 3.5	16400 ± 7000	1830 ± 90	23.5 ± 10.1	43000 ± 18600
N,N-Dimethylformamide	1770 ± 80	9.2 ± 3.9	16200 ± 6900	1940 ± 30	8.7 ± 3.7	16900 ± 7200
Ethylphenylether	--	--	--	820 ± 30	26.0 ± 7.6	21300 ± 6300
Naphthalene	8380 ± 40	7.1 ± 0.45	59400 ± 3800	7930 ± 480	31.9 ± 8.3	253000 ± 68000
Nitrobenzene	10200 ± 400	7.3 ± 3.3	74000 ± 33800	10700 ± 300	16.3 ± 3.8	175000 ± 42000
1-Nitropropane	500 ± 10	10.1 ± 1.4	5150 ± 720	550 ± 10	10.7 ± 5.1	5880 ± 2810
1-Octanol	17900 ± 20	8.4 ± 0.079	149000 ± 1400	17300 ± 700	23.8 ± 5.6	411000 ± 99000
Octyl Aldehyde	--	--	--	440 ± 30	42.3 ± 15.3	18700 ± 6900
Pyridine	420 ± 10	9.6 ± 0.90	4050 ± 380	440 ± 20	20.8 ± 5.9	9230 ± 2640
Pyrrole	--	--	--	30600 ± 200	4.9 ± 1.8	149000 ± 56000
o-Xylene	--	--	--	270 ± 10	27.5 ± 10.0	7340 ± 2700

[a] All partition coefficients are expressed per monomer surfactant.
[b] Dashes indicate partition coefficients were not measured on this series of columns.

Generally, for the SDS-BMIMCl and docSS-BMIMCl stationary phases, the probe molecules studied all preferentially partitioned to the micelle pseudophase over the bulk ionic liquid component. All partition coefficients between the gas phase and the micelle pseudophase (K_{GM}) are significantly larger than those between the gas phase and the bulk ionic liquid portion of the stationary phase (K_{GIL}). Likewise K_{ILM}, the solute partitioning directly between the ionic liquid and the micelle, are all greater than 1, indicating preference toward the micellar pseudophase over the ionic liquid. As a result, the introduction of these micellar

pseudophases to the BMIMCl stationary phase resulted in greater solute retention. In almost all cases, docSS micelles had a greater ability to solubilize these probe molecules than SDS in the BMIMCl ionic liquid, as shown by their larger K_{ILM} and K_{GM} values.

Table 3. Partition coefficients of probe molecules with $BMIMPF_6$ based micellar GLC columns.[a,b]

	Brij700-$BMIMPF_6$			Brij35-$BMIMPF_6$		
	K_{GIL}	K_{ILM}	K_{GM}	K_{GIL}	K_{ILM}	K_{GM}
Acetic Acid	610 ± 80	8.7 ± 1.6	5350 ± 1220	890 ± 90	4.1 ± 1.2	3660 ± 1120
Acetophenone	8520 ± 340	2.5 ± 0.80	21100 ± 6900	10400 ± 400	0.3 ± 0.1	3420 ± 900
Aniline	14500 ± 700	2.8 ± 0.94	41000 ± 13800	14300 ± 2300	1.9 ± 1.8	27100 ± 26200
Benzaldehyde	4110 ± 180	0.5 ± 0.4	2070 ± 1560	4710 ± 170	0.4 ± 0.2	1900 ± 710
Benzonitrile	5530 ± 120	1.2 ± 1.0	6880 ± 5320	5630 ± 190	1.4 ± 0.71	7970 ± 4020
Butanol	190 ± 2	2.0 ± 0.20	390 ± 40	200 ± 10	1.7 ± 0.39	360 ± 80
2-Chloroaniline	20400 ± 500	2.3 ± 0.37	46600 ± 7600	21700 ± 420	2.1 ± 0.23	45700 ± 5100
1-Chlorohexane	200 ± 20	1.9 ± 1.3	390 ± 270	--	--	--
p-Cresol	28000 ± 2400	6.9 ± 1.1	192000 ± 34000	36000 ± 3200	2.8 ± 0.87	99600 ± 32600
Cyclohexanol	1000 ± 30	2.0 ± 0.42	2040 ± 420	1100 ± 10	1.3 ± 0.15	1460 ± 170
Cyclohexanone	--	--	--	1560 ± 100	0.2 ± 0.1	190 ± 140
1,2-Dichlorobenzene	1370 ± 270	3.7 ± 2.4	5130 ± 3400	1640 ± 50	1.4 ± 0.61	2270 ± 1000
N,N-Dimethylformamide	4360 ± 150	0.03 ± 0.01	130 ± 30	4180 ± 190	0.4 ± 0.2	1650 ± 750
Dioxane	290 ± 10	0.7 ± 0.4	190 ± 130	--	--	--
Ethylphenylether	1370 ± 70	1.7 ± 1.1	2290 ± 1460	--	--	--
Methyl Caproate	440 ± 70	3.6 ± 2.5	1590 ± 1150	--	--	--
Naphthalene	8850 ± 200	1.9 ± 0.43	16400 ± 3800	6800 ± 770	3.6 ± 1.0	24600 ± 7530
Nitrobenzene	9670 ± 190	1.4 ± 0.57	13800 ± 5480	9970 ± 300	1.5 ± 0.59	14500 ± 5900
1-Nitropropane	700 ± 10	2.4 ± 0.35	1700 ± 250	--	--	--
1-Octanol	1940 ± 150	3.0 ± 1.0	5780 ± 2030	2240 ± 50	1.5 ± 0.40	3270 ± 900
Octyl Aldehyde	950 ± 100	2.2 ± 1.8	2050 ± 1710	--	--	--
Phenol	17900 ± 1800	7.0 ± 1.2	125000 ± 25000	21700 ± 300	4.0 ± 0.16	87100 ± 3700
Proprionitrile	270 ± 7	0.4 ± 0.10	100 ± 30	300 ± 2	0.10 ± 0.0048	24.9 ± 1.4
Pyridine	540 ± 4	2.9 ± 0.14	1580 ± 80	--	--	--
Pyrrole	2310 ± 70	1.8 ± 0.55	4220 ± 1280	2390 ± 60	1.8 ± 0.33	4370 ± 800
Toluene	170 ± 20	4.0 ± 2.2	700 ± 400	220 ± 30	0.01 ± 0.05	1.6 ± 1.3

[a] All partition coefficients are expressed per monomer surfactant.
[b] Dashes indicate partition coefficients were not measured on this series of columns.

Similar trends can also be seen for the solute partitioning that involves the Brij700-$BMIMPF_6$ and Brij35-$BMIMPF_6$ stationary phases (Table 3). However, in several cases the

probe molecules exhibited more partitioning to the ionic liquid phase than the micelle pseudophase ($0<K_{ILM}<1$). Plots of Eqn. 6 of these analytes will produce slopes that are negative or near zero (e.g. N,N-dimethylformamide with Brij700-BMIMPF$_6$ in Figure 2). This behavior is likely due to an excluded volume effect. Since the analyte preferentially partitions to the ionic liquid over the micellar pseudophase, the apparent partition coefficient of the analyte to the stationary phase decreases with increasing surfactant concentration as more of the stationary phase volume is occupied by micelles. Identical partitioning behavior has been observed previously for micellar LC and TLC [27]. On average, Brij700 achieved higher K_{ILM} and K_{GM} values than Brij35.

Table 4. Binding constants (K_{eq}) of probe molecules to micelles within RTIL stationary phases.[a,b]

	SDS-BMIMCl	docSS-BMIMCl	Brij700-BMIMPF$_6$	Brij35-BMIMPF$_6$
Acetic Acid	--	--	30.6 ± 5.8	3.8 ± 1.1
Acetophenone	1.2 ± 0.3	9.0 ± 1.7	8.7 ± 2.8	0.3 ± 0.1
Aniline	--	--	9.9 ± 3.3	1.8 ± 1.7
Benzaldehyde	2.2 ± 0.8	6.0 ± 1.3	1.8 ± 1.3	0.4 ± 0.1
Benzonitrile	1.0 ± 0.1	5.4 ± 0.3	4.4 ± 3.4	1.3 ± 0.7
Butanol	2.9 ± 0.8	5.5 ± 1.1	7.1 ± 0.7	1.6 ± 0.4
2-Chloroaniline	--	--	8.0 ± 1.3	2.0 ± 0.2
1-Chlorohexane	--	--	6.7 ± 4.6	--
p-Cresol	--	--	24.1 ± 3.7	2.6 ± 0.8
Cyclohexanol	3.0 ± 0.7	5.9 ± 1.2	7.2 ± 1.5	1.2 ± 0.1
Cyclohexanone	2.6 ± 1.3	6.4 ± 3.2	--	0.2 ± 0.1
1,2-Dichlorobenzene	2.2 ± 0.9	9.5 ± 4.1	13.1 ± 8.3	1.3 ± 0.6
N,N-Dimethylformamide	2.5 ± 1.0	3.6 ± 1.5	0.10 ± 0.03	0.4 ± 0.2
Dioxane	--	--	2.3 ± 1.6	--
Ethylphenylether	--	10.5 ± 3.1	5.9 ± 3.7	--
Methyl Caproate	--	--	12.6 ± 8.9	--
Naphthalene	1.9 ± 0.1	13.0 ± 3.4	1.9 ± 0.4	3.4 ± 1.0
Nitrobenzene	2.0 ± 0.9	6.6 ± 1.6	5.0 ± 2.0	1.4 ± 0.6
1-Nitropropane	2.7 ± 0.4	4.3 ± 2.1	8.5 ± 1.2	--
1-Octanol	2.2 ± 0.1	9.6 ± 2.3	10.5 ± 3.6	1.4 ± 0.4
Octyl Aldehyde	--	17.2 ± 6.2	7.6 ± 6.3	--
Phenol	--	--	24.5 ± 4.3	3.7 ± 0.1
Proprionitrile	--	--	1.2 ± 0.3	0.09 ± 0.00
Pyridine	2.6 ± 0.2	8.5 ± 2.4	10.2 ± 0.5	--
Pyrrole	--	2.0 ± 0.7	6.4 ± 1.9	1.7 ± 0.3
Toluene	--	--	14.1 ± 7.9	0.01 ± 0.00
o-Xylene	--	11.2 ± 4.1	--	--

[a] All binding constants are expressed per monomer surfactant.
[b] Dashes indicate binding constants were not measured on this series of columns.

As mentioned previously, the solute equilibrium between the bulk ionic liquid and the micelle component of the stationary phase may also be expressed as an association constant. These calculated values based on Eqn. 8 are shown in Table 4. Most probe molecules shown moderate binding to the micelles, and had the greatest affinity for docSS in BMIMCl and Brij700 in $BMIMPF_6$.

In addition to increasing the retention of these probe molecules, the micellar pseudophase also greatly affects the selectivity of the GLC stationary phase by differentially partitioning solutes. For example, upon the addition of 78.1 mM of Brij700 (to 78.1 mM) surfactant to the $BMIMPF_6$ stationary phase, the separation factor ($\alpha=K_2/K_1$) of 2-chloroaniline and phenol increased from 1.09 to 1.62. Similarly, the α of octyl aldehyde and pyridine was improved from 1.01 to 1.83 by using 36.4 mM of docSS as an additive in the BMIMCl stationary phase. However, in a few cases micelles in the RTIL stationary phase hindered the separation by providing selectivity opposite to that of the bulk liquid component of the stationary phase (See K_{GIL} and K_{GM} in Tables 2 and 3). For instance, cyclohexanol and cyclohexanone exhibited a decrease in their α value (1.42 to 1.11) with the addition of 390.2 mM Brij35 to $BMIMPF_6$.

Characterization of Micelle-IL Stationary Phases. As discussed in the introduction, the complex structure of ionic liquids allows numerous types of solvation interactions to occur, and the introduction of a micellar pseudophase to an ionic liquid can enhance certain interactions [22]. In order to further elucidate the interactions that are involved in probe molecule partitioning to the ionic liquid and micelle components of the stationary phase, the Abraham solvation parameter model was used to characterize these stationary phases [28]. This model utilizes a linear free energy equation that relates a

dependent variable to a series of interaction parameters of the probe molecule and target solvent.

$$\log k = c + rR_2 + s\pi_2^H + a\alpha_2^H + b\beta_2^H + l\log L^{16} \quad (9)$$

The dependent variable may be a solute retention factor (log *k*), partition coefficient (log *K*), or the Ostwald solubility coefficient (log *L*). Each probe molecule possesses a unique set of solute descriptors that are dependent on their structural groups, and therefore the types of solute-solvent interactions it may undergo. These descriptors are the solute's excess molar refraction (R_2), polarizability/dipolarity (π_2^H), hydrogen bond acidity (α_2^H) and basicity (β_2^H), and gas-hexadecane partition coefficient at 298K (L^{16}). The descriptors for all probe molecules in this study are listed in Table 1. In this approach, the stationary phase is characterized by inverse GC by injecting a large number of probe molecules (whose interaction capabilities are known) onto the column of interest. Using the measured solute retention factors and multiple linear regression analysis (Eqn. 9), the interaction parameters of the stationary phase (*r, s, a, b, l*) may be determined. These coefficients are as follows: *r* is the ability of the stationary phase to interact with π- and n-electrons of the solute, *s* is the polarizability/dipolarity of the stationary phase, *a* indicates the stationary phase hydrogen bond basicity, *b* is the hydrogen bond acidity, and *l* is a measure of the dispersion forces and ability of the stationary phase to distinguish between members of a homologous series. This method is described in more detail in another reference [28].

The calculated interaction parameters of the four micelle-ionic liquid stationary phases used here are shown in Table 5, as well as those of the BMIMCl and $BMIMPF_6$ stationary phases with no surfactant from ref. [2]. Clearly, the addition of a micellar pseudophase to the ionic liquid stationary phase has a significant influence on the magnitude

of its solvation interactions. Figure 3 shows the change in the interaction parameters of the stationary phases upon addition of surfactant. All four surfactants enhanced the hydrogen bond basicity of the stationary phase considerably, likely by providing numerous oxygen-based lone pair electrons. The Brij 700 and 35 surfactants increased the *a* term more than SDS and docSS due to their repeating oxyethylene subunits (100 and 23 respectively). However, the *a* term only has an effect on retention if the probe molecule is a hydrogen bond donor. The Brij surfactants also increased the level of π-π and n-π interactions (*r* term) and the degree of dipolar interaction (*s* term). Neither SDS nor docSS significantly affected the dipolarity/polarizability of the stationary phase, however SDS decreased the *r* term slightly. Interestingly, the nonionic surfactants decreased the amount of dispersion interaction provided by the BMIMPF$_6$ stationary phase, while the ionic surfactants in BMIMCl increased the *l* term. Despite the relatively small change in the *l* term, this shift has a major effect on retention since log L^{16} is the largest solute descriptor term (Table 1). This effect can be seen in Figure 4, which shows the change in the Abraham equation terms (Eqn. 9) for 1-octanol upon addition of surfactant to the ionic liquid stationary phase.

Table 5. Interaction parameters of RTIL stationary phases at 70 ºC based on Eqn. 9. [a]Data from reference [2].

		Interaction parameters							
Stationary Phase	[Surf.]	*c*	*r*	*s*	*a*	*b*	*l*	*n*	R^2
BMIM-Cl[a]	0 mM	-2.841	0.291	2.007	5.230	0.000	0.445	22	0.98
BMIM-Cl w/ SDS	119.1 mM	-3.008	0.248	2.008	5.327	0.000	0.481	19	0.98
BMIM-Cl w/ docSS	24.1 mM	-3.001	0.293	2.011	5.274	0.000	0.468	18	0.98
BMIM-PF$_6$[a]	0 mM	-2.622	0.000	1.695	1.579	0.000	0.515	33	0.99
BMIM-PF$_6$ w/ Brij700	60.7 mM	-2.704	0.172	1.904	2.102	0.000	0.468	30	0.96
BMIM-PF$_6$ w/ Brij35	303.9 mM	-2.958	0.143	2.030	2.262	0.000	0.482	29	0.99

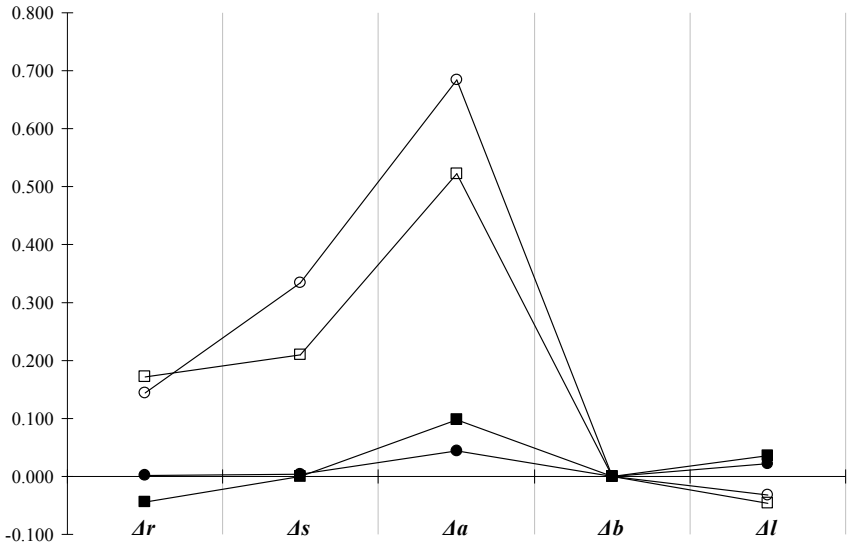

Figure 3. Change in stationary phase interaction parameters upon addition of surfactant for 119.1 mM SDS in BMIMCl (■), 24.1 mM docSS in BMIMCl (●), 60.7 mM Brij700 in $BMIMPF_6$ (□), and 303.9 mM Brij35 in $BMIMPF_6$ (○).

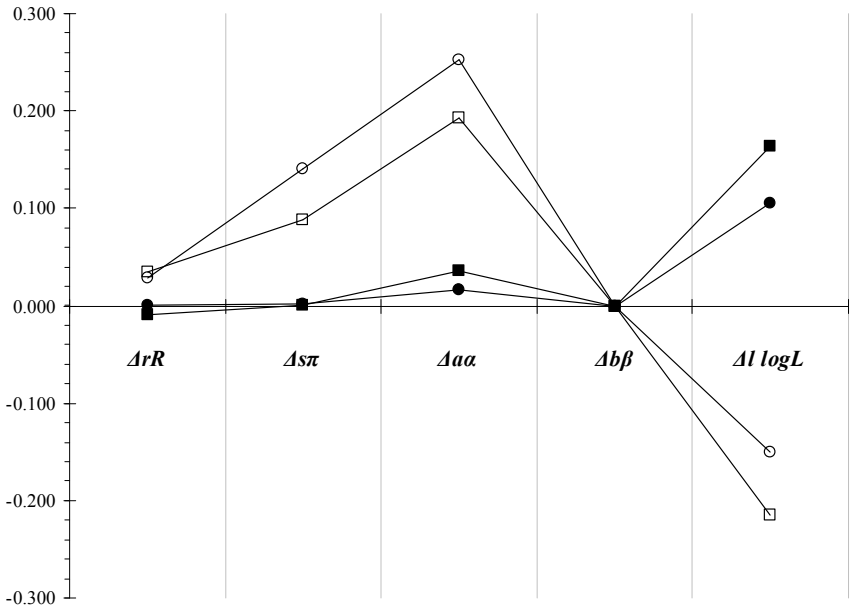

Figure 4. Change in Abraham equation terms of 1-octanol upon addition of surfactant for 119.1 mM SDS in BMIMCl (■), 24.1 mM docSS in BMIMCl (●), 60.7 mM Brij700 in $BMIMPF_6$ (□), and 303.9 mM Brij35 in $BMIMPF_6$ (○).

Based on these data and the partition coefficients and binding constants in Tables 2-4, the analytes that partition most strongly to the Brij surfactants are those that have large α_2^H values (are good hydrogen bond donors). These include solutes such as acetic acid, *p*-cresol, and phenol. Alternately, probe molecules with high log L^{16} terms (naphthalene, octyl aldehyde, and ethylphenylether) associated most strongly with the ionic surfactants, especially docSS. SDS and docSS may be particularly useful as a pseudophase additive to BMIMCl GLC stationary phases for the separation of homologous series of compounds. However, the nonionic Brij surfactants are likely more beneficial for separating arrays of acids and hydrogen bond donor molecules.

Conclusions

The effects of a micellar pseudophase in ionic liquid based GLC stationary phases were examined using the "three-phase" model and Abraham solvation parameters. Generally, probe molecule partitioning to the micellar pseudophase was greater than to the bulk ionic liquid, resulting in an increase in retention with increasing micelle concentration. Furthermore, the addition of surfactant to the ionic liquid stationary phase significantly altered the selectivity of the column. This allows certain solvation attributes of the stationary phase to be enhanced without changing the type ionic liquid used in the coating. All four surfactants (SDS, docSS, Brij700, and Brij35) increased the hydrogen bond basicity of the stationary phase. SDS and docSS increased the level of dispersion interaction in BMIMCl, while this term was decreased by Brij700 and Brij35 in $BMIMPF_6$. Probe molecules that can interact strongly with the stationary phase *via* these interactions were most heavily partitioned to the micelles. As a result, it is possible to predict which analytes will be most highly retained by these micellar-IL stationary phases. Furthermore, SDS and docSS may be

useful as additives to BMIMCl stationary phases for the separation of homologous series of compounds. The Brij surfactants, however, may be used to improve the selectivity of hydrogen bond donor and acidic analytes with $BMIMPF_6$ columns.

References

[1] T. Welton, Chem. Rev., 99 (1999) 2071.

[2] J.L. Anderson, J. Ding, T. Welton, D.W. Armstrong, J. Am. Chem. Soc., 124 (2002) 14247.

[3] S. Carda-Broch, A. Berthod, D.W. Armstrong, Anal. Bioanal. Chem., 375 (2003) 191.

[4] S. Chun, S.V. Dzyuba, R.A. Bartsch, Anal. Chem., 73 (2001) 3737.

[5] P. Bonhôte, A. Dias, N. Papageorgiou, K. Kalyanasundaram, M. Grätzel, Inorg. Chem., 35 (1996) 1168.

[6] T.D. Avery, N.F. Jenkins, M.C. Kimber, D.W. Lupton, D.K. Taylor, Chem. Commun., (2002) 28.

[7] H.M. Zerth, N.M. Leonard, R.S. Mohan, Org. Lett., 5 (2003) 55.

[8] P. Lozano, T. De Diego, D. Carrié, M. Vaultier, J.L. Iborra, J. Mol. Catal. B, 21 (2003) 9.

[9] A.M. Leone, S.C. Weatherly, M.E. Williams, H.H. Thorp, R.W. Murray, J. Am. Chem. Soc., 123 (2001) 218.

[10] V.E. Dickinson, M.E. Williams, S.M. Hendrickson, H. Masui, R.W. Murray, J. Am. Chem. Soc., 121 (1999) 613.

[11] D.W. Armstrong, L. Zhang, L. He, M.L. Gross, Anal. Chem., 73 (2001) 3679.

[12] E.G. Yanes, S.R. Gratz, M.J. Baldwin, S.E. Robison, A.M. Stalcup, Anal. Chem., 73 (2001) 3838.

[13] D.W. Armstrong, L. He, Y. Liu, Anal. Chem., 71 (1999) 3872.

[14] A. Heintz, D.V. Kulikov, S.P. Verevkin, J. Chem. Eng. Data, 46 (2001) 1526.

[15] A. Heintz, D.V. Kulikov, S.P. Verevkin, J. Chem. Thermodyn., 34 (2002) 1341.

[16] J.L. Anderson, D.W. Armstrong, Anal. Chem., 75 (2003) 4851.

[17] J.L. Anderson, D.W. Armstrong, Anal. Chem., 77 (2005) 6453.

[18] J.L. Anderson, R. Ding, A. Ellern, D.W. Armstrong, J. Am. Chem. Soc., 127 (2005) 593.

[19] J. Ding, T. Welton, D.W. Armstrong, Anal. Chem., 76 (2004) 6819.

[20] D.W. Barber, C.S.G. Phillips, G.F. Tusa, A. Verdin, J. Chem. Soc., (1959) 18.

[21] J.E. Gordon, J.E. Selwyn, R.L. Thorne, J. Org. Chem., 31 (1966) 1925.

[22] J.L. Anderson, V. Pino, E.C. Hagberg, V.V. Sheares, D.W. Armstrong, Chem. Commun., (2003) 2444.

[23] D.W. Armstrong, F. Nome, Anal. Chem., 53 (1981) 1662.

[24] H. Nishi, T. Fukuyama, S. Terabe, J. Chromatogr., 553 (1991) 503.

[25] A.W. Lantz, S.M. Wetterer, D.W. Armstrong, Anal. Bioanal. Chem., 383 (2005) 160.

[26] V. Pino, A.W. Lantz, J.L. Anderson, A. Berthod, D.W. Armstrong, Anal. Chem., (2005) in press.

[27] D.W. Armstrong, G.Y. Stine, J. Am. Chem. Soc., 105 (1983) 6220.

[28] M.H. Abraham, Chem. Soc. Rev., 22 (1993) 73.

CHAPTER 6. GENERAL CONCLUSIONS

Future Research

The study of equilibria and interaction phenomenon is a nearly endless area of research in that numerous newly synthesized compounds and pharmaceuticals are developed each year. Furthermore, our ever-increasing understanding of biological systems necessitates the study of interactions between various biomolecules and receptor sites in cells. The activity of these compounds in a particular system is highly dependent on their ability to complex with their target molecules. Therefore, the measurement of association constants will be a continuing field of research for the foreseeable future.

As shown in previous chapters of this dissertation, cyclodextrins are capable of complexing with a wide variety of hydrophobic analytes. Furthermore, these macromolecules are environmentally friendly and nontoxic. Future research could aim to further study cyclodextrins' ability to solubilize and extract hydrophobic compounds, and also examine the effect of cyclodextrin complexation on the degradation of hydrolytically unstable molecules. The sequestering, degradation, and/or removal of pesticides and herbicides are of particular interest today, due to these chemicals' known toxicity and the recent focus on pesticide residues in consumer food products. Many of these compounds are relatively hydrophobic, allowing them to adhere strongly to agricultural and food products even during periods of irrigation or rain. Furthermore, it has been reported that many modern pesticides gradually undergo hydrolytic degradation. Therefore, these substances are excellent model analytes for analyte-cyclodextrin binding and decomposition studies. Preliminary studies have indicated that cyclodextrins are indeed capable of moderately strong

interactions with pesticides. Also, it has been shown that complexation with cyclodextrins can catalyze the degradation of hydrolytically unstable compounds. Therefore, the ability of cyclodextrins to sequester, solubilize, and hasten the degradation of toxic pesticide and herbicide residues would be particularly useful. In addition, cyclodextrins have many advantages over other sequestering techniques including low cost (<$4/kg.), negligible toxicity, and the fact that they are safely metabolized by the body. Further studies are necessary however to 1) understand the effects of cyclodextrin size and derivatization, analyte structure, and solution pH on the strength of the analyte-cyclodextrin complex and analyte degradation, and 2) demonstrate the effectiveness of cyclodextrins as complexation agents for a wide variety of pesticide and herbicide compounds. Moreover, the ability of cyclodextrin to bind to several commonly used pesticides, including endosulfan and chlorpyrifos, has not yet been studied. The effect of cyclodextrin derivatization and cavity size on the rate of analyte degradation may also be studied by using α-, β-, and γ-cyclodextrins whose rim hydroxyls have been substituted with charged and bulky groups.

Another natural extension of the research presented in this section of the dissertation however would be to apply the three-phase model used to describe the partitioning of an analyte is pseudophase gas-liquid chromatography to other separation techniques. A three-phase system also exists in capillary electrophoresis methods that utilize two dissolved pseudophases in the run buffer. One such technique is cyclodextrin modified micellar capillary electrophoresis (CD-MCE). Initially introduced in the early 1990s, CD-MCE is a useful technique that allows the enantioseparation of hydrophobic analytes by using multiple pseudophases (cyclodextrins and micelles) dissolved in the run buffer. Three analyte equilibria are produced with this method: partitioning of the analyte between 1) the run

buffer and dissolved cyclodextrin, 2) the run buffer and the micelle, and 3) the cyclodextrin and micelle directly. Occasionally, sufficient enantioselectivity for a baseline separation cannot be achieved using a single cyclodextrin species, and therefore the micellar pseudophase may be replaced by another cyclodextrin of different charge (and mobility). Interestingly, the three-phase model has never been completely applied to this technique due to either complexities of surfactant-cyclodextrin binding that skew the traditional three-phase equation plots or inaccurate estimations of the analyte-cyclodextrin complex mobility. Therefore, future research could be aimed at deriving proper equations that describe the partitioning of an analyte between all three phases involved in multi-pseudophase capillary electrophoresis. These equations could then be tested experimentally by applying enantioseparation data for a wide variety of chiral analytes using this technique.

Understanding the contributions of all three equilibria to retention and selectivity would greatly benefit the design and optimization process of these separation techniques. Currently, optimization of CE separations utilizing two pseudophases entails altering the concentration ratios of the two pseudophases to determine the ideal conditions that produce the best peak-to-peak separation. This process can be relatively time consuming. By effectively modeling the separation mechanisms and measuring the binding constants of an analyte to the two pseudophases, one could theoretically calculate the ideal concentrations that would maximize selectivity. Furthermore, in cases in which there are multiple cyclodextrin pseudophases, the contribution of each cyclodextrin species to enantioselectivity can be calculated as well. Such equations would greatly speed method development.

Finally, surfactants offer another unique area of future research to pursue. Surfactants are used widely in industrial applications, yet are rarely pure and usually a mixture of

different surfactants. However despite surfactants widespread use, very few studies have been performed that quantitatively measure the effect of introducing an additional surfactant species on the solvation properties of micelles (i.e. mixed micelles). Previous studies have shown that micelles composed of similar structures exhibit nearly ideal thermodynamics of mixing. However, mixed micelles of two or more anionic, cationic, or nonionic surfactants show deviations from ideality. Therefore, there is a great interest in studying and understanding the effects that lead to mixed micelles' solubilization abilities and how they change with varying surfactant ratios. Unlike simple organic solvents, micelles are capable of a wide variety of interaction types including hydrophobic, dipole-dipole, hydrogen bonding, and electrostatic interactions. By examining the relationship between the relative concentrations of the two surfactants and the solvation parameters of the mixed micelles, one may gain better understanding into the solubilization properties of the mixed micelle system. Initial studies on the interaction properties of pure surfactants have indicated that solubilization of organic molecules is greatly promoted by larger micelle volumes and hindered by micelles with increased hydrogen bond basicity. Therefore, studying how mixed micelles' parameters of hydrogen bonding change with varying surfactant ratios would be of particular interest.

The solvation parameters of a wide variety of mixed micelles could be measured using the Abraham solvation parameter model. The solvation parameters of the mixed micelles could then be examined in relation to the surfactant ratio to determine if a linear or nonlinear relationship exists. Nonlinear relationships would suggest that 1) the ratio of surfactants in the mixed micelle may be different than the ratio of free surfactants or 2) that there are significant interactions between the surfactant species in the micelle producing

unique solvation characteristics. In addition, the effect of the surfactants' nonpolar chain length may be examined by studying homologous series of surfactants.

Conclusions

In Part 1 of this dissertation, we have reviewed the general methods for measuring binding constants and partition coefficients, and discussed the mathematical treatment of the data to gather information regarding the magnitude and types of interactions involved in solute-ligand associations. The proper understanding of these concepts allows important information regarding the thermodynamic nature of chemical processes to be elucidated. Here, we have shown that cyclodextrins are capable of including a wide array of malodorous compounds with varying degrees. The formation of analyte-cyclodextrin complexes that precipitate out of solution is of particular interest as it greatly increases the cyclodextrin's ability to suppress and extract odor. Volatile compounds may also bind with cyclodextrin and its derivatives, however to a lesser extent. The aqueous solubility of these vapors increases in the presence of dissolved cyclodextrin, as a result of the three-phase equilibria that is established. It was also shown that this three-phase equilibria system is analogous to the solute partition equilibria of cyclodextrin gas-liquid chromatography and equations were developed to model this system. The contributions to retention and selectivity for all three equilibria could be ascertained. Finally, the equations developed to model pseudophase gas-liquid chromatography were applied to a new class of GC columns: micellar ionic liquid stationary phases. This methodology allowed us to probe the solvation interactions of the ionic liquid and micellar components of the stationary phase. Such studies are particularly useful in understanding the types of interactions that are responsible for separation

selectivity, and this in turn provides insight into the types of molecules that a particular stationary phase is selective towards.

PART II: DEVELOPMENT OF A RAPID TEST FOR MICROBIAL CONTAMINATION

CHAPTER 1. GENERAL INTRODUCTION

Introduction

As of the late 1990s, the global industrial microbiology testing market was estimated at almost $2 billion annually, a majority of these tests are being performed in the food and pharmaceutical industries for routine product safety checks.[1] In addition to these fields, the medical and public sectors (e.g. water treatment, homeland security, etc.) also have a considerable need for rapid and accurate microbial tests to confirm the absence of pathogenic species on medical supplies and water sources. Nonspecific tests for the detection and analysis of all microbial contaminants account for over 75% of microbiological tests. Most of the remaining percentage of methodologies target specific indicator organisms (such as coliforms, unicellular fungi, or mold) that point toward the presence of other more pathogenic species. Only a minor fraction of the microbial tests performed in industry are used to detect specific cellular contaminants in a sample.[1] Sterility testing is essential in industry to ensure consumer/patient safety, maintain product quality, and meet regulatory requirements.

However current standard methods for sterility testing are greatly lacking in numerous aspects. In fact, most methods still in widespread use today are based on techniques over 100 years old. For example, direct inoculation was originally developed for the isolation and identification of diseases in the late 1800s. Using this method, a growth media or agar is inoculated with a sample and any microorganisms present are allowed to grow under a certain set of conditions. The plate or solution is then inspected visually for colony formation or turbidity. This traditional culture method is still the "gold standard" of

current sterility tests.[2] Microbiological tests that rely on the growth of bacteria/fungi fail to meet the demands of modern industry, mainly due to the slow speed of analysis. According to the U.S. Pharmacopeia, growth media inoculated with a sample must be allowed to incubate for 14 days before a definitive results may be established concerning the sample's sterility.[2] Furthermore, microorganisms may differ in their requirements for nutrients, cofactors or other environmental conditions, the absence of which can impact their ability to grow in synthetic media. Sub-lethal injury (induced via heat, salt, starvation, antimicrobial or other environmental stress) is another potentially confounding factor affecting microbial growth. As a result, direct inoculation based methods may be biased – able to only detect only those contaminants capable of growing under the conditions used. Currently, it is estimated that defined methodologies exist to culture less than 2% of microorganisms on earth, highlighting the potential limitations of growth based detection methods.[3] Therefore, since no one set of conditions will grow all bacteria or fungi, growth based sterility tests are also fundamentally flawed in the conclusiveness of their results.[4]

Because of these factors and the increasing demand on industries to become more streamlined (*i.e.* producing products more cheaply and quickly with no loss in quality), new methods of microbiological analysis are being developed that lack many of the shortcomings of traditional methods. Impedance measurements may be used for detecting the presence of living organisms within a sample. Growth media often are comprised of large uncharged (or near net neutral) molecules such as fats, proteins, carbohydrates, etc. Microbes metabolize these nutrients into smaller components (organic acids, amino acids, etc.), which are usually charged. As a result of this metabolic process the resistance and conductivity of the growth media changes. By monitoring the impedance of the sample under constant voltage, the

presence of viable organisms may be detected. A change in the conductivity of the sample can usually be detected once the culture grows to ~10^6 cells/mL.[5] While this may be used to detect a variety of microorganisms, it still retains some of the basic flaws of plating methods, such as media specific growth and long analysis time.

Another nonspecific technique for the detection of viable organisms in a sample utilizes bioluminescence. Here, adenosine triphosphate (ATP), which is present in all living cells, is used to oxidize D-luciferin *via* the luciferase enzyme. This process, in the presence of oxygen and magnesium ions, produces light that may then be detected by a luminometer. The level of light emitted is proportional to the amount of ATP, and therefore the approximate microbial load, in the sample. However since the level of ATP may vary between individual cells and between species, this technique is often used strictly as a test for the presence/absence of cells in a sample. ATP-bioluminescence is a rapid technique, capable of producing a result within minutes, and is relatively simple to perform. However, several drawbacks exist. The technique's low sensitivity (~10^3 cells) requires that a preconcentration or growth step be used for a true sterility determination, increasing the length of the test to 24 hours or more. The enzymatic reaction is also sensitive to the sample matrix in that other components in the system may quench bioluminescence. Unfortunately, the process of releasing ATP from the cells results in cell lysis, making any further microbial analysis impossible.[6]

Flow cytometry is a popular technique that allows characterization and counting of cell populations on a single cell basis.[7] Flow cytometry is a general analytical technique that can be applied to many different aspects of cell physiology, including viability. For example, a sample may be stained by the passive diffusion of a fluorescein-like derivative which is

subsequently metabolized within the cell to a fluorescent form. Cells are then passed one-by-one in front of a laser and their fluorescence signal is detected. Other fluorescent tags may be used to identify cell type or monitor cellular processes. Higher-end instruments may also be able to physically sort the resulting populations based on cell fluorescence. The technique is highly sensitive (single cell) and analysis times usually run on the order of several hours. However, most flow cytometers are designed as basic research instruments, and are therefore fairly expensive and difficult to maintain. It is unlikely that anything but lower-end, task-dedicated machines will be adopted for routine use in the sterility analyses of bulk samples. Flow cytometry-based sterility tests are presently capable of detecting ~10 cells/mL. Additional increases in sensitivity are needed to detect individual contaminant cells.[8]

Several other techniques currently exist for the detection and analysis of specific microorganisms in a sample. Enzyme immunoassays can be used to detect the presence of particular types of bacteria.[9] In these techniques specific antibodies (free or bound to a substrate) interact with antigens on the surface of the target cells. This interaction is then usually monitored *via* enzymatic techniques and fluorescence. Total analysis times usually run between 24-48 hours with detection limits of immunoassays around 10^4 cells/mL, making pre-enrichment a necessity. Non-specific binding may also produce false-positives. Immuno-magnetic separations (IMS) are being explored as ways to couple organism-specific pre-concentration with immunoassay or other test formats. IMS utilizes super-paramagnetic beads with attached antibodies that may bind to certain bacterial strains. After the beads bind to the cells (within 1 hr), a magnet may be used to isolate the bound cells from the remaining matrix. Often times, IMS is used as a preconcentration method for other molecular-based detection techniques.[9]

Molecular-based techniques allow the characterization and identification of specific types or species of microorganisms by detecting the presence of certain molecular components in the cell (e.g. DNA or RNA sequences). The polymerase chain reaction (PCR) is a commonly applied technique for amplifying organism-specific nucleic acid sequences. PCR utilizes short DNA sequences (primers) to direct the DNA polymerase-mediated synthesis of target sequences. Although DNA replication is linear in the first few rounds of PCR, it quickly becomes exponential, enabling low quantities of specific sequences to be detected against a high background of non-target DNA. After amplification, an external method, such as gel electrophoresis may be used to verify that the PCR product matches the size of the expected sequence. Alternatively, amplicon-specific probes can be used to detect the presence of the expected products as they are formed (e.g. real-time PCR). Generally, around 10^3 cells/mL are necessary for reliable DNA amplification with this technique, and, unless a specialized approach is used (e.g. ethidium monoazide treatment for selective detection of live cells), PCR does not differentiate between viable and dead cells.[10]

Fluorescence *in situ* hybridization (FISH) is another molecular-based technique for the characterization of cells. Here, a fluorescently-labeled nucleic acid probe is used to detect organism-specific (e.g. "signature") sequences occurring within whole, permeabilized ("fixed") cells. These probes are usually ~18-25 nucleobases in length and are typically composed of DNA. Alternatively, DNA mimics or analogs, such as peptide nucleic acid (PNA) or locked nucleic acid (LNA) may also be used, as these molecules may have additional functional advantages over DNA, including faster hybridization times or greater affinity for target sequences vis-à-vis DNA. After cell fixation, the probe enters the cell via passive diffusion and hybridizes with its target, usually on the 16S or 23S ribosomal RNA

(rRNA) subunit. Ribosomal RNA is commonly used as a target sequence due to the high number of copies present in most cells (~10^3-10^5 ribosomes per bacteria). After removal of unbound (or non-specifically bound) probe via washing, target cells are identified on the basis of their fluorescence. [11]

Although a number of potential rapid diagnostic methods exist, as outlined above, sensitive, low cost, user friendly and widely applicable detection approaches are still needed by industry to address sterility testing needs. The purpose of the work presented here is to develop a test for microbial contamination that fulfills the requirements of modern industry, namely rapid analysis, method simplicity, nonspecific detection of contaminants, and easily interpreted results. Additionally, further characterization and identification of the contaminants may be performed in this procedure. Recently, considerable interest has developed in the microbiology and bioanalytical fields in using capillary electrophoresis (CE) for the analysis of microorganisms. Traditionally used as a molecular technique for the separation of biomolecules, CE is an attractive technique for microbial studies due to its aqueous running environment and rapid analysis times.

In capillary electrophoresis, a fused-silica capillary (usually 25-250 μm inner diameter and 20-80 cm in length) is filled with an aqueous buffer, and a plug of analyte solution is injected by pressure or voltage. A high voltage (up to 25 kV) is then applied. Ions present in the buffer and sample zones undergo electrophoresis and migrate towards the oppositely charged electrode based on their electrophoretic mobility, μ. This mobility is dependent on the charge on the molecule, q, and the translational friction coefficient, f, in the following relationship:

$$\mu = \frac{q}{f} \tag{1}$$

Assuming that the molecule is present in solution in a spherical shell of hydration, the frictional coefficient may be determined using Stokes' law:

$$f = 6\pi\eta R \tag{2}$$

where η is the viscosity of the surrounding solution and R is the hydrodynamic radius of the particle. Therefore smaller, more highly charged molecules possess a greater electrophoretic mobility than larger molecules with lower net charges. Neutral molecules, however, will have no electrophoretic mobility and reside in the bulk solution.[12]

At pHs greater than ~3, the surface of the silica capillary is negatively charged due to exposed silanol groups. As a result, cationic buffer ions concentrate near the capillary wall and an electrical double-layer is formed. Upon application of the electric field, these positively charged ions move toward the negatively charged electrode. Because these cations are highly solvated by water molecules, their migration also results in the flow of the bulk solution toward the cathode. This phenomenon is known as electroosmosis or the electroosmotic flow (EOF). The charge on the capillary wall and the electric double layer that is formed may be greatly affected by the buffer properties, such as pH, ionic strength, and buffer additives. These factors are often used to control the speed and direction of the EOF. Alkylamine salts are commonly used to reverse the direction of the EOF by coating the capillary surface with a positive charge, resulting in anionic buffer ions forming a double layer adjacent to the capillary wall.[12]

Usually, conditions are chosen so that the EOF is capable of sweeping all ionic analytes of interest toward the capillary outlet. By placing a detector (commonly UV-Vis or

fluorescence) near the end of the capillary, analytes may be analyzed as they are swept into the outlet buffer vial. The combination of electroosmosis and electrophoresis allows CE to separate molecules based on their mass-to-charge ratio. Capillary electrophoresis may be operated in numerous modes including capillary zone electrophoresis (CZE), micellar capillary electrophoresis (MCE or MEKC), capillary gel electrophoresis (CGE), capillary isoelectric focusing (CIEF), isotachophoresis (ITP), capillary electrophoresis using entangled polymers, and capillary electrochromatography (CEC). These methods differ mostly by the nature of the buffer additives or capillary treatment employed and the sample injection method. The details of these techniques are beyond the scope of this dissertation introduction and are described in detail in other literature sources.[12]

While CE has seen significant success in the separation of molecules, its crossover to microbiological analysis is still in its infancy. The slow progress of adapting CE to cellular studies is due to the inherent characteristics of microorganisms, many of which are dissimilar to molecular analytes. Unlike molecules, bacteria and unicellular fungi are living biocolloids that are highly sensitive to their environment. Extreme conditions of pH, ionic strength, voltage, or organic solvents may result in cell lysis and death. In order to effectively characterize and detect microbial species, steps must be taken to ensure that the cells remain intact and, preferably, alive for during analysis. Microbial diversity also presents a set of variables that must be taken into account, particularly in the development of a non-specific universal sterility test. Microbial contaminants can vary widely in their size, shape and surface characteristics. For example, bacteria conform to a variety of shapes from spherical cocci to rod-like cells with diameters anywhere from 100 nm to several μm. Yeast and other unicellular fungi however are significantly larger than bacteria (often 10-100 fold). In

addition, the surfaces of these cells are quite diverse. Gram-positive bacteria possess a multi-layer surface composed of a plasma membrane and a thick outer peptidoglycan layer. Peptidoglycan is a rigid polymeric structure of peptides and carbohydrates, which provides protection and structural stability to the cell. Teichoic acids are interwoven in the peptidoglycan, creating a highly negatively charged bacterial surface. Gram-negative bacteria, however, have a relatively thin layer of peptidoglycan and a second plasma membrane on its outer surface. This second plasma membrane is relatively neutral with only a small amount of charge produced by proteins that extrude from the membrane. Furthermore, under certain growing conditions bacteria may produce a capsule, a sticky excretion often made of polypeptides or polysaccharides that coats the cell that provides protection and allows the cell to adhere to various surfaces.[13,14]

As a result of these size and surface variations, the electrophoretic mobility of microorganisms may vary drastically. Compounding the issue is the fact that a single species of cells may also have a wide distribution of mobilities, a term called electrophoretic heterogeneity.[14] A population of bacterial species may include cells at various growth stages, resulting in diverse surface characteristics and sizes. Therefore, it can be very difficult to control the migration of microorganisms within the applied electric field. Often times an injection of a pure bacteria culture will result in numerous peaks and broad bands, causing data analysis and peak identification to be nearly impossible. Adhesion of the cells to the capillary wall may also add to peak variance/irregularity and possibly prevent the cells from being detected altogether.[14] Several strategies have been employed to overcome these hurdles, many of which are described below in the literature review and the main body of this dissertation.

Organization

Part 2 of this dissertation is organized in a chronological manner, beginning with a review of previous works aimed at applying capillary electrophoresis to the analysis and separation of biocolloids and microorganisms. In the chapters following this review, several journal publications will be presented that detail our development of a rapid capillary electrophoresis based test for microbial contamination. Chapter 2 describes our initial experimental progress that resulted in the current fundamental methodology for a CE sterility test. This publication also demonstrates the principles and theory of the method and reports preliminary data that was obtained using concentrated culture samples of lab grown bacteria. Chapter 3 builds upon our previous work by optimizing our method so that a single cell present in the sample injection may be detected- a primary requirement of a true sterility test. This method appears to be non-specific and universal for a wide rage of unicellular fungi and bacteria. Current areas of research will be summarized in Chapter 4, and preliminary data will be reported on the application of our CE-based sterility test to the identification of microorganisms and detection of microbial contaminants in various "real-world" sample matrices. Finally, general conclusions and the direction of future research will be discussed in Chapter 5.

Literature Review

Viruses. Some of the very first applications of capillary electrophoresis to the analysis of biocolloids focused on viruses and examined their behavior in the capillary under an applied electric field. Viruses are relatively simple biocolloids composed of a protein encapsulated nucleic acid strand. Their structures are often symmetrical and their surface compositions are primarily controlled by ionizable groups on their protein sheath. One of the

first studies was performed by Hjerten *et al.* in the late 1980s.[15] This work examined the mobility of the tobacco mosaic virus (TMV) under the applied electric field. It was found that the virus, as well as a bacteria species *Lactobacillus casei*, possessed migration times similar to that of the electroosmotic flow. This result indicated that the surfaces of these biocolloids were not highly charged. Capillaries coated with either methylcellulose or polyacrylamide were necessary in order to prevent the viruses from adhering to the capillary wall. Many of these initial works focused on methods to prevent adsorption to the capillary wall using either capillary coatings or buffer additives to solubilize the viruses without denaturing their protein capsule. Studies using TMV were continued by Grossman and Soane and focused on the effect of the virus' orientation in the capillary on its electrophoretic mobility.[16] Generally, higher applied voltages resulted in greater virus mobilities. This trend was attributed to alignment of the virus parallel to the electric field (and bulk solution flow), decreasing the frictional component, f, of its mobility. Numerous publications were released by Kenndler *et al.* several years later that further characterized TMV by measuring its isoelectric point and producing a reproducible migration time. Surfactant additives were used to prevent capillary wall adhesion. Their work eventually shifted toward identifying the products of the virus' degradation, such as the 80S structural unit.[17-19] In addition to TMV, attempts to analyze adenoviruses using capillary electrophoresis have also been made. Mann and co-workers obtained irregularly shaped virus peaks within a 7-10 minute band by using polyvinyl alcohol coated capillaries. Proteins were then used as standards for the estimation of virus concentration in the sample.[20]

Bacteria and Yeasts. In the early 1990s, the first attempts to separate bacteria using capillary electrophoresis were made. However, due to the wide range of sizes and surface

characteristics of bacterial cells within a single species (resulting in electrophoretic heterogeneity), obtaining efficient peaks of living cells proved to be much more difficult than for viruses. Broad bands of four bacteria (*S. agalactiae, E. faecalis, S. pyogenes,* and *S. pneumoniae*) were detected by Ebersole *et al*. However the electrophoretic velocities of these species were quite low, resulting in significant overlap with the EOF. This problem was overcome by using very long capillaries (250 cm) that allowed sufficient time for the bacteria to migrate from the sample zone. Unfortunately, the result was long analysis times (up to 80 minutes) and broad bacteria peaks (often 10 minutes wide).[21] Other studies using this methodology with different species have produced similar results.[22] Electrophoretic mobility data for a wide variety of microorganisms has been collected and compiled in the literature as well.[23] In order to further assess the applicability of capillary electrophoresis to the analysis of microorganisms, Yamada and co-workers assessed the separation of *A. tumifaciens* and *C. cartae* by capillary zone electrophoresis (CZE) and capillary gel electrophoresis (CGE). Overall, CGE separations produced greater band resolution and peak purity than traditional CZE, however analysis times were significantly longer with CGE (a result of the extreme viscosity of the running buffer).[24] Very few of these techniques were widely pursued however. The effects of electrophoretic heterogeneity within bacteria populations resulted in extremely poor peak efficiencies, requiring that the species being separated have large differences in their electrophoretic mobilities. Conversely, molecular analysis using capillary electrophoresis obtains very high efficiencies, enabling analytes with only small differences in mass or charge to be completely resolved.

In order to overcome the problems of electrophoretic heterogeneity and poor efficiency with bacteria in capillary electrophoresis, numerous studies were performed to

attempt to stack or aggregate cells during the separation process. In 1999, our research group developed a method using a dilute solution (0.025% w/w) of polyethylene oxide (PEO) as a running buffer that enabled highly efficient, sharp peaks for the separation of bacterial cells. Species such as *S. cerevisiae, P. fluorescens, E. aerogenes,* and *M. luteus* were separated with analysis times ranging from 10 to 60 minutes using a 27 cm capillary.[25] Several mechanisms were proposed in a later publication to explain the apparent compression of bacteria bands into sharp peaks.[26] One model described a "hairy" coating of polymer on the surface of the bacteria which slows the movement of small ions near the cell. This effect results in a localized decrease in conductivity (and increase in electric field) around the bacteria that can lead to focusing of the band *via* electrophoretic migration. Another theory suggests that the differences in size and shape of the bacterial cells may promote cellular aggregation by causing cells to have a range in electrophoretic mobilities. The presence of polymer additive may enhance cell-cell adhesion and slow the EOF to allow adequate time for aggregation to occur. This process may be also be affected by field induced aggregation in which particles form flat, disc-like aggregates aligned perpendicularly with the electric field. These aggregates traverse the capillary more slowly in this orientation and result in a higher frequency of cell collisions, further enhancing agglomeration.[26] Armstrong has applied this dilute polymer method to a variety of applications. Bacteria present in dietary tablets were quantitated using fluorescent nucleic acid dyes and correlating the peak areas to calibration curves.[27] The cell viability of these bacteria and others were also examined with this CE method by using a red fluorescent dye that selectively permeates dead cells.[27,28] Bacterial contaminants (*S. saprophyticus* and *E. coli*) present in urine were also separated and removed from the major matrix components.[29] Several other dilute polymer solutions

have been explored to enhance the efficiency of bacterial separations with capillary electrophoresis. Polyvinylpyrrolidone was found to effectively stack bacterial bands,[30] while sodium alginate polymers have been successful in obtaining sharp peaks for various *Salmonella* strains.[31]

Coated capillaries have also been used in bacterial separations to suppress cell adsorption to the capillary wall when no other additives are present in the buffer to solubilize the bacteria. Buszewski and co-workers successfully separated three of four bacteria in a mixture of *P. vulgaris, E. coli, B. cereus,* and *P. fluorescens* using acrylimide coated capillaries.[32] As this coating suppressed the EOF, reverse polarity was used to allow the negatively charged cells to reach the detector. Analysis was accomplished in under 7 minutes due to the short length of the capillary (8 cm effective length). Polyvinyl alcohol coatings were also used for determining the net charge on the surface of *A. oxydans*.[33]

A few papers have also reported on the use of capillary isoelectric focusing (CIEF) for the separation of bacteria and other biocolloids. In CEIF, the capillary is initially coated with a polymer to suppress the bulk solution flow. The entire capillary is filled with running buffer that contains both the analyte and a series of ampholytes that create a pH gradient across the capillary. Upon application of the voltage, analytes traverse toward the oppositely charged electrode until they experience a pH environment that equals their isoelectric point (pI), at which point they loose all electrophoretic mobility. This allows separation of analytes (and microorganisms) based on their pI values. Armstrong et al. published the separation of three bacteria of similar size, *S. rubidiae, P. putida*, and *E. coli,* with CEIF.[25] Pressure was used to mobilize the cells after focusing. Yeast cells have also been isolated using CEIF by Shen and co-workers using hydroxypropyl methylcellulose coated

capillaries.[34] The pI values of yeast cells ranged from 5.2 to 6.4 depending on the stage of cell development.

Eukaryotic Cells and Organelles. The initial successes of applying capillary electrophoresis to the separation and analysis of viruses and bacteria have opened the door to the study of more complex cellular structures. Red blood cells (RBC) are among the most simple of eukaryotic cells and were one of the first to be separated by CE. A variety of RBCs including human, rabbit, chicken, and porcine erythrocytes were electrophoresed in a fluorinated ethylene-propylene coated capillary by Zhu and Chen.[35] Hydroxypropyl methylcellulose was added to the phosphate running buffer to enhance peak shape and efficiency. The differences in the electrophoretic mobilities of each species' RBCs were quite large, with migration times ranging from 14 minutes to 33 minutes. Canine erythrocytes have also been analyzed using a microfluidic CE device by Li and Harrison.[36]

The viability of boar sperm has also recently been assessed by He and co-workers using capillary electrophoresis and a dilute PEO buffer solution.[37] Ionic strength and PEO concentration were found to have a significant impact on the fluorescent signal strength and the speed of analysis. Semen extender was used for the cell suspension and was found to exhibit multiple benefits such as prolonging the sperm stability and greatly improving peak shape and efficiency.

The analysis of intact intracellular organelles using capillary electrophoresis has also gained significant interest in recent years. Arriaga and others have employed capillary electrophoresis and fluorescence detection for the analysis of individual organelles lysed from eukaryotic cells. The electrophoretic mobility of mitochondria of NS1 and CHO cells were measured using capillary electrophoresis to characterize the mitochondrial surface.[38] In

addition, capillary electrophoresis has been used to determine the average mitochondria per cell, and quantitate Cardiolipin, an important phospholipid in the function of mitochondria, from NS1 cells.[39,40]

Concluding Remarks. Despite the significant progress made in the past decade in the analysis of microorganisms using capillary electrophoresis, the field is still in its infancy. Numerous challenges still exist before the technique gains widespread use. For example, up to this point no single methodology is capable of separating or analyzing a wide variety of bacteria or unicellular fungi. Also previous methods require significant method optimization before a reliable signal may even be obtained. Solutions to problems such as electrophoretic heterogeneity, wall adsorption, and cell lysis have come in the forms of buffer additives to coat cells' surfaces, capillary wall coatings, and gentle running conditions to maintain cell viability. These publications are an important foundation for future studies (this dissertation included) and provide necessary fundamental theory into the electrophoretic behavior of microorganisms in capillary electrophoresis.

References

(1) Industrial Microbiology Market Review-2nd Edition, Strategic Consulting, Inc., March 2004.

(2) United States Pharmacopeia, 26th ed.; Webcon Ltd.: Toronto, Ontario, Canada, 2003; pp 2011-2016. Anal. Chem. 2006, 78, 4759-4767.

(3) Pratten, J.;Wilson, M.; Spratt, D.A. *Oral Microbiol. Immun.* **2003**, *18 (1)*, 45-49.

(4) Moldenhauer, J.; Sutton, S. V. W. *PDA J. Pharm. Sci. Technol.* **2004**, *58* (6), 284-286.

(5) Silley, P.; Forsythe, S. *J. Appl. Bacteriology* **1996**, *80*, 233-243.

(6) Bussey, D.M.; Tsuji, K. *Appl. Environ. Microbiol.* **1986**, *51*, 349-355.

(7) Alverez-Barrientos, A.; Arroyo J.; Canton, R.; Nombela, C.; Sanchez-Perez, M. *Clin. Microbiol. Rev.*, **2000**, *13*, 167-195.

(8) Johnson, R. *Euro. Pharma. Rev.* **1999**, *4 (1)*, 55-59.

(9) McCarthy, J. *Detecting Pathogens Food* **2003**, 241-258.

(10) Fung, D.Y.C. Overview of Rapid Method of Microbial Analysis. In *Food Microbiological Analysis New Technologies Series no. 12*, New York: Marcel Dekker, 1997.

(11) Moter, A.; Gobel, U.B. *J. Microbiol. Methods* **2000**, *41*, 85-112.

(12) Grossman, P.D.; Colburn, J.C. (Eds.) *Capillary Electrophoresis: Theory and Practice*, London: Academic Press, 1992.

(13) Dart, R.K. *Microbiology for the Analytical Chemist*, Cambridge: The Royal Society of Chemistry, 1996.

(14) Rodriguez, M.A.; Armstrong, D.W. *J. Chromatogr. B* **2004**, *800*, 7-25.

(15) Hjerten, S.; Elenbring, K.; Kilar, F.; Liao, J.; Chen, A.J.C.; Siebert, C.J.; Zhu, M. *J. Chromatogr.* **1987**, *403*, 47.

(16) Grossman, P.D.; Soane, D.S. *Anal. Chem.* **1990**, *62*, 1592.

(17) Scnabel, U.; Groiss, F.; Blass, D.; Kenndler, E. *Anal. Chem.* **1996**, *68*, 4300.

(18) Okun, V.; Ronacher, B.; Blass, D.; Kenndler, E. *Anal. Chem.* **1999**, *71*, 2028.

(19) Okun, V.; Blass, D.; Kenndler, E. *Anal. Chem.* **1999**, *71*, 4480.

(20) Mann, B.; Traina, J.A.; Soderblom, C.; Murakami, P.M.; Lehmberg, E.; Lee, D.; Irving, J.; Nestaas, E.; Pungor, E.J. *J. Chromatogr. A* **2000**, *895*, 329.

(21) Ebersole, R.C.; McCormick, R.M. *Bio/Technology* **1993**, *11*, 1278.

(22) Pfetsch, A.; Welch, T. *Fres. J. Anal. Chem.* **1997**, *359*, 198.

(23) Torimura, M.; Ito, S.; Kano, K.; Ikeda, T.; Esaka, Y.; Ueda, T. *J. Chromatogr. B* **1999**, *721*, 31.

(24) Yamada, K.; Torimura, M.; Kurata, S.; Kamagata, Y.; Kanagawa, T.; Kano, K.; Ikeda, T.; Yokomaku, T.; Kurane, R. *Electrophoresis* **2001**, *22*, 3413.

(25) Armstrong, D.W.; Schulte, G.; Schneiderheinze, J.M.; Westenberg, D.J. *Anal. Chem.* **1999**, *71*, 5465.

(26) Armstrong, D.W.; Girod, M.; He, L.; Rodriguez, M.A.; Wei, W.; Zheng, J. Yeung, E.S. *Anal. Chem.* **2002**, *210*, 245.

(27) Armstrong, D.W.; Schneiderheinze, J.M.; Kullman, J.P., He, L. *FEMS Microbiol. Lett.* **2001**, *194*, 33.

(28) Armstrong, D.W.; He, L. *Anal. Chem.* **2001**, *73*, 4551.

(29) Armstrong, D.W.; Schneiderheinze, J.M. *Anal. Chem.* **2000**, *72*, 4474.

(30) Girod, M.; Armstrong, D.W. *Electrophoresis*, **2002**, *23*, 2048.

(31) Shinitani, T.; Tamada, K.; Torimura, M. *FEMS Microbiol. Lett.* **2002**, *210*, 245.

(32) Buszewki, B.; Szumski, M.; Klodzinska, E.; Dahm, H. *J. Sep. Sci.* **2003**, *26*, 1045.

(33) Tsibakhashvilli, N.Y. *Biomed. Chromatogr.* **2002**, *16*, 327.

(34) Shen, Y.; Berger, S.J.; Smith, R.D. *Anal. Chem.* **2000**, *72*, 4603-4607.

(35) Zhu, A.; Chen, Y. *J. Chromatogr.* **1989**, *470*, 251.

(36) Li, P.C.H.; Harrison, D.J. *Anal. Chem.* **1997**, *69*, 1564-1568.

(37) He, L.; Jepsen, R.J.; Evans, L.E.; Armstrong, D.W. *Anal. Chem.* **2003**, *75*, 825.

(38) Duffy, C.F.; Fuller, K.M.; Malvery, M.; O'Kennedy, R.; Arriaga, E.A. *Anal. Chem.* **2002**, *74*, 171.

(39) Fuller, K.M.; Duffy, C.F.; Arriaga, E.A. *Electrophoresis* **2002**, *23*, 1571.

(40) Strack, A.; Duffy, C.F.; Malvey, M.; Arriaga, E.A. *Anal. Biochem.* **2001**, *294*, 141.

CHAPTER 2. CAPILLARY ELECTROPHORETIC METHOD FOR THE DETECTION OF BACTERIAL CONTAMINATION

Published in *Analytical Chemistry*

Michael A. Rodriguez, Andrew W. Lantz, and Daniel W. Armstrong*

Department of Chemistry & Biochemistry, University of Texas at Arlington, Arlington, Texas 76019-0065

Abstract

There has been growing interest in separations-based techniques for the identification and characterization of microorganisms because of the versatility, selectivity, sensitivity, and short analysis times of these methods. A related area of analysis that is scientifically and commercially important is the determination of the presence or complete absence of microbes (in essence, a test for sample sterility). In such a test, it is not of immediate importance to identify a particular microorganism, but rather, to know with a high degree of certainty whether any organism(s) is (are) present. Current regulations require culture-based tests that can take up to 2 weeks to complete. As a rapid alternative, capillary electrophoresis- based methods are examined. Experimental formats are developed that promote the consolidation of all cell types into a single zone (peak) which is separated from the electroosmotic flow front and any other interfering molecular constituents. This process can be accomplished using a segment of dilute cetyltrimethylammonium bromide, which serves to temporarily reverse the migration direction of the cells, and another segment of solution containing a "blocking agent", which serves to stop the cell migration and focus

them into a narrow zone. Relatively wide-bore capillaries can be used to increase sample size. This approach appears to be effective for a broad spectrum of bacteria, and analyses times are less than 10 min.

Introduction

Testing for the presence of microbes, whether they are bacteria, fungi, or even viruses, in laboratory samples is an important and necessary procedure for many areas of science. The food industry must be sure that there is minimal microbial contamination in products, especially contamination that could cause consumers illness upon ingestion.[1] Microorganism testing is important in the pharmaceutical industry as well, as it produces a large number of medicinal products for consumer use.[2] The health care industry must be very careful that tissues or other important biological samples (i.e., blood or plasma) are not infected with microbial agents.[3] A transplant of these materials to an otherwise healthy patient could prove disastrous. It is important for hospitals to have the ability to diagnose bacteremia or urinary tract infections (UTIs) and to do so quickly; a quicker diagnosis leads to faster treatment and recovery.[4] Furthermore, it is essential that the large amount of water processed by treatment plants is suitable for use by the general public, and that special sterile water/aqueous solution samples used in medicinal and microbiological research are indeed microbe free.[5]

There are numerous methods to test for potentially dangerous microbial agents. The simplest and most common approach employed for bacterial detection is the direct inoculation method.[6] This method, updated in 2004, is outlined in detail in the United States Pharmacopeia.[6] A sample is homogenized, a small aliquot is taken, and the aliquot is placed directly into a medium capable of sustaining microbial growth. After a few days the sample

is checked for turbidity or examined under a microscope for the presence of bacteria; a positive test in either case indicates contamination of the original sample. There are a few drawbacks to this testing method. The test requires several days to complete, and great care must be taken to prevent any contamination during the analysis, since one spurious bacterium could produce a false positive. There is a modification of the direct inoculation technique called membrane filtration.[6] This test is appropriate for samples that are too large to analyze by direct inoculation or samples that have a low enough number of bacteria to require concentration. The sample is simply filtered through a membrane with pores small enough to prevent the microorganisms from passing, yet large enough for the surrounding solution to flow freely. The membrane containing the filtered bacteria is placed in the growth medium, as opposed to the sample aliquot in the direct inoculation method, and the same procedure as in the direct inoculation method is followed from that point on.[6] Other methods have been developed to alleviate the shortcomings of these standard methods (mainly the time factor) yet still provide equally accurate results. All other tests are compared to these methods when it comes to obtaining a reliable answer about the presence and quantity of viable bacteria. Recently, molecular techniques have come to the forefront as an alternate means of microbial detection. They are divided into three types: hybridization, amplification, and immunoassay techniques. Hybridization involves the use of fluorescently labeled nucleic acid probes that bind to complementary nucleic acid sequences present in bacteria.[7] These complementary nucleic acid strands specifically bind only to the probe (in some cases its fluorescence is greatly enhanced). Once the probe binds to the complement strand of nucleic acid, the fluorescent bacteria can be visualized microscopically. Amplification techniques, such as PCR (polymerase chain reaction), extract a small amount of genetic material from the

bacteria and amplify it to a level that can be quantified for identification.[8] Immunoassay methods make use of the very specific reaction between antigens on the surface of bacteria and the antibodies the immune system produces in response to them.[9] The most common immunoassay test is ELISA (enzyme-linked immunosorbent assay). These techniques are all very specific and allow for identification of bacteria, in most cases, at the species level. The time needed for these tests is considerably less than that for culture-based methods, in most instances requiring only several hours to complete. However, they are very complex to perform, and significant personnel training may be necessary to carry them out. For tests such as PCR the operator must also be trained to interpret the results. The reagents and materials these types of tests require are also expensive to produce. Therefore, despite their faster analysis time, there are several disadvantages to these methods. Also, they are not general methods but rather in most cases specific to a particular microorganism. Hence, for a general contamination test they would miss all other sources of contamination.

Other methods have been developed to detect bacteria that do not fall under the specific label of molecular techniques. One example is the electrochemical detection that has been employed to detect pathogenic bacteria.[10] In this instance the cathodic peak current of oxygen is measured during growth with an electrochemical voltammetric analyzer. The rapid consumption of oxygen during growth leads to a discernible change in the cathodic peak current. Along the same lines, a dye that responds to bacterial growth through color shifts has been used to detect bacteria in blood samples.[11] Raman and Fourier transform infrared spectroscopy were also used to identify bacteria on the basis of their infrared protein spectra.[12] Other techniques have been used with some degree of success as well, but also have not come into common use for one or more of several reasons. For example, they

frequently lack the ability to compete with other techniques in terms of accuracy or time requirements, the costs are too high, or the method is simply too limited and/or technical.[13]

It is clear that a number of different choices are available when testing for microorganisms, each with its own advantages and disadvantages. Standard culture methods can provide accurate information about the presence and number of bacteria by using serial dilutions and colony counting, yet they are very time consuming and do not count dead microorganisms or microorganisms that do not grow in a particular medium. Molecular methods can reduce this time requirement considerably and can even provide information about the very genetic makeup of the bacteria. However, to detect general contamination, this degree of specificity is not needed, and indeed the high degree of specificity of these methods will result in false negatives as other microorganisms go undetected. Another example is a case where the source of contamination is not known; it is only known that the sample has been in an environment where contamination from any number of bacteria is likely. Tests that are developed for specific bacteria will not always give meaningful information in such a case, unless by chance the sample was contaminated with the same microorganism the test was designed for. There is need for an efficient/effective method capable of providing a simple, rapid, and binary (yes/no) answer in regard to the presence/ absence of any/all microorganisms. Such a test would greatly reduce the time requirements in cases where specificity is not needed, and also when it is used as a first-step analysis where specificity is required (to ensure that more complex or time consuming tests are not performed on samples that have not been contaminated with bacteria in the first place). The test should combine the reduced analysis time of molecular techniques, possibly even reducing them further, and the broad applicability of culture techniques.

Analytical techniques, in particular capillary electrophoresis (CE), have been used recently to address some of the problems associated with microbial detection and identification methods.[14] CE is an attractive technique because of its fast analysis times and very small sample requirements (which often is the case with microbial samples). Some of the earliest work in microbial CE was performed by Hjerten et al. with the tobacco mosaic virus.[15] Grossman and Soane also studied this virus; however, while Hjerten was simply probing the movement of particles with the electroosmotic flow (EOF) in a direct current electrical field, Grossman and Soane were examining the actual effect of the orientation of the virus on its electrophoretic mobility.[16] There has been extensive work on the human rhinovirus by Kendler and co-workers, who studied several of its electrophoretic properties and developed a method for identification.[17-19] A few other attempts were made at viral analysis by CE as well.[20] However, a majority of the work with microorganisms and CE has focused on bacteria. Initial experiments yielded broad peaks and long migration times (mostly due to the long capillaries used to distance the bacteria from the EOF), but they showed the potential for identification and separation.[21] With the use of polymer additives in the run buffer very sharp peaks and a good separation of several bacteria were reported by Armstrong and co-workers.[22,23] Other reports of success with these polymer additives have been reported as well.[24] Short, coated capillaries also were used to separate a number of bacteria, in addition to the use of other additives to the run buffer.[25-27]

However, there have been very few reports on the identification of the presence or complete absence of a large number of diverse microorganisms by CE, in essence a sterility test. In this paper we present a procedure that is capable of issuing a binary answer to the presence/absence of a broad array of microorganisms in a single sample by using capillary

electrophoresis in conjunction with surfactants and an injection spacer technique. This method is capable of discerning the presence of microbes in a very short amount of time. In these respects we are utilizing the best elements of culture techniques (broad applicability) and molecular techniques (fast analysis times). While it is not capable of the specificity of molecular techniques in terms of identifying bacteria at the species and sometimes strain level (and this is not necessarily a drawback for reasons mentioned previously), it could prove to be useful as a stand-alone sterility test or as a quick first step analysis when specificity is desired.

Experimental

Materials. Tris(hydroxymethyl)aminomethane (TRIS), sodium hydroxide, hydrochloric acid, and cetyltrimethylammonium bromide (CTAB) were all purchased from Aldrich (Milwaukee, WI). Citric acid was obtained from Fisher Scientific. Dimethyl sulfoxide (DMSO) was a product of EM Science (Gibbstown, NJ). Luria broth was obtained from Sigma (St. Louis, MO). Brain heart infusion and nutrient broths were obtained from Difco Laboratories (Franklin Lakes, NJ.). BacLight fluorescent dye was obtained from Molecular Probes, Inc. (Eugene, OR). Uncoated fused silica capillaries with inner diameters of 100, 150, and 200 μm and outer diameters of 365 μm were obtained from Polymicro Technologies (Phoenix, AZ). *Escherichia coli* (ATCC no. 10798), *Salmonella subterreanea* (ATCC no. BAA-836), *Listeria innocua* (ATCC no. 33090), *Brevibacterium taipei* (ATCC no. 13744), *Corynebacterium acetoacidophilum* (ATCC no. 13870), *Aerococcus viridans* (ATCC no. 11563), *Pseudomonas fluorescens* (ATCC no. 11150), Escherichia blattae (ATCC no. 29907), and *Staphylococcus aureus* (ATCC no. 10390) were all obtained from the American Type Culture Collection (Manassas, VA).

Methods. The CE separations were performed on a Beckman Coulter P/ACE MDQ capillary electrophoresis system equipped with a 488 nm laser-induced fluorescence and a photodiode array detector. UV detection was used in all experiments except those that involved the use of *S. aureus* (Figures 4 and 5). Laser-induced fluorescence detection was used in these instances since it provided a more intense signal. The following procedure for staining the microorganisms with BacLight dye was used when LIF detection was necessary. Briefly, a 1 mM stock solution of BacLight Green dye was prepared in DMSO. A working solution of 100 µM was then made by adding 2 µL of the 1 mM stock solution to 18 µL of DMSO. The cells were stained by adding 1 µL of the working dye solution/mL of bacteria solution, and then incubated at room temperature for at least 15 min. The signal for the bacteria varied on the basis of the type of bacteria, but generally the lowest number of bacteria detectable was around 50-200 entities. The capillaries used in these experiments varied in length from 30 to 60 cm (20 and 50 cm to the detector, respectively). The inner diameters also varied from 100 to 200 µm; both dimensions are specified in each experiment. When a capillary was first used, it was rinsed with water for 30 s, 1 N NaOH for 5 min, and the running buffer for 2 min. Prior to each run the 100 µm i.d., 30 cm capillary was rinsed with water for 1 min, base for 1 min, and buffer for 1 min at 10 psi. The 200 µm i.d., 30 cm capillary was rinsed with water for 10 s, base for 10 s, and buffer for 10 s at 5 psi. When 60 cm length capillaries were used, the rinse time was doubled while the pressures remained the same. DMSO was used as a neutral marker at a concentration of ~10 µL/0.5 mL. This concentration of DMSO did not have an observable effect on the bacteria when examined microscopically. Stock solutions of 10 mM TRIS/3.3 mM citric acid were prepared and diluted 10x for a working solution concentration of 1 mM TRIS/0.33 mM citric acid as

needed. Surfactants were added to these working concentration buffers in the appropriate concentrations as they were needed daily. Sodium hydroxide and hydrochloric acid were used to adjust the pH when necessary. The standard running buffer concentration is 1 mM TRIS/0.33 mM citric acid with 1 mg/mL CTAB, pH 7, unless otherwise noted in the figure legends. The standard sample buffer is 1 mM TRIS/ 0.33 mM citric acid, pH 7, unless otherwise noted in the figure captions. All bacteria were grown according to the directions supplied by the manufacturer. The microorganisms were initially grown in liquid broth, then plated on agar plates, and stored under refrigeration until needed. When used for experiments, a single colony was taken from the agar plate and again grown in a liquid medium. The cells were harvested for use when in the stationary phase of growth when the concentration was ~10^8 CFU/mL. The microorganisms were centrifuged down, the excess broth was removed, and the microorganisms were washed with working concentrations of the TRIS/citric acid buffer (pH 7) once, then recentrifuged and decanted, and finally suspended in a working concentration of TRIS/citric acid buffer of the same volume as the broth that was originally removed. The final concentration of the cells was ~10^8 CFU/mL. These were then used as samples for analysis. This was done each day to produce new samples.

Safety. A majority of the microorganisms in this study fall into the biosafety level one category, and standard microbiological practices can be employed in their use. Two microorganisms used in this study (*Pseudomonas aeruginosa* and *S. aureus*) fall into the biosafety level two category, and when handling these microorganisms, extra precautions should be used. This includes using extreme caution when handling sharps or needles contaminated by the microorganism. Procedures that produce aerosols or have the potential to splash should be done in biosaftey cabinets or safety centrifuge cups. Splash shields, face

protection, gowns, and gloves are recommended. Waste decontamination must be available as well.[28]

Results and Discussion

Method Development. The ultimate goal of this research was to develop a method capable of giving a rapid, unambiguous answer as to the presence/absence of bacteria/ microbes. A method capable of providing a single peak at the desired time, regardless of the bacterial species, its heterogeneity, or the number of different species present, seemed to be the best option. This task was somewhat more daunting than it was first expected to be. There are few options to minimize the effects of electrophoretic heterogeneity as documented by Arriaga and coworkers. [29] One possibility is to treat the surface of the bacteria to eliminate or minimize the charge before analysis. Even if possible, this approach would not allow the bacteria to migrate away from the EOF front. Alternatively, the bacteria could be compressed at a point inside the capillary. This would result in all of the aggregated bacteria migrating together at the same velocity, as long as all other forces inside the capillary (e.g., turbulent flow, thermal effects, etc.) were insufficient to break them apart. Even if multiple bacterial species are present, it should not pose a problem since interspecies aggregation is not uncommon.[30]

It is well-known that acidic conditions can induce aggregation in bacteria, and initial experiments with a method developed using pH boundaries had some success (see Figure 1).[31] This method worked well for some bacteria but not for others. In our experiments it was mainly Gram-positive bacteria (e.g., *Bacillus subtilis, L. innocua*) that aggregated under acidic conditions. Although it may not be broadly applicable, this procedure may be useful as a secondary analysis for the identification of Gram positive bacteria. To accomplish the main

goal, however, a method that was capable of causing a wider number of different bacteria to associate well away from the EOF front was sought.

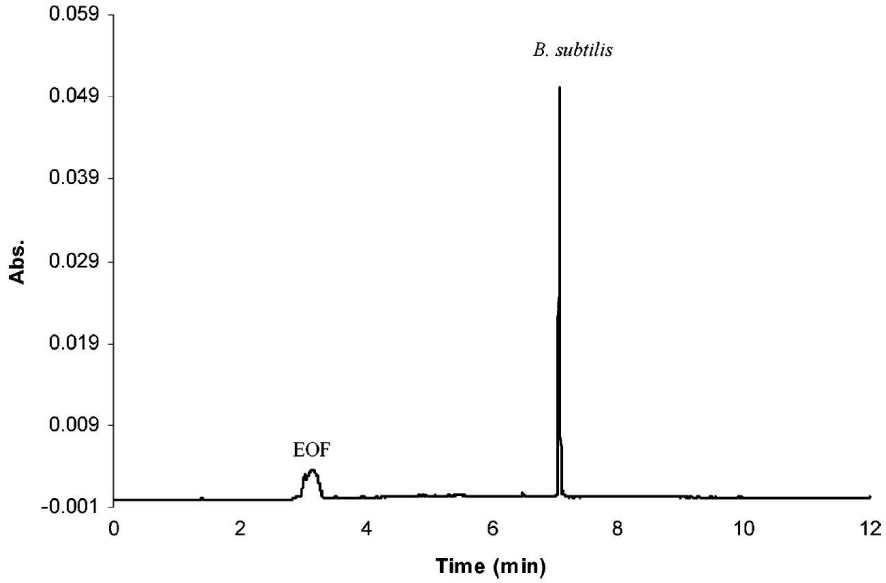

Figure 1. Differential pH method. Detection is at 254 nm. The small broad peak at ~3 min is the EOF, and the sharp tall peak at 7 min is the microbe peak (*B. subtilis*) Conditions: capillary, 30 cm long (20 cm to detector), 100 µm inner diameter. The capillary is filled with pH 9 (adjusted with dilute NaOH), 1 mM TRIS/0.33 mM citric acid before any injections are made, and the outlet buffer is the same. The inlet running buffer is 1 mM TRIS/0.33 mM citric acid, pH 4 (adjusted with dilute HCl). The voltage is +4 kV. The sample is injected for 3 s at 0.4 psi.

The addition of CTAB to samples caused some bacteria to undergo aggregation. However, this was not the case for a number of others. The concentration of CTAB used was low (~1 mg/mL) and did not lyse the cells (as indicated by inspection microscopically). Fortunately, a large number of bacteria aggregated when CTAB was added to the bacterial samples in the presence of a specific nutrient medium. (It is interesting to note that this is not a coprecipitation process; no precipitate forms when only CTAB and nutrient broth are combined.) It appeared that the combination of CTAB and nutrient broth had a synergistic effect toward consolidation of all types of bacteria. Also it was not sensitive to the effects of microbial electrophoretic heterogeneity. Now, an appropriate CE system utilizing this effect

had to be devised. It would have to allow the bacteria, migrating as a single band, to distance themselves from the EOF, to distinguish them from contaminants appearing there.

The first experiments were set up in the following manner. The sample injection contained both nutrient broth and the microorganisms (no CTAB), while the surrounding run buffer contained CTAB in an appropriate concentration. It was thought that the CTAB would move into the region containing the broth and bacteria (since it had a current motion counter to the electroosmotic flow) to induce aggregation and produce a sharp peak. A sharp peak did appear; however, the bacteria could not migrate out of the region containing the nutrient broth (the neutral region). Recall that the pH method allowed the microbial peaks to move away from this region, but it mainly worked for Gram-positive bacteria.

Similar experiments were then performed in which the nutrient broth component from the sample injection was removed. The bacteria yielded peaks with migration times longer than that of the EOF in this instance. This is a direct result of the nutrient broth no longer inhibiting their movement out of the neutral region. An interesting point to note is that bacteria are known to be negatively charged at conditions similar to those at which these experiments were performed. Under normal circumstances this type of electropherogram (a peak with a longer migration time than the EOF) would be further evidence of the negative charge of the bacteria; however, under conditions where both the electroosmotic flow and polarity are reversed (as in these experiments), it indicates exactly the opposite. It was apparent that the dilute CTAB was having a significant effect on the mobility of the bacteria. The following experiment was performed to examine the exact effect of CTAB on the bacteria. The capillary was filled with buffer containing CTAB, then an initial injection of buffer lacking CTAB was made, and finally a sample consisting of bacteria and an EOF

marker was injected. The migration time of the bacteria in this instance was the same as that of the EOF marker. This was sufficient to show that the CTAB in the region adjacent to the bacteria (on the anodic side) was responsible for imparting some positive charge to their surface.

Due to the opposite direction of migration of the bacteria and the EOF (which carried the nutrient broth), it was thought that separating the two regions, with the bacterial sample on the anodic side of the capillary and the nutrient segment on the cathodic side, would allow them to converge in an area between the two injected segments. Also, this could solve the problem of any interference that could be present near the EOF front since the CTAB is capable of carrying the bacteria well away from that region.

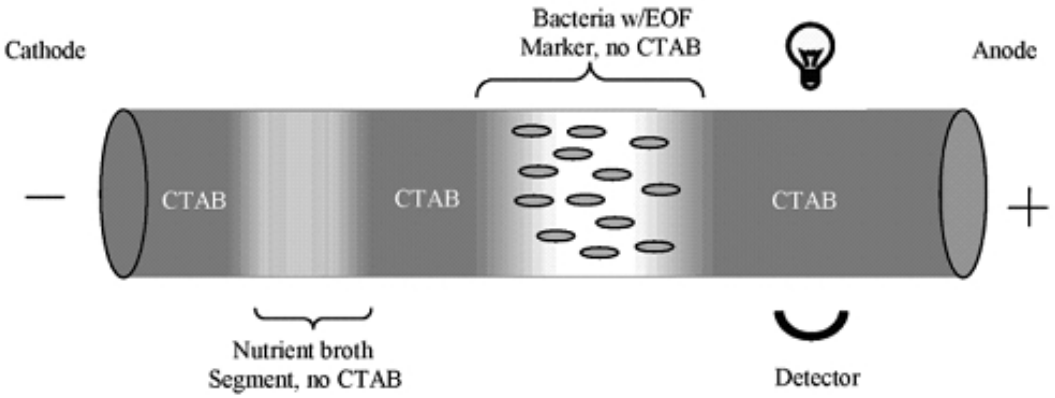

Figure 2. Schematic of the finalized spacer method. An injection of bacteria that contains no CTAB is made first (after the capillary is filled with run buffer (see the Experimental Section for the concentration)), then a spacer of run buffer (5 s at 0.4 psi), and finally an injection (1.5 s at 0.2 psi) of nutrient broth (8 g/L). The voltage is then applied (-2 kV). The CTAB on the anodic side of the bacteria migrates toward the cathode and coats the bacteria as it moves through the sample plug. This imparts a positive charge on the bacteria and moves them toward the cathode until they meet the nutrient broth segment (which is traveling with the EOF). The bacteria begin to aggregate and lose charge, and from that point on, they travel as a macroparticle with minimal mobility along with the nutrient broth segment toward the detector.

Figure 2 is a diagram showing the starting reagent and sample segmentation conditions needed to compress all microbes and separate them from the electroosmotic flow front. The capillary is rinsed with water and base and then filled with run buffer (see the

Experimental Section for the exact conditions) containing CTAB. The sample of bacteria is then injected (it does not contain CTAB), and next a spacer containing the same CTAB concentration as the rest of the run buffer is injected. Last, a segment of nutrient broth (which also does not contain CTAB) is placed in the capillary. The dissolved CTAB residing in front of the bacteria (on the anodic side) migrates toward the cathode when the voltage is applied. As it passes through the sample zone it carries the bacteria with it. The electroosmotic flow is reversed under these conditions, and it flows toward the anode, as does the segment of nutrient broth that was injected (see Figure 2). The combination of the anodic movement of the nutrient broth segment and the cathodic movement of the bacteria allows them to converge at a point between the two zones in the capillary. The bacteria begin to aggregate and eventually form a large macroparticle. As the macroparticle forms, it quickly loses mobility, and from that point on it migrates in the anodic direction while residing in the nutrient segment.

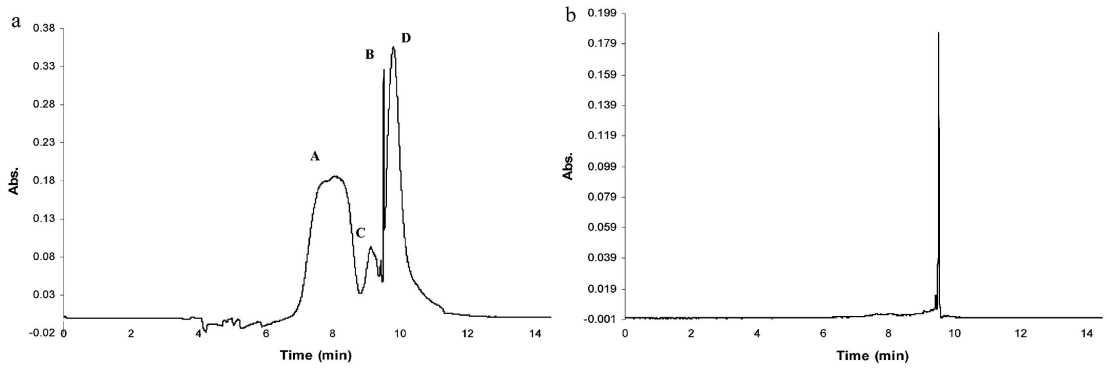

Figure 3. (a) Electropherogram obtained when the spacer method is used. Detection is at 214 nm. Peak A is the EOF marker (DMSO), peak B is the microbe peak (*E. coli*), and peaks C and D result from the nutrient broth. Conditions: capillary, 30 cm long (20 cm to detector), 100 μm inner diameter. The running buffer is 1 mM TRIS/0.33 mM citric acid with 1 mg/mL CTAB, pH 7. The sample buffer is 1 mM TRIS/0.33 mM citric acid, pH 7. The nutrient broth concentration is 8 g/L. The voltage is -2 kV. The sample is injected for 6 s at 0.5 psi, the spacer injected for 5 s at 0.4 psi, and the nutrient broth for 1.5 s at 0.2 psi. (b) Same electropherogram as in (a). However, detection is at 449 nm.

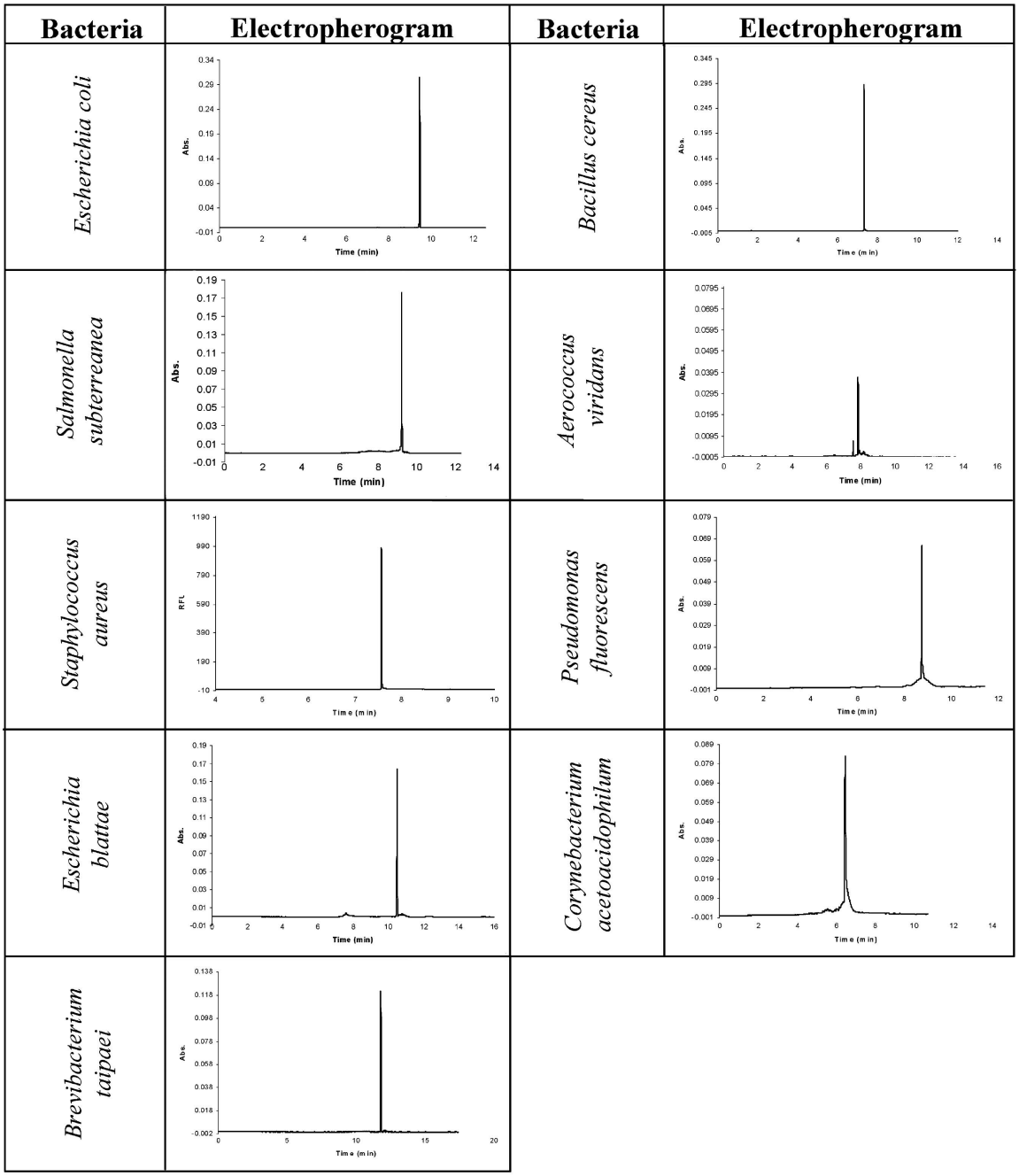

Figure 4. Nine different bacteria successfully adapted to this method. Conditions for all electropherograms are the same as those listed in Figure 3a except for the detection wavelength (449 nm) and some conditions for *S. aureus*, which was stained with BacLight and analyzed with LIF detection at 514 nm. The rest of the conditions for *S. aureus* are similar to those in each other electropherogram.

The resulting electropherogram is shown as Figure 3a. The first broad peak (A) is the EOF marker DMSO (mixed with the bacteria prior to injection), the second (C) and third (D)

broad peaks result from the segment of nutrient broth injected into the capillary after the microbes. The middle and sharpest peak (B) is from the bacteria, in this case E. coli. This electropherogram is obtained when the UV detector is set to 214 nm and illustrates the migration of each injected component. The bacteria in the sample injection are the only species present capable of giving a signal (largely due to Mie scattering) when detected at 449 nm. The resulting electropherogram shows only a single sharp bacterial peak (Figure 3b). This same procedure can be applied to a number of different bacteria as shown in Figure 4.

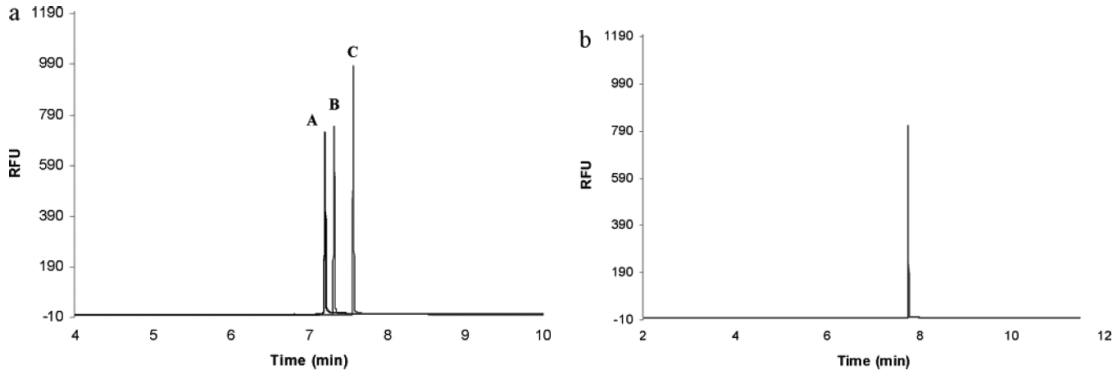

Figure 5. Three separate overlaid electropherograms showing *E. coli* (C), *S. aureus* (A), and *S. subterreanea* (B) individually (a) and in a mixed sample (b). Conditions are identical to those listed in Figure 3a, with the following exceptions: Laser-induced fluorescence detection was used, and the monitored wavelength was 517 nm. The bacteria were all stained with BacLight.

Figure 5a shows the composite electropherograms of three different bacteria analyzed individually (note the slight variation in migration times, which is inherent to CE). When these three bacteria are combined in one sample and subjected to this method, a single peak is still obtained, as shown in Figure 5b. These experiments indicate the possibility that this set of conditions may apply broadly to many microorganisms. Regardless of whether the sample contains many bacteria, such as those listed in Figure 4, or just a single species, the same sharp peak will occur at the same point in the capillary in each instance. Also note that

it takes less than 10 min for any combined bacterial band to migrate to the detector. Hence, it could be used to obtain rapid information as to the presence or absence of microorganisms in a sample. It could also be multiplexed for high-throughput analysis.[32]

Analysis Optimization. The system used in these experiments is fairly complex. Not only are there the standard factors of pH, ionic strength, and additive concentration, which are commonly optimized for all CE experiments, but also there are other factors that must be considered. The sample injection amounts were optimized in an effort to introduce as much sample into the capillary as possible. This was done by increasing either the injection time or the inner diameter of the capillary. Introduction of larger amounts of sample could prove useful when dealing with very dilute samples. The spacer length, nutrient broth concentration, and nutrient broth injection length all had only a minimal effect on the results and therefore are not discussed.

Three different pHs were tested using this method: 4, 7, and 9. Each pH yields a very sharp single peak for the bacteria (*E. coli*); however, pH 7 seemed to consistently give peaks with a higher absorbance. It is interesting to note that the peaks do not tend toward longer migration times as the pH is lowered. This is because of the complex nature of the dependence of electroosmotic flow on the CTAB concentration.[33]

A combination of TRIS and citric acid at fairly low concentrations was used as the running buffer for this system. There is a narrow window of workable ionic strengths as compared to pH. A single peak is obtained at 5 times the normal concentration of TRIS/citrate used; however, it is slightly widened and skewed. The peak converts back to its normal shape upon addition of more CTAB. However, a further increase to 10 times the normal concentration of TRIS/citrate completely destroys the single peak, and it cannot be

reconstituted even if further amounts of CTAB are added. A solution consisting of only CTAB and water can be used to obtain similar results; therefore, only the upper limit of ionic strength significantly affects the peak number and shape. When the run buffer concentration in these experiments is varied, it is imperative that the sample buffer be of the same concentration (in buffer salt content). If the sample buffer is significantly higher or lower in ionic strength than the surrounding run buffer, an adequate peak is not obtained (i.e., multiple peaks or inconsistent migration times occur). In the case where the sample buffer is of lower concentration than the surrounding run buffer, multiple peaks are obtained. If the sample is of higher ionic strength than the surrounding run buffer, the bacteria again become trapped in the neutral zone well before they reach the nutrient segment. It is reasonable to assume that CTAB has an effect on the surface of the bacteria since the mobility of the bacteria has been shown to be affected by it. There are a number of counterions around any charged particle in solution, and the density of the ions depends on the ionic strength of the solution. It could be reasoned that, at higher ionic strengths, when the diffuse layer becomes more compact, it may be harder for the CTAB to reach the surface of the bacteria. Thus, the CTAB may not be able to affect the surface of the bacteria in the way it does at lower ionic strengths. An alternate explanation is that when this ionic layer becomes compact the bacteria tend to aggregate slightly (as charged particulates are known to do).[34] The larger aggregates, as opposed to mostly single bacteria at low ionic strengths, may not be affected as greatly by the CTAB.

The concentration of CTAB in the run buffer was varied to study its effect on the system; Figure 6 shows the results. The optimal concentration of CTAB is between 1 and 2 mg/mL; the peak height drops considerably if the concentration is raised. This phenomenon

may be possibly due to the lysis of cells as the concentration of CTAB increases. The highest signal obtained while still exhibiting a single peak is most desirable, since a major goal is detecting bacteria at very low levels. The sharp single peak that is usually obtained breaks apart at CTAB levels of ~0.5 mg/ mL.

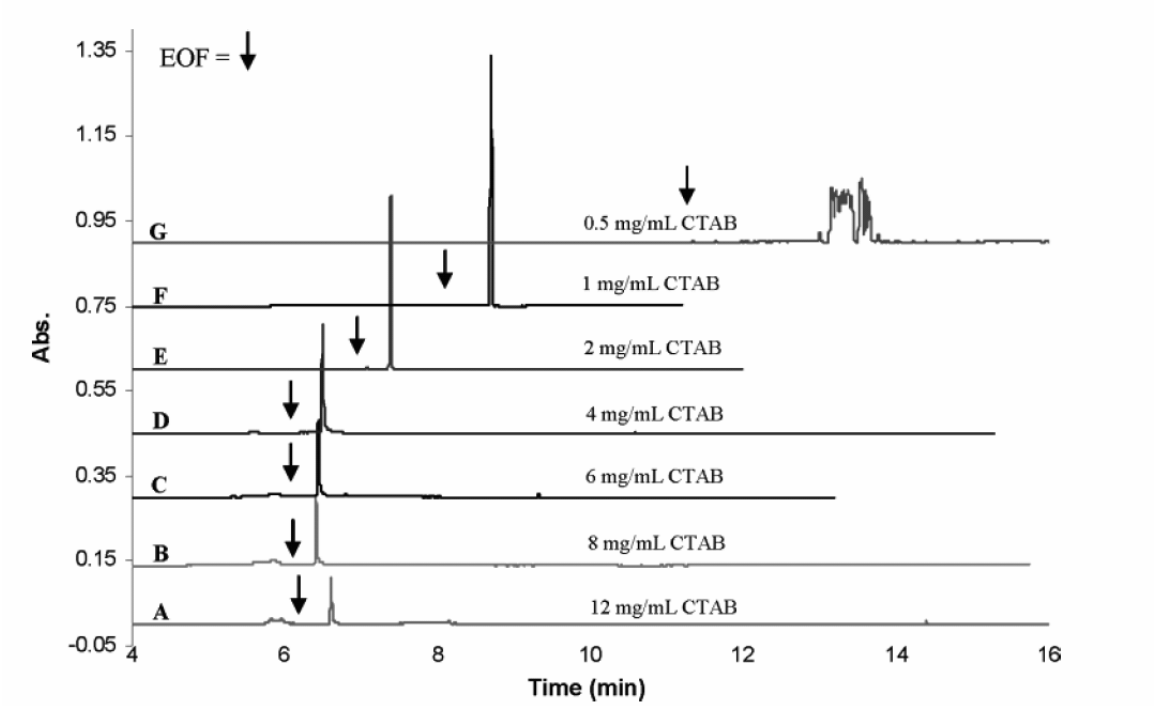

Figure 6. Optimization of CTAB concentration with *S. subterreanea*. Electropherogram A conditions: run buffer, 1 mM TRIS/0.33 mM citric acid with 12 mg/mL CTAB, pH 7; sample buffer, 1 mM TRIS/0.33 mM citric acid, pH 7. Each of the electropherograms B-G have identical salt contents, but contain CTAB concentrations of 8, 6, 4, 2, 1, and 0.5 mg/mL, respectively. Detection is at 449 nm. Injections, voltage, and capillary dimensions are the same as those listed for Figure 3a.

As mentioned above, part of the goal was to obtain as large of a signal as possible by optimizing the conditions. This would allow detection of bacteria at the very low levels. In addition, it would also help to compensate for the low number of bacteria injected and detected due to the inherently low volume of the capillaries used. Therefore, experiments were undertaken to maximize the bacterial injection volume. This was accomplished by use of both longer capillaries and larger inner diameter capillaries. The longer capillaries were

used to increase the length of the injected bacteria zone. Filling the capillary with too long of a sample segment adversely affects the EOF since the sample does not contain CTAB, and CTAB is responsible for coating the capillary and reversing the EOF. If the sample zone gets too large, the amount of CTAB present to reverse the flow would be insufficient and it would lead to prohibitively long migration times. Use of longer capillaries helps to minimize this effect. More of the remaining capillary is filled with CTAB for two equal-length injections when a longer capillary is used. The longer capillary also affords the bacteria more time to reach the nutrient segment. The use of larger inner diameter capillaries allows larger volumes of the bacterial sample solution to be injected for equal injection lengths.

A comparison was made between the use of a 30 cm capillary and a 60 cm capillary. The peak shape is normal for injections of 6 and 9 s (at 0.5 psi) for the 30 cm capillary, but the injection of 12 s (at 0.5 psi) shows multiple peaks. Experiments have shown that CTAB cannot be present in the segment containing bacteria and also that CTAB is responsible for moving the bacteria in the cathodic direction; therefore, the distance over which the CTAB must carry the bacteria becomes increasingly large as the bacteria are injected over longer time periods. It seems that a limit is reached at which the CTAB cannot carry all of the bacteria in the CTAB free sample segment back to the interface of the nutrient segment. In this case multiple peaks are observed. A 60 cm capillary was used in an attempt to give the CTAB additional time to carry the bacteria back to the nutrient segment and help unify the multiple peaks obtained for long injection times. The injection pressure was identical to that of the 30 cm capillary (0.5 psi), but the length of time for each injection was doubled; this was done so that direct comparisons could be made between capillaries. The injections of 12 and 18 s on the 60 cm capillary, which correspond to the 6 and 9 s injections on the 30 cm

one, both gave reasonable peaks. However, similar to the 30 cm capillary, additional peaks appeared when the injection time was increased to 24 s (12 s on the 30 cm capillary). Therefore, the additional time afforded to the CTAB did not improve the microbial peak.

Increasing the inner diameter of the capillary proved to be much more useful for increasing the overall number of bacteria and volume of solution injected. Two different inner diameter (i.d.) capillaries (100 and 200 μm, both 30 cm in length) were used for these experiments. The concentration of bacteria injected was identical in each experiment as were the lengths (not in seconds but in millimeters) of the injected spacer, nutrient segment, and bacterial sample segment. The time and pressures were adjusted for injections made on the 200 μm i.d. capillary to compensate for the larger flux of materials and to give injection lengths similar to those of the 100 μm i.d. capillary. Both experiments produce sharp bacterial peaks. However, it is clear that a much larger peak is obtained when using the 200 μm i.d. capillary. The doubling of the diameter leads to a 4-fold increase of the volume injected if the injection length (again in millimeters, not seconds) is held constant. The increased number of bacteria injected in this larger capillary most likely leads to the larger signal, since they are compacted into the same length as in the smaller diameter capillary. In addition there is an added benefit of increased (double) path length for detection when using the larger inner diameter; this also adds to a larger signal in accordance with Beer's law. There are some interesting points that should be mentioned with the use of larger capillaries. For instance, molecular species would be broadened significantly in 200 μm capillaries (compared to 100 μm), due to increased Joule heating, siphoning, and other effects. This is not the case with this microorganism procedure. Upon aggregation they travel as a single macroparticle and cannot be separated by the forces of thermal mixing or other dispersive

actions within the capillary. Theoretically, even larger diameter capillaries could be used; however, practical concerns become a problem. For instance, these larger i.d. capillaries are more brittle and prone to breakage. Also, most commercial CE instruments are only capable of accepting common outer diameters of the capillary (usually 360 μm).

Experiments were also performed to determine the maximum injection length for a capillary that is 30 cm long and has an inner diameter of 200 μm. The injection lengths used ranged in time from 4 to 7 s (at 0.2 psi). As is expected, the peak height increases with the injection time, due to the greater number of bacteria being injected. The migration time also increases as the injection time increases; this is a result of the length of the CTAB-free sample zone. As mentioned previously, the reversed flow of the EOF is dependent on the amount of CTAB in the capillary. As the concentration of CTAB decreases, the velocity of the reversed EOF decreases as well, resulting in longer migration times. At a 7.0 s injection, the peak begins to broaden and split slightly. This is roughly the limit of the injection for a capillary of this diameter. This 6.0-7.0 s maximum injection time for the 200 μm i.d. capillary is of particular interest. This time corresponds to an injection length of 43-50 mm and an injection volume of 1360-1580 nL (using the Poiseuille equation). This is nearly identical to the maximum injection length of 40-53 mm for a 100 μm i.d. capillary. However, the volume injected is of course much lower for the 100 μm i.d. capillary at 317-423 nL. Though there is a limitation as far as the injected sample length is concerned, the injected sample volume (and hence number of bacteria) can be increased significantly by simply increasing the inner diameter of the capillary. Fortunately, doing so does not adversely affect the results.

Conclusions

There is a pressing need for a rapid test that is capable of providing a binary answer regarding the presence/absence of a wide variety of microorganisms. Culture methods and modifications of them are still the universally accepted procedures for determining microbial contamination, but these types of tests suffer from long analysis times. Other techniques such as hybridization, amplification, and immunoassays can considerably reduce the time required for microbial analysis; however, they all have specific drawbacks as well. Some of these techniques require considerable training and expertise to perform. They do provide a high level of specificity, in terms of identifying species, but this is not always desired or needed for a simple "sterility" test. The method presented here is capable of providing a quick (a few minutes) answer regarding the presence or absence of microorganisms. It is also applicable to a variety of different bacteria, even to samples containing a variety of different species. In this manner it is able to utilize the best elements of other available tests. It can potentially be used to diagnose bacteremia or UTIs; these are cases where a quick answer can be much more beneficial than a detailed answer (providing genus, species, and strain information) which may consume precious extra time. Future experiments will focus on applying this test to just such "real world" samples for diagnosis and also on applying these tests to many other bacteria as well as other microorganisms including fungi and viruses. In addition, the limit of detection must be improved for this method. The ideal method is capable of detecting at the single-cell level. This method is currently capable of analyzing bacterial samples that have been diluted slightly, ~106 CFU/mL; this number is larger than that at the single-cell level. Laser-induced fluorescence should theoretically be able to detect extremely low levels of bacteria (and these methods have been used), but background fluorescence from both the

nutrient broth and BacLight dye have hampered efforts to reach these low levels. We have begun experiments using other staining methods and have had some success in reducing the background further. Once the component of the nutrient broth that is responsible for the synergistic effect with CTAB is isolated, the background will be reduced to near zero and the lower limit of detection should approach single-cell levels. This may prove to be the most useful form of the sterility test using CE.

References

(1) Duffy, G. B.; Kilbride, B.; Fitzmaurice, J.; Sheridan, J. J. *Routine Diagnostic Tests for the Detection of Food Borne Pathogens*; The National Food Center: Teagasc, Dansinea, Castleknock, Dublin 15, ISBN 1 84170 1890; January 2001.

(2) Sutton, S. V. W.; Cundel, A. M. *Pharmacopeial Forum* **2004**, *30 (5)*, 1884- 1894.

(3) Peters, R. P. H.; van Agtmael, M. A.; Danner, S. A.; Savelkoul, P. H. M.; Vanderbroucke-Grauls, C. M. J. E. *Lancet Infect. Dis*. **2004**, *4*, 751-760.

(4) Muhldorfer, Inge; Ziebuhr, Wilma; Hacker, Jorg. *Mol. Med. Microbiol*. **2002**, *2*, 1515-1540.

(5) Emmerson, A. M. *Emerging Infect. Dis*. **2001**, *7 (2),* 272-276.

(6) *United States Pharmacopeia, 26th ed*.; Webcon Ltd.: Toronto, Ontario, Canada, 2003; pp 2011-2016.

(7) Schweickert, B.; Moter, A.; Lefmann, M.; Goebel, U. B. APMIS 2004, 112 (11/12), 856-885.

(8) Bej, A. K.; Mahbubani, M. H.; Atlas, R. M. *Crit. Rev. Biochem. Mol*. **1991**, *26 (3-4),* 301-334.

(9) McCarthy, J. *Detecting Pathogens Food* **2003**, 241-258.

(10) Li, Y.; Yang, L.; Ruan, C. U.S. Pat. Appl. Publ., Appl. No. US 2003-635164 20030806, 2004; 18 pp. (11)

(11) Osanai, T.; Saito, M.; Tamura, N.; Watanabe, T.; Mikami, T.; Matsumoto, T. *Yakugaku Zasshi* **2004**, *124 (12),* 983-987.

(12) Maquelin, K.; Kirschner, C.; Choo-Smith, L. P.; et al. *J. Clin. Microbiol*. **2003**, *41*, 324-329.

(13) Gracias, K. S.; McKillip, J. L. *Can. J. Microbiol*. **2004**, *50 (11),* 883-890.

(14) Rodriguez, M. A.; Armstrong, D. W. *J. Chromatogr., B* **2004**, *800*, 7-25.

(15) Hjerten, S.; Elenbring, K.; Kilar, F.; Liao, J.; Chen, A. J. C.; Siebert, C. J.; Zhu, M. *J. Chromatogr.* **1987**, *403*, 47-61.

(16) Grossman, P. D.; Soane, D. S. *Anal. Chem*. **1990**, *62*, 1592-1596.

(17) Scnabel, U.; Groiss, F.; Blaas, D.; Kenndler, E. *Anal. Chem*. **1996**, *68*, 4300- 4303.

(18) Okun, V.; Ronacher, B.; Blaas, D.; Kenndler, E. *Anal. Chem*. **1999**, *71*, 2028-2032.

(19) Okun, V.; Blaas, D.; Kenndler, E. *Anal. Chem*. **1999**, *71*, 4480-4485.

(20) Mann, B.; Traina, J. A.; Soderblom, C. Murakami, P. M.; Lehmberg, E.; Lee, D.; Irving, J.; Nestaas, E.; Pungor, E., Jr. *J. Chromatogr., A* **2000**, *895*, 329-337.

(21) Ebersole, R. C.; McCormick, R. M. *Bio/Technology* **1993**, *11*, 1278-1282.

(22) Armstrong, D. W.; Schulte, G. Schneiderheinze, J. M.; Westenberg, D. J. *Anal. Chem*. **1999**, *71*, 5465-5469.

(23) Armstrong, D. W.; Scneiderheinze, J. M.; Kullman, J. P.; He, L. *FEMS Microbiol. Lett.* **2001**, *194*, 33-37.

(24) Hoerr, V.; Stich, A.; Holzgrabe, U. *Electrophoresis* **2004**, *25 (18-19)*, 3132- 3138.

(25) Buszewski, B.; Szumski, M.; Klodzinska, E.; Dahm, H. *J. Sep. Sci*. **2003**, *26*, 1045-1056.

(26) Shinitani, T.; Yamada, K.; Torimura, M. *FEMS Mirobiol. Lett*. **2002**, *210*, 245-249.

(27) Szumski, M.; Klodzinska, E.; Buszewski, B. *J. Chromatogr., A* **2005**, *1084*, 186-193.

(28) U.S. Department of Health and Human Services, Centers for Disease Control and Prevention and National Institutes of Health. *Biosafety in Microbiological and Biomedical Laboratories, 4th ed.;* U.S. Government Printing Office: Washington, DC; 1999; pp 12-13.

(29) Duffy, C. F.; McEathron, A. A.; Arriaga, E. A. *Electrophoresis* **2002**, *23 (13)*, 2040-2047.

(30) Xfiloche, S. K.; Zhu, M.; Wu, C. D. *J. Dent. Res*. **2004**, *83 (10),* 802-806.

(31) Beniasch, M. Z. *Immunitaetsforsch. Exp. Ther., 1* **1912**, *12*, 268-315.

(32) Yeung, E. S.; Li, Q. *Chem. Anal*. **1998**, *146*, 767-789.

(33) Tavares, M. F. M.; Colombara, R.; Massaro, S. *J. Chromatogr., A*. **1997**, *772*, 171-178.

(34) Verwey, E. J.; Overbeek, J. T. G. *Theory of the Stability of Lyophobic Colloids*; Elsevier: Amsterdam, 1948.

CHAPTER 3. SINGLE CELL DETECTION: A RAPID TEST OF MICROBIAL CONTAMINATION USING CAPILLARY ELECTROPHORESIS

Published in *Analytical Chemistry*

Andrew W. Lantz, Ye Bao[‡], Daniel W. Armstrong*[‡]

Iowa State University, Chemistry Department, 1605 Gilman Hall, Ames, Iowa 50011, USA.

Abstract

Single cells of bacteria and fungi were detected using a capillary electrophoresis based test for microbial contamination in laboratory samples. This technique utilizes a dilute cationic surfactant buffer to sweep microorganisms out of the sample zone and a small plug of "blocking agent" to negate the cells' mobility and induce aggregation. Analysis times are generally under 10 minutes. Previously, a nutrient broth media was reported as an effective blocking agent, however the natural background fluorescence from the nutrient broth limited the detection sensitivity to ~50 cells. In order to enhance the sensitivity of the technique down to a single cell, an alternative synthetic blocking agent was sought. Various potential blocking agents were screened including salts, polypeptides, small organic zwitterions, and surfactants. Zwitterionic surfactants are shown to be attractive alternatives to a nutrient broth blocker, and mimic the nutrient broth's effects on cellular aggregation and mobility. Specifically, caprylyl sulfobetaine provided the sharpest cell peaks. By substituting caprylyl sulfobetaine in place of the nutrient broth the fluorescence of the blocker plug is reduced by as much as 40x. This reduction in background noise enables the detection of a single

[‡] Current Address: University of Texas Arlington, Department of Chemistry and Biochemistry, Arlington, TX 76091 email: sec4dwa@uta.edu

microorganism in a sample, and allows this technique to be potentially used as a rapid sterility test. All single cells analyzed using this technique displayed signal-to-noise ratios between 5 and 9.

Introduction

The detection of microbial contamination in test samples is a crucial component of safety and quality control in the food,[1] pharmaceutical,[2] and medical industries,[3] as well as in the public sector (e.g., homeland security[4] and water treatment[5]). Pathogenic bacteria and fungi can cause serious diseases in patients and consumers when introduced internally *via* food or medical products. Therefore, there is a great need for rapid methods of analysis that test for the presence or complete absence of microorganisms. Current standard methods involve inoculating a sterile growth medium with an aliquot of sample, and allowing it to incubate over several days or weeks. The medium is then examined for the presence of bacteria or fungi.[6] While this technique is capable of detecting the presence of a single cell in the original aliquot, it is very time-consuming to complete. Several variations of this method have been developed to compensate for its poor speed, however these tests still require days for definitive results.[6] Furthermore, all methods that utilize growth media have a fundamental shortcoming: they may only detect organisms capable of growth on the particular medium and under specific experimental conditions. Therefore, current methods of sterility tests are often considered flawed.[7]

As a means of overcoming the shortcomings of standard microbiological methods, molecular techniques have attracted considerable attention for the analysis of microorganisms. These methods include nucleic acid hybridization or amplification (PCR, polymerase chain reaction) as a means of microbial identification,[8,9] and immunoassay

techniques.[10] However, these methods are highly specific (i.e., not particularly useful for general sterility test purposes), and are relatively complex procedures requiring significant training to perform. Recently, capillary electrophoresis (CE) has been explored as a technique for the separation and identification of microorganisms.[11] Traditionally used as an analytical technique for the separation of molecules by their mass-to-charge ratio, CE possesses unique attributes (aqueous running buffers, fast analysis time, and low sample requirements) that make it an attractive approach for "biocolloid" analysis. In the late 1980s, Hjerten et al. demonstrated that CE of viruses and bacteria was possible by examining the flow of the tobacco mosaic virus and *Lactobacillus casai* through a capillary with an applied electric field.[12] Since then, several studies have been published on the analysis of microorganisms using CE, including a mobility study on the human rhinovirus,[13] and separations of several different bacteria strains utilizing dilute polymer additives[14] and coated capillaries.[15,16]

Few publications currently exist, however, concerning the development of a rapid sterility test with CE.[17,18] Recently, our research group reported a versatile, rapid CE method for the examination of bacterial contamination.[18] A wide variety of bacteria are compatible with this method, and analysis times are typically less than 10 minutes. Microbial entities may be detected using either ultraviolet-visible (UV-Vis) or laser-induced fluorescence (LIF) detection. However, the natural fluorescence of some of the reagents in these experiments limited the detection sensitivity of the method to ~50 cells. In order to be used successfully as a "sterility test" a detection limit of a single cell is an absolute requirement. This technical note reports the successful completion of this study. By attaining single cell detection, this

method is now capable of indicating the presence or complete absence of microorganisms in a sample-the primary requirement of a sterility test.

Experimental

Materials. Buffer additives, including tris(hydroxymethyl)aminomethane (TRIS), cetyltrimethylammonium bromide (CTAB) sodium dodecyl sulfate (SDS), sodium hydroxide, sodium chloride, and hydrochloric acid were obtained from Aldrich Chemical (Milwaukee, WI). Citric acid was purchased from Fisher Scientific (Fair Lawn, NJ). 3-(Decyldimethyl-ammonio)propanesulfonate or caprylyl sulfobetaine (SB3-10), as well as octyl sulfobetaine (SB3-8), lauryl sulfobetaine (SB3-12), myristyl sulfobetaine (SB3-14), and palmityl sulfobetaine (SB3-16) were all ordered from Sigma (St. Louis, MO). Taurine, betaine, sarcosine, triethylamine N-oxide, and all peptides and poly amino acids were purchased from Sigma. Molecular Probes, Inc. (Eugene, OR) supplied the BacLight Green fluorescent dye. Nutrient and brain heart infusion broths were products of Difco Laboratories (Franklin Lakes, NJ), while luria broth was obtained from Sigma. *Brevibacterium taipei* (ATCC no. 13744), *Corynebacterium acetoacidophilum* (ATCC no. 13870), *Escherichia blattae* (ATCC no. 29907), *Bacillus cereus* (ATCC no. 10702), *Bacillus subtilis* (ATCC no.12695), *Candida albicans* (ATCC no. 10231), *Rhodotorula* (ATCC no. 20254), and *Bacillus megaterium* (ATCC no. 10778) were all purchased from American Type Culture Collection (Manassas, VA). Uncoated fused silica capillaries with inner and outer diameters of 100 μm and 365 μm respectively, were purchased from Polymicro Technologies (Phoenix, AZ). All microorganisms examined in this study are rated biosafety level one. Therefore, standard microbiological practices may be employed.

Methods. Analyses were performed on a Beckman Coulter P/ACE MDQ capillary electrophoresis system equipped with photodiode array and 488 nm laser-induced fluorescence detectors (Fullerton, CA). Fluorescence emission from BacLight Green stained cells was detected at 516 nm, while Mie scattering was detected at 449 nm. Capillaries used were 30 cm in total length (20 cm to the detector) with an inner diameter of 100 μm. New capillaries were initially conditioned with the following rinses: 1 N NaOH, 1 N deionized water, 1 N HCl, and running buffer each for 3 min. Between runs, the capillaries were washed with 1 N NaOH, deionized water, and running buffer for 1 min each. Working buffers were prepared by adding appropriate amounts of TRIS and citric acid to deionized water to produce a 10 mM TRIS/3.3 mM citric acid solution, and diluting this solution 10x to a final concentration of 1 mM TRIS/ 0.33 mM citric acid. pH was adjusted to 7 using dilute sodium hydroxide or hydrochloric acid. The final running buffers were prepared by dissolving CTAB in the working buffer to a concentration of 1 mg/mL. Blocking solutions contained the blocking agent of interest at varying concentrations in working buffer adjusted to pH=7. These solutions were all made fresh daily. All bacteria and fungi were grown as specified by the supplier. All cell concentrations were approximated by serial dilutions and plate-count methods. Initially, the microorganisms were grown in the appropriate liquid broth, and then plated on agar growth media and stored under refrigeration. All broths and agar were autoclaved (Primus autoclave, Omaha, NE) for 1 hr prior to inoculation. For experiments, fresh liquid broth was inoculated with a single microbe colony that was extracted from the agar plate. These cells were grown at 30-37 ºC under gentle agitation for approximately 24 hrs, producing a cellular concentration of ~10^8 colony forming units (CFU)/mL. The microorganisms were centrifuged down, and the excess broth was removed.

The cells were then washed with working TRIS/citric acid buffer, recentrifuged, and finally resuspended in fresh buffer for analysis. All samples were vortexed for 30 sec and sonicated briefly prior to analysis to disperse cellular aggregates. Serial dilutions of the microbial solutions were made using working buffer when necessary. BacLight Green fluorescent dye was used to stain the cells for LIF detection. This dye was initially prepared in DMSO to produce a 1 mM solution, as directed by the manufacturer. The cells were stained by adding 1 μL of dye solution per 1 mL of microbial solution (to a final concentration of 1 μM) and incubating the cells at room temperature for at least 30 min. Experiments were performed with varying amounts of BacLight to ensure cells were saturated with the fluorescent dye to maximize the signal-to-noise ratio at this concentration.

After all wash cycles, the capillary was filled with running buffer containing CTAB. Three injections were made prior to the run: 1) sample plug consisting of microorganisms, 2) spacer plug of running buffer, and 3) plug containing blocking agent. Unless otherwise noted, sample injections were made for 5 s at 0.5 psi (158 nL), spacer injections for 4 s at 0.5 psi, and blocker injections for 2 s at 0.1 psi. For single cell analysis, microbial solutions were diluted down to ~10^4 CFU/mL and stained with BacLight Green dye as described above. A small drop (~2 μL) of this solution was applied to a sterile microscope slide, and using an autoclaved micro-utensil the drop was smeared across the slide to produce numerous drops of smaller volume. These drops were then inspected visually by microscopy until a drop that contained only a single microorganism was identified and isolated. This entire drop was then injected into the capillary *via* capillary action (in place of the sample plug mentioned above). All run buffers, solutions, and vials used in the CE analysis were

autoclaved prior to the run. Run voltage was set to –2 kV in reverse polarity (current: -1.4 μA), due to reversal of the electroosmotic flow (EOF) by CTAB.

Results and Discussion

Blocking Agent. As reported previously, a CE/microfluidic-based test for the presence of microbes can be accomplished by filling the capillary with a dilute cationic surfactant (CTAB) buffer and injecting a series of plugs consisting of the microbial sample, running buffer spacer, and blocking agent (see Figure 1).[18]

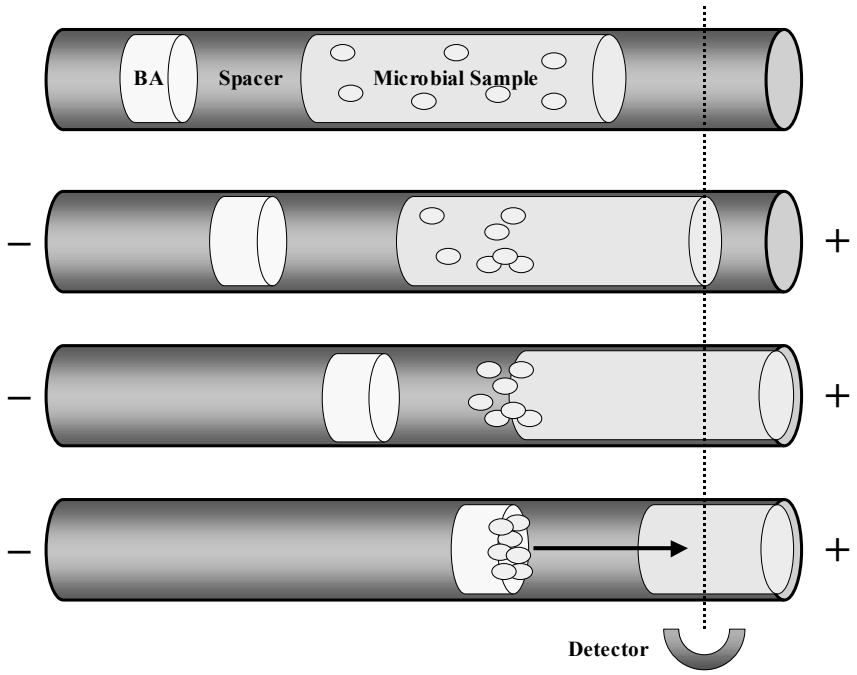

Figure 1. Schematic of CE/microfluidic-based test for microbial contamination. The entire capillary is initially filled with running buffer containing CTAB surfactant. Three injections are made prior to the run: 1) a large plug of sample containing microorganisms, 2) a spacer plug of running buffer and CTAB, and 3) a short plug of blocking agent (BA). Cells present in the sample are represented by ovals. See Experimental and Results sections for details.

Upon application of a voltage to the capillary, the cationic surfactant migrates through the sample zone. Since the electrophoretic mobility of a biocolloid is based on its surface charges,[11] the coating of the microorganisms' surface by CTAB results in a cationic migration of the cells. These bacteria and/or fungi then traverse the sample and spacer zones

until they come in contact with the blocking agent, at which point cellular aggregation occurs and their electrophoretic mobility is lost. Effectively, the microorganisms change direction twice during the separation. However, the natural fluorescence of the original nutrient broth blocking agent hindered the method's detection sensitivity, with a limit of detection of ~50 cells. It was clear that if this technique was to be an effective sterility test, the background problem had to be eliminated while preserving the unique aggregation and mobility effects on the microorganisms.

An alternate blocking agent was sought based on the following observations of the synergistic qualities of the CTAB/nutrient broth system: (a) in the presence of both CTAB *and* nutrient broth microorganisms often formed aggregates, however this seldom occurred in the presence of only one of these additives; (b) CTAB and nutrient broth do not precipitate when combined, indicating that a unique mechanism involving both CTAB and the nutrient broth is likely responsible for cellular aggregation (not simply a co-precipitation); and (c) the cells lose their electrophoretic mobility in the presence of both CTAB and nutrient broth, signifying neutralization or masking of the surface charge on the microorganisms. Cellular aggregation may be induced in several ways including neutralization of surface charges on the cells or coating the microorganism with a polymeric or uncharged material.[19-21]. Growth media (including nutrient broth) are often composed of beef or other protein extracts such as peptone, containing various water-soluble protein derivatives obtained by acid or enzyme hydrolysis of natural protein. It was initially hypothesized that the active agent in nutrient broth responsible for cellular aggregation was a hydrolyzed protein or peptides with multiple charges, either zwitterionic or simply ionic. Due to the previous success of surfactant

coatings on the surface of bacteria,[18] we postulated that this agent could potentially also be a surface-active species.

Table 1. List of potential blocking agents tested.

Salts	TRIS-citrate NaCl
Peptides	Poly-L-glutamate (MW~10000) Poly-L-arginine (MW~40000) Gly-Gly-Gly-Gly-Gly-Gly Arg-Gly-Glu-Ser Gly-Gly-Gly Leu-Leu-Leu
Zwitterions	Triethylamine N-oxide Sarcosine Taurine Betaine
Zwitterionic Surfactants	Octyl sulfobetaine (SB3-8) Caprylyl sulfobetaine (SB3-10) Lauryl sulfobetaine (SB3-12) Myristyl sulfobetaine (SB3-14) Palmityl sulfobetaine (SB3-16)

Numerous compounds were examined as potential blocking agents prior to method optimization and single cell analysis (Table 1). All additives were tested with concentrations ranging from 1 mM to 50 mM, with the exceptions of poly-L-glutamic acid and poly-L-arginine which were examined up to 10 mM due to their high molecular weights. To confirm that the focusing effect of the cells seen at the blocking agent front is not simply due to a stacking effect by the high ionic strength of the nutrient broth, small plugs of TRIS-citrate (up to 50 mM TRIS/ 16.7mM citrate) and sodium chloride (up to 50 mM) were substituted in place the nutrient broth. While some peak focusing occurred, these agents were not effective at preventing the cells from passing through the blocker plug. Poly-L-glutamate and poly-L-arginine were then examined to test the effectiveness of acidic and basic long chain polypeptides as blocking agents. These amino acid polymers appeared to have no effect on the migration of the microorganisms, allowing the cells to pass completely through the

blocker plug. Shorter peptides of 3-6 amino acid units with either nonionizable side chains (polyglycine and polyleucine) or both acidic and basic functional groups (Arg-Gly-Glu-Ser) were then assessed. Interestingly, while these peptides only blocked a small percentage of the cells in the sample, these agents proved to be more effective at negating the cells' electrophoretic mobility than the longer polypeptides. Therefore, it was theorized that small zwitterionic molecules might be responsible for the observed cell aggregation. Small zwitterionic molecules, such as sarcosine, taurine, betaine, and trimethylamine N-oxide, belong to a class of compounds known as osmolytes (or reverse denaturants). These molecules are well known to be involved in the stabilization and folding of proteins' tertiary and quaternary structures, and therefore may have a significant effect on the charge of proteins on the surface of microorganisms.[22] All four small zwitterionic molecules examined did indeed step a significant percentage (though not all) of certain microorganisms from passing through the blocker plug. However, these agents were not as effective as the nutrient broth, nor were they universal in their effect. For example, sarcosine blocked a majority of *Corynebacterium acetoacidophilum* cells while having little effect on the mobility of *Escherichia blattae*.

The apparent universal ability of the surfactant CTAB to efficiently coat and sweep microorganisms out of the sample zone directed our study toward zwitterionic surfactants. Anionic surfactants, such as SDS, were also examined however these surfactants precipitate in the presence of the cationic CTAB buffer additive. A series of zwitterionic sulfobetaine surfactants of varying carbon chain length (from 8 to 16) was evaluated. All five of the zwitterionic surfactants evaluated successfully induced aggregation of the cells in the presence of CTAB and negated the electrophoretic mobility of microorganisms. In addition,

these blocking agents appear to be universal for the bacteria and fungi tested in this study. Surprisingly, the length of the carbon chain on the surfactant tail appears to have a significant effect on the ability of the blocking agent to focus the cells. While all the sulfobetaine surfactants focus the cells into a single peak, the sharpest peaks were obtained using caprylyl sulfobetaine (SB3-10). Equimolar solutions of surfactants with more (SB3-12, -14, -16) or fewer (SB3-8) than 10 carbons in their tail produced significant peak tailing, resulting from stray cells passing through the blocker plug. Based on these studies SB3-10 was chosen as a synthetic alternative blocking agent for further studies of this CE-based sterility test.

Single Cell Detection. Substituting the zwitterionic surfactant SB3-10 in place of the nutrient broth greatly reduced the background fluorescence of the blocker plug. Electropherograms of ~25 cells of *Brevibacterium taipei* illustrate how the background signal from the blocker plug is decreased by a factor of ~40 by switching from nutrient broth (Figure 2A) to SB3-10 (Figure 2B) blocking agent.

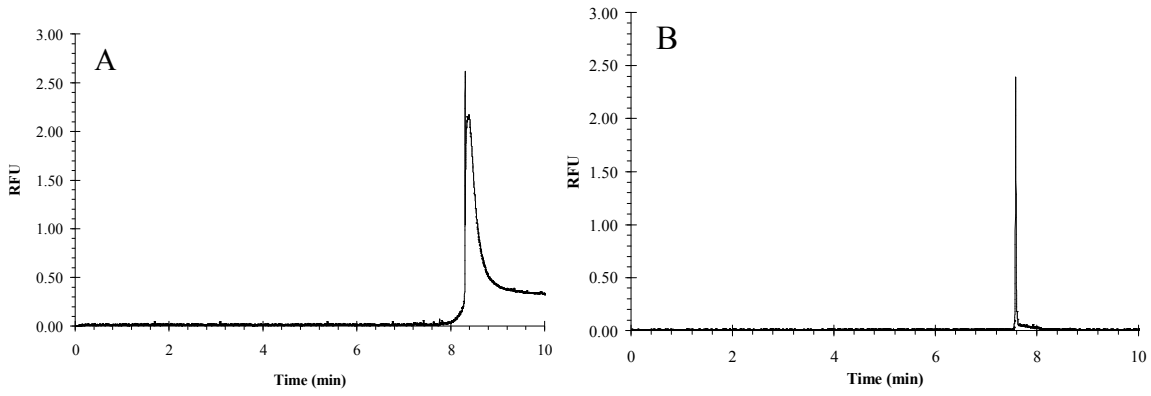

Figure 2. Electropherograms of ~25 cells of *Brevibacterium taipei* using A) 8 mg/mL of nutrient broth and B) 5 mg/mL of SB3-10 as a blocking agent. LIF detection at 516 nm. See Experimental section for method details.

This background reduction allows a single cell initially residing in the sample plug to be detected, which is an essential characteristic of a true sterility test. Samples containing a

single cell of one of several bacteria or fungi species were tested in order to confirm the detection limit of the method. Figure 3 shows example electropherograms of single cell detection for four bacteria (both gram negative and positive) and one fungus.

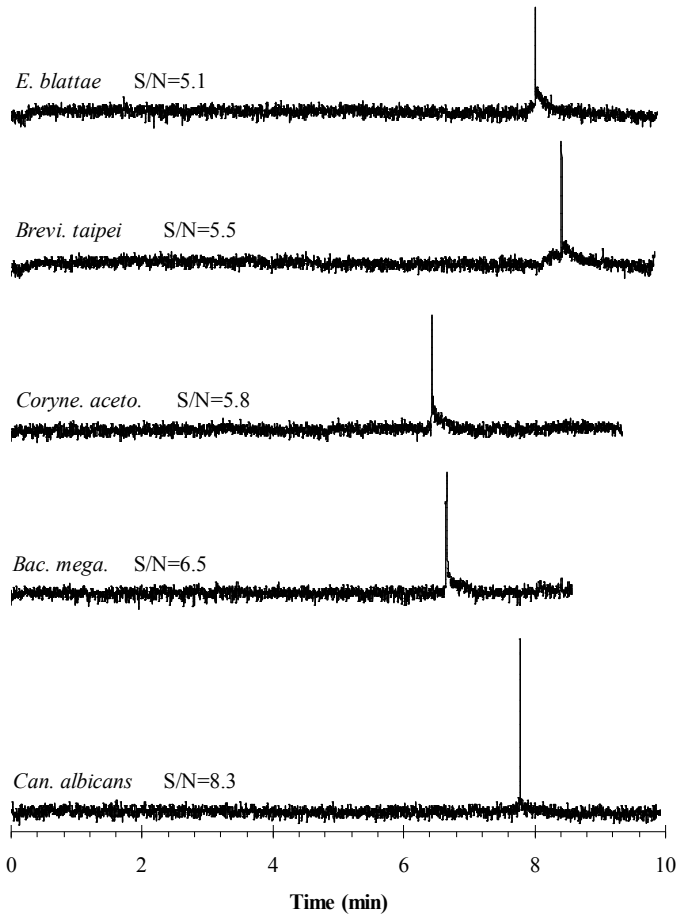

Figure 3. Electropherograms of single cells of various bacteria and fungi using the revised CE based sterility test. LIF detection at 516 nm. Concentration of SB3-10 blocking agent, 5 mg/mL. See Experimental section for method details.

Small variations in the migration times of the cells (and blocker plug) are the result of slight changes in the EOF. All single cell runs in this study displayed signal-to-noise ratios (S/N) between 5 and 9 and were repeated at least 3 times. Slight background fluorescence exists from the SB3-10 blocker plug behind the cell peak. This fluorescence occurs even when BacLight dye is not introduced into the capillary, indicating that this signal is likely due to

slight fluorescence from the SB3-10 or trace impurities present in the zwitterionic surfactant solid. Simple recrystalization of the SB3-10 did not significantly lower the background fluorescence. The background fluorescence signal however is directly proportional to the concentration of SB3-10 in the blocker plug. Therefore, the background noise may be minimized by limiting the concentration of blocking agent used. For most samples containing a relatively low concentration of microbial contamination ($<10^6$ CFU/mL), an SB3-10 concentration of 5 mg/mL is sufficient and exhibits negligible background fluorescence (see Figures 2 and 3). More turbid solutions of cells may require higher concentrations of blocking agent to adequately (and rapidly) stack all microorganisms into a single peak and negate their mobility. However, at such high cell counts the detection limit of this technique no longer becomes an issue. The effect of increasing blocking agent concentration on a solution of *Corynebacterium acetoacidophilum* (~10^8 CFU/mL) is shown in Figure 4.

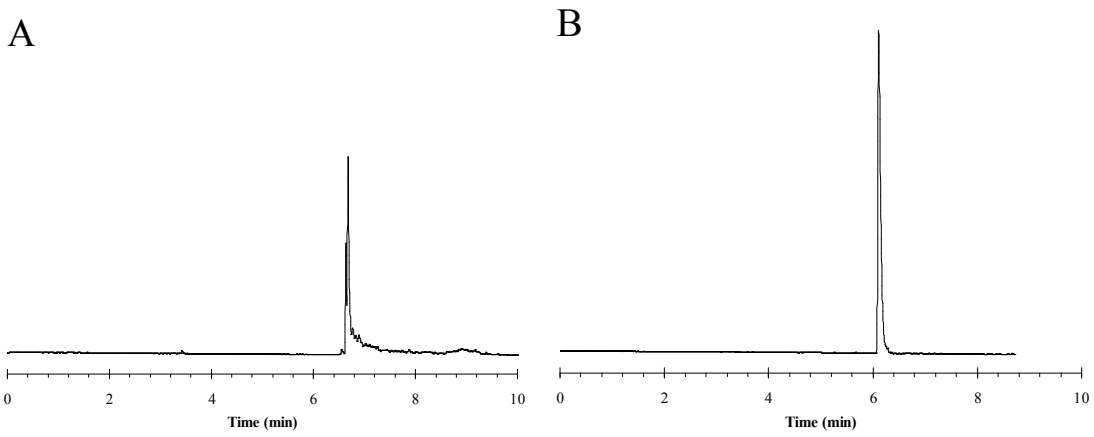

Figure 4. Effect of SB3-10 blocking agent concentration on high cell count samples. *Corynebacterium acetoacidophilum* at ~10^8 CFU/mL. A) 5 mg/mL SB3-10, B) 10 mg/mL SB3-10. Detection by Mie scattering at 449 nm. See Experimental section for method details.

The peak tailing in Figure 4A is the result of cells passing through the blocker plug due to an insufficient SB3-10 concentration. Simply doubling the concentration of the blocking agent (Figure 4B) eliminates the tailing.

Sample Preparation. Prior to CE analysis, samples must be prepared in such a manner so that the contaminating microorganisms are included in the injected volume. In most real-world scenarios, the original sample volumes are quite large and the number of bacteria or fungi cells present may be very low. Centrifugation is a rapid and effective technique for concentrating moderate volume microbial solutions down to several microliters. For significantly larger volumes membrane filtration may be used, where a sample is passed through a porous membrane capable of sequestering colloidal particles and microorganisms. The cells may then be removed from the membrane with a wash solution and concentrated further *via* centrifugation. These sampling techniques are also widely used and necessary for current sterility tests such as plating/streaking by direct inoculation, and are described in detail elsewhere.[6] In order to further ensure that the sample injected into the capillary would contain any potential microbial contamination, the volume of the sample injection may be increased by using larger inner diameter capillaries. As shown in a previous publication, sample injections of several microliters may be accomplished by using a 200 μm I.D. capillary with this CE-based sterility test.[18] Because the migration of the microorganisms within the capillary depends heavily on the conductivity and composition of the sample and buffer solutions, proper sample preparation must also include removal of ionic species and other interferences in the original sample matrix. This may easily be accomplished by a series of wash cycles that involve centrifugation of the sample and resuspension of the microbial pellet into sterile working buffer.

Conclusions

The development of single cell detection is the last significant hurdle to the development of a rapid, microfluidic sterility test for use in public and private industries. By substituting an easily obtained, relatively inexpensive synthetic compound (SB3-10) in place of the nutrient broth blocking agent, the background noise was decreased by a factor of 40 allowing a single cell present in the sample zone to be detected. This small procedural change has a huge impact on the practicality and effectiveness of the method. Future work that is necessary prior to commercial applications includes the assessment of "real world" samples using this technique, and a statistical analysis of the method's robustness and accuracy.

References

(1) Duffy, G. B.; Kilbride, B.; Fitzmaurice, J.; Sheridan, J. J. *Routine Diagnostic Tests for the Detection of Food Borne Pathogens*; January 2001.

(2) Sutton, S. V. W.; Cundel, A. M. *Pharmacopeial Forum* **2004**, *30* (5), 1884-1894.

(3) Peters, R. P. H.; van Agtmael, M. A.; Danner, S. A.; Savelkoul, P. H. M.; Vanderbroucke-Grauls, C. M. J. E. *Lancet Infect. Dis.* **2004**, *4*, 751-760.

(4) Rogers, J. V.; Sabourin, C. L. K.; Choi, Y. W.; Richter, W. R.; Rudnicki, D. C.; Riggs, K. B.; Taylor, M. L.; Chang, J. *J. Appl. Microbiol.* **2005**, *99*, 739-748.

(5) Emmerson, A. M. *Emerging Infect. Dis.* **2001**, *7* (2), 272-276.

(6) *United States Pharmacopeia*, 26th ed.; Webcon Ltd.: Toronto, Ontario, Canada, 2003; pp 2011-2016.

(7) Moldenhauer, J.; Sutton, S. V. W. *PDA J. Pharm. Sci. Technol.* **2004**, *58* (6), 284-286.

(8) Schweickert, B.; Moter, A.; Lefmann, M.; Goebel, U. B. *APMIS* **2004**, *112* (11/12), 856-885.

(9) Bej, A. K.; Mahbubani, M. H.; Atlas, R. M. *Crit. Rev. Biochem. Mol.* **1991**, *26* (3-4), 301-334.

(10) McCarthy, J. *Detecting Pathogens Food* **2003**, 241-258.

(11) Rodriguez, M. A.; Armstrong, D. W. *J. Chromatogr. B* **2004**, *800*, 7-25.

(12) Hjerten, S.; Elenbring, K.; Kilar, F.; Liao, J.; Chen, A. J. C.; Siebert, C. J.; Zhu, M. *J. Chromatogr.* **1987**, *403*, 47-61.

(13) Okun, V.; Ronacher, B.; Blaas, D.; Kenndler, E. *Anal. Chem.* **1999**, *71*, 2028-2032.

(14) Armstrong, D. W.; Schulte, G. Schneiderheinze, J. M.; Westenberg, D. J. *Anal. Chem.* **1999**, *71*, 5465-5469.

(15) Buszewski, B.; Szumski, M.; Klodzinska, E.; Dahm, H. *J. Sep. Sci.* **2003**, *26*, 1045-1056.

(16) Szumski, M.; Klodzinska, E.; Buszewski, B. *J. Chromatogr., A* **2005**, *1084*, 186-193.

(17) Palenzuela, B.; Simonet, B. M.; García, R. M.; Ríos, A.; Valcárcel, M. *Anal. Chem.* **2004**, *76*, 3012-3017.

(18) Rodriguez, M. A.; Lantz, A. W.; Armstrong, D. W. *Anal. Chem.* **2006**, *78(14)*, 4759-4767.

(19) Singleton, P. In *Bacteria in Biology, Biotechnology and Medicine*; John Wiley and Sons: New York, 1997.

(20) Fletcher, M. (Ed) *Bacterial Adhesion*; Wiley-Liss: New York, 1996.

(21) Armstrong, D. W.; Girod, M.; He, L.; Rodriguez, M. A.; Wei, W.; Zheng, J.; Yeung, E. S. *Anal. Chem.* **2002**, *74*, 5523-5530.

(22) Bolden, D.W. *Methods*. **2004**, *34(3)*, 312-22.

CHAPTER 4. CURRENT RESEARCH: IDENTIFICATION OF MICROBIAL CONTAMINANTS AND ANALYSIS OF CONSUMER EYE CARE PRODUCT STERILITY BY CAPILLARY ELECTROPHORESIS

Yet to be published

Andrew W. Lantz, Byron Brehm-Stecher, Daniel W. Armstrong*‡

Iowa State University, Chemistry Department, 1605 Gilman Hall, Ames, Iowa 50011, USA.

Introduction

In the past few decades, capillary electrophoresis has gained popularity in molecular analytical separations due to its inherent advantages (fast analysis time, low solvent consumption, aqueous running buffers) over other chromatographic techniques. Recently, this technique has been extended to the separation and analysis of colloidal particles including viruses, bacteria, and fungi, as there is a great need for a rapid assay (identification and quantitation) of these microorganisms in various branches of the food, pharmaceutical, and medical industries.[1] These "biocolloids" possess numerous charged groups on their surface from exposed amino acid residues, charged sugars, and glycolipids. As a result, these microorganisms are capable of electrophoretic migration in an applied electric field. However, several challenges have existed in the development of a capillary electrophoretic method for microbial analysis. Cell compatible ("gentle") run conditions (ionic strength, pH, voltage) are necessary in order to maintain cell functionality and prevent cell lysis. Also

‡ Current Address: University of Texas Arlington, Department of Chemistry and Biochemistry, Arlington, TX 76091 email: sec4dwa@uta.edu

limiting the effect of the cells' growth stage and size can also be a problem. Cells of varying size and surface charge will have a range of electrophoretic mobilities and therefore will not migrate as a single zone; a phenomenon termed "electrophoretic heterogeneity". Several techniques have been employed to overcome these hurdles, including coating the cells with surfactants or polymers to produce a uniform surface charge, adding ionic run buffer additives to induce cellular aggregation, and stacking methods to compact the cells into a single zone.[1-5]

As discussed in previous chapters of this dissertation, we have recently developed a capillary electrophoretic technique for the analysis of microbial contamination that is capable of single cell detection.[4,5] This method utilizes a cationic surfactant buffer additive to effectively sweep microorganisms out of their initial sample zone and a short injection plug of blocking agent (a zwitterionic surfactant) to stack the cells into a single, sharp peak. The presence or absence of this peak signal is used to designate sample sterility. The focus of our current research is to expand the use of this system to the identification of microbial contamination and to test the applicability of the methodology to consumer products.

Fluorescence *in situ* hybridization (FISH) is a rapid molecular technique for fluorescently labeling target cells based on their genetic characteristics.[6] Typically, a fluorescently labeled nucleic acid probe is allowed to permeate whole, fixed target cells and hybridize with its complementary DNA or RNA sequence within these cells. Ribosomal RNA (rRNA) is often used as a target as it is highly amplified within the cell, with most active cells having between 10^3 and 10^4 copies present.[7] If the target sequence is unique for a specific species or class of microorganisms, selective tagging of the cells is possible. Fairly strong signals are commonly obtained using FISH due to the large number of rRNA binding

sites available for the fluorescent probe. Because of their negatively charged sugar-phosphate backbone, DNA-based nucleic acid probes are inherently limited in their abilities to detect Gram-positive bacteria, as these cells possess permeability barriers to their free diffusion, including thick and anionic cell walls. Additionally, DNA probes are hybridized under fairly high salt concentrations (0.7 M to 0.9 M NaCl) and therefore may also be limited in their abilities to target highly structured rRNA sequences, which are stabilized by charge-shielding effects at these salt concentrations.[8] Peptide nucleic acid (PNA) probes were recently developed to overcome these difficulties and are composed of a synthetic peptide-like backbone that replaces the sugar-phosphate backbone of DNA.[9] Because PNA backbones are synthetic and uncharged, these probes do not encounter electrosteric resistance in hybridizing to natural nucleic acids and therefore display rapid hybridization kinetics. Additionally PNA probes hybridize independently from salt concentration. This allows them to be used at low salt conditions (0 – 100 mM NaCl) which promote destabilization of higher order nucleic acid structures, enabling otherwise "buried" sequences to be targeted. Because they are uncharged, we sought to combine PNA-FISH probes with our previously developed capillary electrophoretic sterility test in order to provide additional discriminatory power to this approach. Coupling these two complementary techniques would not only allow verification of sample sterility, but also identification of contaminants through species specific fluorescent signals.

An important step in any analytical separation technique is proper sample preparation. This step applies especially to the case of "real-world" samples whose matrices contain numerous components besides the analyte(s) of interest. The electrophoretic migration of analytes in capillary electrophoresis is highly dependent on the ionic strength and

composition of the sample and bulk solution. Therefore, in order to control the mobility of target cells within the electric field, the sample must be prepared so that any interfering species that may alter the conductivity of the solution or interact with the capillary wall are removed. Since biocolloids are many orders of magnitude larger than molecular species present in the sample, centrifugation may be used to pellet and resuspend the target cells into a buffer solution free of any adverse components. Larger insoluble constituents may be removed by filtration, however a membrane with the proper pore size to allow microorganisms to pass but capture particulates must be used. Sterility tests are often used in the pharmaceutical and personal care industries to ensure that their products are free of any pathogenic contaminants. Recently, contact lens solutions have been a focus of concern due to *fusarium* fungi contamination in Bausch and Lomb contact lens solution products. This outbreak resulted in numerous cases of fusarium keratitis in consumers.[10] Here, we also report on the sample preparation and analysis of several consumer eye care products, including contact lens solutions and multi-purpose eye drops using this CE-based microbial contamination test.

Experimental

Materials. Tris(hydroxymethyl)aminomethane (TRIS), cetyltrimethylammonium bromide (CTAB), sodium hydroxide, and hydrochloric acid were obtained from Aldrich Chemical (Milwaukee, WI). Citric acid was purchased from Fisher Scientific (Fair Lawn, NJ). 3-(Decyldimethyl-ammonio)propanesulfonate (SB3-10) was ordered from Sigma (St. Louis, MO). Formalin was obtained from E&K Scientific (Santa Clara, CA). Molecular Probes, Inc. (Eugene, OR) supplied the BacLight Green™ fluorescent dye. A fluorescein-labeled, *Salmonella*-specific PNA probe (Sal23S15; Am-ACC TAC GTG TCA GCG-Cbx ;

"Am" represents the amino terminus of the PNA, analogous to the 5' end of DNA, and "Cbx" represents the carboxyl terminus of the PNA, analogous to the 3' end of DNA) was obtained from Boston Probes (Boston, MA). Nutrient and brain heart infusion broths were products of Difco Laboratories (Franklin Lakes, NJ). *E. coli* (ATCC no. 25922), *Salmonella enterica* Ser. Typhimurium, and *Candida albicans* (ATCC no. 10231), were all purchased from American Type Culture Collection (Manassas, VA). Bausch and Lomb ReNu MultiPlus® Multi-Purpose Solution and Visine® eye drops were purchased locally. Uncoated fused silica capillaries with inner and outer diameters of 100 μm and 365 μm respectively, were purchased from Polymicro Technologies (Phoenix, AZ).

Cell Growth and Preparation. Working buffers were prepared by adding appropriate amounts of TRIS and citric acid to deionized water to produce a 10 mM TRIS/3.3 mM citric acid solution, and diluting this solution 10x to a final concentration of 1 mM TRIS/ 0.33 mM citric acid. pH was adjusted to 7 using dilute sodium hydroxide or hydrochloric acid. All bacteria and fungi were grown as specified by the supplier. All biosafety level 2 microorganisms were handled in an approved BSL-2 lab. Microorganisms were grown in the appropriate liquid broth, and then plated on agar growth media, incubated until colonies were formed, and subsequently stored refrigerated for storage. All broths and agar were autoclaved (Primus autoclave, Omaha, NE) for 1 hr prior to inoculation. For experiments, fresh liquid broth was inoculated with a single microbe colony that was extracted from the agar plate. These cells were grown at 30-37 ºC under gentle agitation for approximately 24 hrs, producing a cellular concentration of ~10^8 colony forming units (CFU)/mL. The microorganisms were pelleted via centrifugation, and the excess broth was removed. Microorganism solutions were washed with working TRIS/citric acid buffer,

centrifuged, and suspended in sample matrix or fresh buffer for analysis. All samples were vortexed for 30 sec and sonicated briefly prior to analysis to disperse cellular aggregates. Serial dilutions of the microbial solutions were made using working buffer when necessary. For sample preparation of consumer eye care products, approximately 5 mL of ReNu MultiPlus® solutions or Visine® eye drops were spiked with 2 µL of water containing resuspended microorganisms at ~10^8 CFU/mL. As needed, these solutions were then centrifuged and the pelleted cells resuspended in 0.5 mL working buffer. For sterility assessments, all vials and suspension solutions were autoclaved prior to use. Bacteria used in CE-FISH studies (*E. coli* ATCC 25922 and *Salmonella* Typhimurium) were grown overnight and fixed with 40:60 10% buffered formalin:ethanol. These treated cultures were then centrifuged and resuspended in 50:50 phosphate:ethanol prior to hybridization.

Hybridization and Staining. BacLight Green™ fluorescent dye was used as a universal dye for LIF detection. This dye was initially prepared in DMSO to produce a 1 mM solution, as directed by the manufacturer. The cells were stained by adding 1 µL of dye solution per 1 mL of microbial solution (to a final concentration of 1 µM) and incubating the cells at room temperature for at least 30 min. For CE-FISH experiments, the fluorescein-labeled PNA probe Sal23S15 (Am-ACC TAC GTG TCA GCG-Cbx) was used. This probe selectively binds to rRNA present in the 23S ribosomal subunit of *Salmonella* species. Centrifuged cell pellets were suspended in 50 µL of PNA hybridization buffer (20 mM Tris and 100 mM NaCl at pH 9, 0.5% SDS, 100 pmol/ml Sal23S15 probe). Cells were hybridized in PCR tubes using a heat block set at 55 °C for 30 minutes. A solution consisting of 10 mM Tris and 1 mM EDTA at pH 9 was then used to wash the hybridized cells for 10 minutes.

These cells were then centrifuged into a pellet and resuspended in the appropriate buffer for CE analysis.

Capillary Electrophoresis. Analyses were performed on a Beckman Coulter P/ACE MDQ capillary electrophoresis system equipped with photodiode array and 488 nm laser-induced fluorescence detectors (Fullerton, CA). Fluorescence emission was detected at 516 nm, while Mie scattering was detected at 449 nm. Capillaries used were 30 cm in total length (20 cm to the detector) with an inner diameter of 100 μm. The final running buffers were prepared by dissolving CTAB in the working buffer to a concentration of 1 mg/mL. Blocking solutions contained 10 mg/mL SB3-10 in working buffer adjusted to pH=7. These solutions were all made fresh daily. New capillaries were initially conditioned with the following rinses: 1 N NaOH, 1 N deionized water, 1 N HCl, and running buffer each for 3 min. Between runs, the capillaries were washed with 1 N NaOH, deionized water, and running buffer for 1 min each. After all wash cycles, the capillary was filled with running buffer containing CTAB and the following injections were performed: were made in order: bacteria sample for 5 s at 0.5 psi, spacer plug of running buffer and CTAB for 5 s at 0.5 psi, and blocker plug of SB3-10 for 2 s at 0.1 psi. For the analysis of sterile samples, all run buffers, solutions, and vials used in the CE analysis were autoclaved prior to the run. Voltage was set to –2 kV in reverse polarity (current: -1.4 μA), due to reversal of the electroosmotic flow (EOF) by CTAB.

Results and Discussion

Fluorescence *in situ* Hybridization. PNA-FISH was coupled with a capillary electrophoretic test for microbial contamination in order to assess the ability to specifically identify the presence of *Salmonella* Typhimurium in sample injections. Different sample

solutions containing *E. coli* or *S.* Typh. were allowed to hybridize with the *Salmonella* specific PNA probe Sal23S15 as stated in the Experimental section. These samples were run with our developed CE method to determine the specificity of the PNA probe to *Salmonella* over *E. coli* and also to estimate the limit of detection using this PNA probe as a fluorescent marker. Figure 1A shows the electropherogram for the Sal23S15 hybridized culture of *E. coli*. No significant signal was produced by *E. coli*, indicating both the selectivity of the probe and a lack of non-specific bindng of the probe to the surfaces of non-target cells.

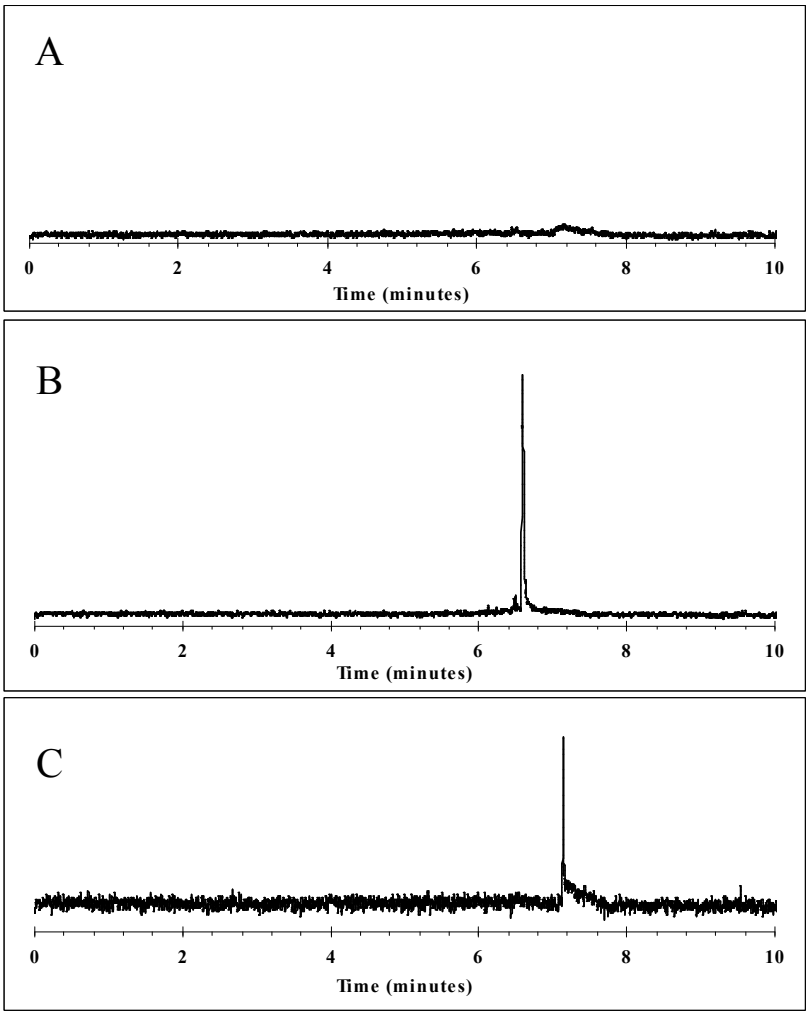

Figure 1. Electropherograms of A) ~10^8 CFU/mL *E. coli*, B) ~10^8 CFU/mL *Salmonella* Typh. and ~10^8 CFU/mL *E. coli*, and C) ~10^6 CFU/mL *Salmonella* Typh. and ~10^8 CFU/mL *E. coli*. All samples were hybridized with *Salmonella* specific Sal23S15 PNA probe as described in the Experimental section.

In contrast, strong fluorescent signals were obtained from hybridized *Salmonella* Typhimurium as seen in Figure 1B. This sample consisted of undiluted *E. coli* and *Salmonella*, both of which were allowed to react with the PNA probe. These data demonstrate the successful combination of capillary electrophoresis and fluorescence *in situ* hybridization for the characterization of sample contamination. The Sal23S15 probe was effective as a genus specific probe for the detection of *Salmonella* species in the sample injection.

In order to approximate the detection limit of this technique using this particular PNA probe, a series of mixtures of *Salmonella* Typhimurium and *E. coli* was prepared consisting of a fixed *E. coli* count (~10^8 cells/mL) and serial 10x dilutions of ~10^8 cells/mL *Salmonella*. Signal-to-noise ratios of ~7.2 were obtained with a 100x dilution of *Salmonella* (Figure 1C), and fell to ~1.6 with a 1000x dilution. Based on the Poiseuille equation, a 5 second injection at 0.5 psi in a 100 μm i.d. capillary corresponds to an approximate injection volume of 158 nL. Therefore, the number of Salmonella cells injected at the 100x dilution may be calculated as ~158 cells. This detection limit is significantly higher than that reported using BacLight Green™ dye in our previous publication (single cell).[5] This is likely due to a difference in the relative number of bound fluorescent molecules per cell. PNA-probes are designed to be highly specific for certain rRNA sequences, and therefore their net signal is dependent on the number of ribosomal copies present in the cell. BacLight Green™ on the other hand is a relatively non-specific dye that binds to membrane bound proton channels and other proteins. The detection sensitivity of PNA probes could potentially be improved by using more than one *Salmonella*-specific probe, or by optimizing experimental variables such

as probe concentration and hybridization time. Although PNA probes possess certain attributes (lack of charge, rapid hybridization kinetics, ability to penetrate "difficult" microbial structures, etc.) that suggest they may be a superior choice for combination with CE, additional work with DNA probes must also be performed in order to confirm these expected benefits.

Consumer Eye Care Products. The applicability of consumer eye care products to this CE-based test for microbial contamination was also examined in this study. Bausch and Lomb ReNu MultiPlus® Multi-Purpose Solution and Visine® eye drops were chosen as sample matrices and inoculated with lab cultured *Candida albicans*. Injections of spiked samples (without any special preparation treatments) produced numerous peaks and broad bands of cells, many of which remaining in the original sample zone (Figure 2A). Contact lens solutions and eye drops often contain a variety of constituents ranging from simple salts to surfactants and long organic polymers for lubrication. For example, besides purified water, major components of ReNu MultiPlus® solutions include 9% w/w polyhexamethylene, 1% NaCl, 1% poloxamine, and 0.9% sodium borate. Visine® drops also contain 1% w/w polyethylene glycol, 1% povidone, and 0.1% dextran. These matrix components likely interfere with the ability of CTAB to effectively coat the surface of the microorganisms and extract the cells out of the sample plug. Furthermore, the increased ionic strength of the eye solutions increases the conductivity of the sample zone, thus lowering the electric field in this region and limiting the migration velocity of the cells. Therefore, it is necessary to remove these compounds from solution prior to CE analysis. In order to isolate the contaminating cells from the sample matrix, inoculated eye care solutions were centrifuged and the supernatant was decanted.

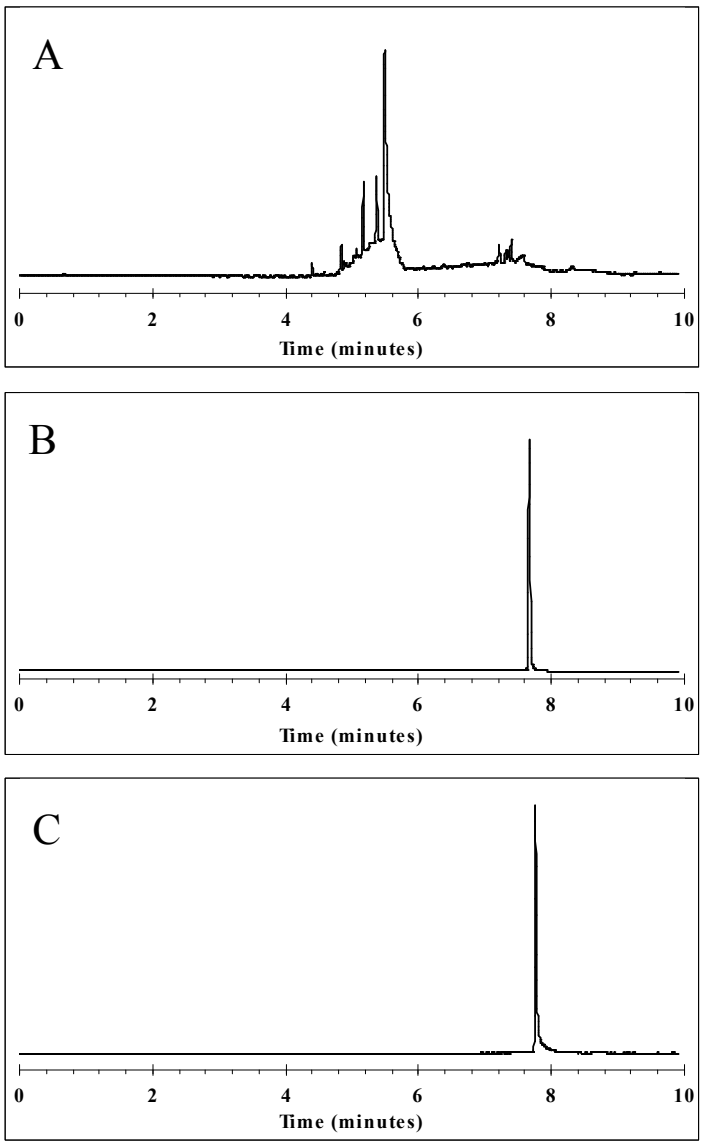

Figure 2. Electropherograms of *Candida albicans* in A) ReNu MultiPlus® solution, B) ReNu MultiPlus® solution after resuspension in working buffer, and C) Visine® solution after resuspension in working buffer. See text for details.

The remaining pelleted cells were washed in working buffer, recentrifuged and resuspended in buffer once again for analysis. Successful removal of matrix interferences resulted in a sharp peaks for fungal contaminants detected at the appropriate location (i.e. front of the blocking plug) *via* CE analysis (Figures 2B and 2C).

The sterility of Bausch and Lomb ReNu MultiPlus® Multi-Purpose Solution was tested using fluorescence detection. A fresh 5 mL aliquot of ReNu solution was transferred to an autoclaved vial using a sterile transfer pipette and centrifuged to pellet any cells present. The supernatant was decanted and any potential contaminants were resuspended in ~250 µL of sterile working buffer and stained with BacLight Green dye. After incubation, the sample was analyzed using the CE sterility test method. No measurable signal was detected for the injected samples (Figure 3A). This process was repeated 3-fold. Based on the single cell detection capabilities demonstrated in the previous dissertation chapter using BacLight Green dye, these results indicate that the injected samples of ReNu solution were indeed sterile.

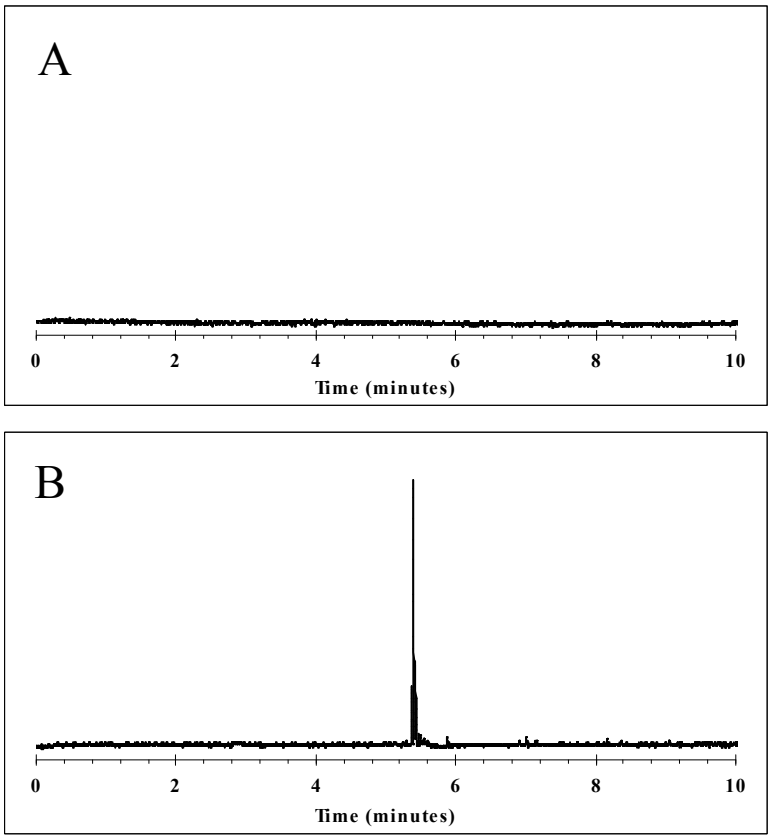

Figure 3. CE-based sterility test of ReNu MultiPlus® solution with A) an uncontaminated sample, and B) a sample inoculated with a non-sterilized instrument. See text for details.

The ability of this technique to detect low levels of cellular contaminants in ReNu solution was examined by exposing 5 mL of the lens solution to a non-sterile inoculation loop. This solution was then concentrated down to approximately 250 µL via centrifugation, resuspended in sterile working buffer, and stained with BacLight Green dye. A relatively small, but easily detectable, peak was obtained for these trials (Figure 3B), indicating that microbial contamination was present from exposure to non-sterile environments.

Conclusions

The development of a rapid capillary electrophoresis based test for microbial contamination was expanded here to demonstrate the potential for cellular identification with this method. Fluorescence *in situ* hybridization was coupled with our CE method for specific fluorescent tagging of microorganisms present in the sample. PNA probes were used as specific biomarkers for the detection of relatively low levels of *Salmonella* strain contaminants, even in the presence of high concentrations of *E. coli*. Initial sensitivity studies showed a detection limit of ~10^2 injected cells. While this sensitivity is lower than that obtained using the nonspecific BacLight Green dye, further work to enhance the intensity of the PNA tagged cells may lead to lower detection limits. In addition, commercial consumer products were applied to this CE-based sterility test for the first time. The sample preparation and sterility results of contact lens solutions and eye drops are reported here. Removal of the microbial contaminants from the sample matrix was necessary to allow adequate CTAB coating of the cells during electrophoresis. Test results indicated that these eye care products were indeed sterile, and intentional inoculation of the samples produced a detectable peak signal indicating contamination.

References

(1) Rodriguez, M. A.; Armstrong, D. W. *J. Chromatogr. B* **2004**, *800*, 7-25.

(2) Armstrong, D.W.; Schulte, G.; Schneiderheinze, J.M.; Westenberg, D.J. *Anal. Chem.* **1999**, *71*, 5465.

(3) Armstrong, D.W.; Girod, M.; He, L.; Rodriguez, M.A.; Wei, W.; Zheng, J.; Yeung, E.S. *Anal. Chem.* **2002**, *74*, 5523.

(4) Rodriguez, M.A.; Lantz, A.W.; Armstrong, D.W. *Anal. Chem*. **2006**, *78(14)*, 4759-4767.

(5) Lantz, A.W.; Bao, Y.; Armstrong, D.W. *Anal. Chem.* **2006,** *79*, 1720-1724.

(6) Brehm-Stecher, B.F.; Hyldig-Nielsen, J.J.; Johnson, E.A. *Appl. Environ. Microbiol.* **2005**, *71*, 5451-5457.

(7) Amann, R.I.; Ludwig, W.; Schleifer, K.H. *Microbiol. Rev.* **1995**, *59*, 143-169.

(8) O'Donnell, A.G.; Whitley, A.S. C. Edwards (ed.) In *Methods in Biotech. Vol 12*, Humana Press: Totowa, N.J., 1999, pp. 221-235.

(9) Stender, H.; Fiandaca, M.; Hyldig-Nielsen, J.J.; Coull, J. *J. Microbiol. Methods* **2002**, *48*, 1-17.

(10) Margolis, T.P.; Whitcher, J.P. *J. Am. Med. Assoc.* **2006**, *296*, 985-987.

CHAPTER 5. GENERAL CONCLUSIONS

Future Research

While significant progress has been made toward the separation and analysis of microorganisms using capillary electrophoresis, numerous areas of study remain uninvestigated. The problems of electrophoretic heterogeneity and capillary wall interactions have been overcome through a variety of methods including the use of buffer additives (e.g. surfactants, polymers, multivalent additives) and stacking techniques, as described in the literature review and other chapters of this dissertation. In regard to this capillary electrophoresis based sterility test, further work primarily falls into two main areas: optimization of identification techniques and real-world sample preparation.

In chapter 5 of this dissertation, we introduced the application of fluorescence *in situ* hybridization to capillary electrophoresis as a means to specifically identify microorganisms in the sample injection. However, detection limits were significantly higher for this PNA probe than with a non-specific dye such as BacLight Green, which enabled single cell detection. Future research may be aimed at exploring additional nucleic acid apporoaches, including side-by-side comparisons of DNA and PNA probes, the use of more than one *Salmonella*-specific probe and a rigorous evaluation of experimental variables, including the effects of ionic strength, hybridization time and probe concentration, and how these can be manipulated to yield bright, yet specific hybridizations.

Other methods of identification involve a physical separation of different cell types and strains. The sterility test reported here involves a method that detects the presence or absence of microorganisms in a sample, regardless of species or class. However, after this

initial screening for contamination is complete, a second method may be used to differentiate such characteristics as bacteria vs. fungi, gram positive vs. negative, cell size and shape, and surface isoelectric point. Isoelectric focusing has seen some success in the separation of bacteria species in the past. In this technique, a pH gradient is generated within the capillary using an ampholyte mixture solution. Cells then migrate in the applied electric field until they reach a pH where their net charge is zero (i.e. their pI). If the bacteria have differing pI values, they will be separated. However isoelectric focusing can be difficult to perform as it requires chemical modification of the capillary wall to suppress the electroosmotic flow of the bulk solution. One possible alternative to isoelectric focusing would be to utilize a spacer plug technique where a series of pH boundaries within the capillary are produced via multiple buffer injections of varying pH. This could potentially allow cells to migrate with their native electrophoretic mobility until they reach an injected pH boundary that negates their surface charge. Diffusion of the pH boundaries may be possibly overcome by utilizing large bulky buffer ions whose electrophoretic mobilities and diffusion coefficients are low. This technique may also be applied to the separation of gram-negative and gram-positive bacteria, as it is well known that these two classes of bacteria have large differences in their surface composition and therefore surface charge and isoelectric points.

Other possibilities for microbial separations include introducing additives to the run buffer that preferentially bind to specific bacteria species, such as sugars or proteins. As bacteria bind to these buffer additives, their surface charge and mobility may change allowing them to be separated from other bacterial species in the original sample zone. Glycomics, the study of glycan recognition in biological systems, provides a potentially useful source of information regarding selective binding of carbohydrates to bacteria.

Studies have shown that carbohydrates play critical roles in important physiological cell-cell recognition, adhesion and signaling. In addition, certain bacterial species adhere strongly to specific types of saccharides based on multivalent interactions. Mannose, for example, binds more strongly to certain strains of E. coli over other bacteria. One could potentially utilize these selective sugar-bacteria interactions in the separation of microorganisms.

Future work should also focus on the preparation of samples to be tested using this CE-base technique. As discussed in chapter 5, components in the sample matrix can greatly affect the electrophoretic migration of analytes. Differences between the ionic strength of the sample bulk buffer solution can result in decreased mobility of the microorganisms and ineffective sweeping out of the sample zone. Other dissolved compounds may also compete with CTAB for interaction with the cell's surface. As a result, it is necessary to remove these matrix components prior to analysis and resuspend the target cells in working buffer. For simple liquid matrices, this may easily be accomplished *via* centrifugation. However, for solid samples the procedure may be significantly more complex. After dissolution of the solid sample, filtration may be necessary to isolate the microorganisms from particulate matter. Special care must be taken so that no single cell is removed from the sample during this process; otherwise the sterility test result is meaningless. Another difficulty that must be addressed relates to the testing of food, produce, and meat. These samples likely contain cellular matter that may produce false positives, in addition to any bacteria or fungi. Therefore, sample preparations must be developed to remove these cellular components prior to analysis, or detection methods that are specific to only bacteria or fungi (such as DNA or PNA probes) must be implemented.

Conclusions

Despite the numerous avenues available for future studies, significant progress has been made in the past several years toward robust methodologies for the characterization of microorganisms using capillary electrophoresis. The solutions discussed in this dissertation to the problems of electrophoretic heterogeneity, cell viability, and detection limit provide a stable foundation for continued development in this area. Controlling the electrophoretic mobility of these highly variable microorganisms is essential to reproducible analysis using CE. Buffer additives such as polymers and surfactants appear to be the most effective means of altering the surface composition of the cells, allowing the effects of electrophoretic mobility to be reduced. The microbes may then migrate as a single unit regardless of their individual mobilities by stacking the cells into a single peak and inducing cellular aggregation.

The coupling of other biomolecular techniques with capillary electrophoresis is also proving to be very advantageous. As demonstrated here, fluorescence *in situ* hybridization allows species specific detection of microbial contaminants through binding of a fluorescent nucleic acid probe to its complementary rRNA sequence. Other methods such as enzyme immunoassays and immunmagnetics may also be beneficial to selective separation and analysis of microorganisms in CE. Such combinations are essential to further development in this field of research, which straddles the gap between analytical chemistry and microbiology.

A great need exists for rapid microbiological testing techniques in numerous areas of industry. Traditional growth based methods are no longer adequate for a business culture that demands low cost, fast analysis, and definitive results. Biochemical, fluorescence, and

nucleic acid based technologies are being developed that will eventually replace these outdated procedures. Capillary electrophoresis provides an attractive platform for microbial analysis (specific and universal) that may be coupled with other modern detection techniques to provide additional specific cellular characterization. The method's rapid analysis time and relatively simple setup is ideal for automated routine testing of sample contamination. The current progress being made in the field of microbiological analysis will likely produce significant improvements and changes to commercial sample testing in the next decade.